

AD-A051623

①

ROTARY VANE POSITIVE
DISPLACEMENT AIR CYCLE MACHINE
FOR ECS APPLICATIONS

TEST AND DEMONSTRATION REPORT

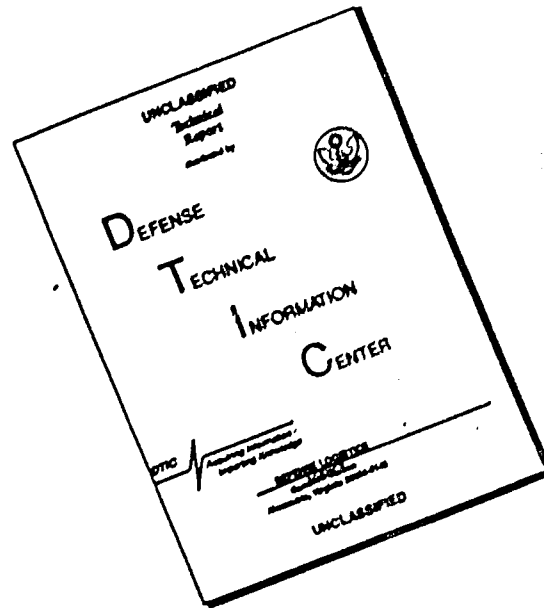
T. C. EDWARDS
W. R. Sanders

The ROVAC Corporation

SP
DDC
RECEIVED
MAR 22 1978
RECEIVED
D

DISTRIBUTION STATEMENT A
Approved for public release;
Distribution Unlimited

DISCLAIMER NOTICE



THIS DOCUMENT IS BEST QUALITY AVAILABLE. THE COPY FURNISHED TO DTIC CONTAINED A SIGNIFICANT NUMBER OF PAGES WHICH DO NOT REPRODUCE LEGIBLY.

0

ROTARY VANE POSITIVE DISPLACEMENT
AIR CYCLE MACHINE FOR ARMY ECS APPLICATIONS

TEST AND DEMONSTRATION REPORT

The ROVAC Corporation
100 Rovac Parkway
Rockledge, Florida 32955

August 1977

The Government does not necessarily endorse or approve of the projections or predictions made in this report. Contracting officer's technical representatives

DDC
RECEIVED
MAR 22 1978
ACCEPTED

U.S. ARMY MOBILITY EQUIPMENT RESEARCH AND DEVELOPMENT CENTER
FORT BELVOIR, VIRGINIA 22060

DISTRIBUTION STATEMENT A
Approved for public release;
Distribution Unlimited

ACCESSION TO	
RTIS	White Section <input checked="" type="checkbox"/>
DDC	Buff Section <input type="checkbox"/>
UNANNOUNCED	<input type="checkbox"/>
JUSTIFICATION	
Per Htr. on file	
BY	
DISTRIBUTION/AVAILABILITY CODES	
Dist.	AVAIL. and/or SPECIAL
A	

ABSTRACT

This report presents the results of laboratory tests and calculations conducted on a Model 606 air conditioning system designed for U. S. Army Mobile applications. The tests were performed in the laboratory of The ROVAC Corporation at 100 Rovac Parkway, Rockledge, Florida. Testing was performed in accordance with ASHRAE Standards at the environmental conditions specified in U. S. Army Contract DAAG53-76-C-0052. The specified test conditions were as follows: an outside or sink temperature of 125°F, and inside or cooling load conditions of 90°F dry bulb and 67°F wet bulb. The results of performance testing a steady state cooling capacity of 7200 Btu/hr at a COP of 0.544 was measured during testing. This performance compares favorably with an overall COP on the order of 0.35 produced by well-developed conventional air cycle turbo-machine and air cycle system technology.

Also included in this report are calculations predicting the performance of this Model 606 compressor-expander with ports designed to minimize port losses and internal thermal barriers to minimize adverse intra-Circulator heat transfer. These projections provide a basis for expecting a dry air COP in the vicinity of 1.5 for a further developed ROVAC Circulator and system at the specified operating conditions. Calculations are also included which demonstrate expected 606 performance in a system using industry-standard heat exchangers. Notably, these calculations show that the use of an industry-standard regenerative heat exchanger alone would increase the existing hardware COP to 0.715.

TABLE OF CONTENTS

<u>SECTION</u>	<u>TITLE</u>	<u>PAGE</u>
1	INTRODUCTION AND SUMMARY	1
1.1	System Configuration	1
1.2	Test Facilities	1
1.3	Instrumentation	2
1.4	Test Conditions	2
1.5	Test Procedure	2
1.6	Calculation of Performance	2
2	SYSTEM CONFIGURATION	3
3	TEST FACILITY	6
3.1	Calorimeter	6
3.2	Calormetric Environmental Controls	8
4	INSTRUMENTATION	11
5	TEST CONDITIONS	17
6	TEST PROCEDURE	18
7	PERFORMANCE DETERMINATION	20
7.1	Cooling Capacity	20
7.2	Coefficient of Performance	22
7.2.1	Example Calculation of Cooling Capacity (H) and COP of System	25
7.2.2	Heat Exchanger Performance	29
7.3	Performance Projections & Discussion	32
7.3.1	Performance Estimates of 606 System with Industry-Standard Regenerator Performance	36
7.3.2	Calculation of System COP with Optimized Constant-Area High Pressure Porting and Industry Standard Heat Exchangers	39
7.3.3	Calculation of System COP with Optimized Heat Exchangers, High Pressure Porting, and Minimized Intra-Circulator Heat Flux	41

TABLE OF CONTENTS (Continued)

	<u>PAGE</u>
APPENDICES	47
A. Instrumentation, Calibration, Certification	47
B. Test Data	68
C. Enriched Loop - Technical Papers	79

LIST OF ILLUSTRATIONS

<u>FIGURE</u>	<u>TITLE</u>	<u>PAGE</u>
2.1	System Configuration with Oil Separator	5
3.1	Test Cell Floor Plan	7
3.2	Test Cell with System Installed	9
4.1	Test Cell with System and Instrumentation	12
7.1	Computer Predicted Heat Loss From Cooling Load Chamber versus Ambient Temperature	23
7.2	5 HP Motor Calibration Curve	24
7.3	5 HP Motor Calibration Curve	26
7.4	7 1/2 HP Motor Calibrated Motor Curve	27

LIST OF TABLES

<u>TABLE</u>	<u>TITLE</u>	<u>PAGE</u>
4.1	Measurement Location and Purposes	14
7.1	Performance Test Log for ROVAC 606	44

SECTION I

INTRODUCTION AND SUMMARY

A ROVAC positive displacement rotary vane air cycle air conditioning system was designed, fabricated and tested at The ROVAC Corporation under Army Contract DAAG53-76-C-0052. This report describes the system configuration, test facilities, instrumentation, test procedure, calculation of performance and calculations of predicted performance of an improved system.

1.1 System Configuration

The ROVAC Model 606 air conditioning system consists of a ROVAC positive displacement rotary vane compressor-expander, heat exchangers, fans and accessories assembled in a lubricated, closed cycle configuration. The Model 606 compressor-expander was designed and fabricated by The ROVAC Corporation specifically for integration into the system. The heat exchangers, fans and peripherals were purchased and modified to comply with the overall system design. The heat exchangers were not industry-standard air cycle units and, hence, did not provide optimum system performance.

1.2 Test Facilities

Performance tests of the Model 606 air conditioning system were conducted in the ROVAC test facilities in Rockledge, Florida. The construction of a calorimetric test chamber and the test procedures were performed in accordance with ASHRAE standards. The test cell itself consisted of a modified refrigeration chamber with full instrumentation.

1.3 Instrumentation

The instrumentation utilized during the tests was designed to provide data for analyzing the performance of the entire system. The test cell is instrumented to enable measurement of cooling capacity and COP. Also, heat exchanger effectiveness and pressure loss calculations can be made from data recorded during performance tests.

1.4 Test Conditions

Performance tests were conducted in the calorimeter at the environmental conditions specified in contract DAAG53-76-C-0052. The environmental conditions were 125°F outside or sink temperature and inside or cooling load conditions of 90°F dry bulb and 67°F wet bulb.

1.5 Test Procedure

Performance tests of the Model 606 system were conducted according to a test procedure which was based on ASHRAE standards and subject to the approval of the Army Technical Representative. The test procedure was written in accordance with ASHRAE standards 16-69, 31-69 and 41-66. The procedure which was incorporated into a Test Plan was submitted to the Army contracting officer's representative for approval.

1.6 Calculation of Performance

The cooling capacity, COP and heat exchanger performances were calculated from the data recorded during calorimetric testing. The cooling capacity of the system was determined to be 7200 Btu/hr on 9 April 1977 operating with dry air in the system. At this time the COP was calculated to be 0.544.

SECTION 2

SYSTEM CONFIGURATION

The air conditioning unit under test consisted of a ROVAC compressor-expander installed in a lubricated closed loop system configuration with regeneration. For testing, the system was installed in a fully instrumented calorimetric test chamber. The following sections describe the physical configuration of the ROVAC Model 606 air conditioning system tested.

The prototype test system is a ROVAC closed loop, lubricated air cycle system with regeneration. Figure 2.1 is a system schematic. The heart of the system is the compressor-expander. It performs the function of compressing, expanding and pumping the air. After the air is compressed it is pumped into the primary heat exchanger, HX_1 . HX_1 is a cross flow plate-fin heat exchanger. Here heat is rejected and oil which has been entrained in the hot compressed air is separated and falls into the sump of the heat exchanger. The air flows out of the primary heat exchanger to the oil separator where the remainder of the oil is removed. Then the air passes on to the regenerator. Here the warm (approximately 125°F) compressed air is further cooled by the approximately 90°F low pressure air from the secondary heat exchanger. The high pressure air flows to the expander where work is removed to produce cooling. The cold low pressure air is pumped into the secondary heat exchanger, HX_2 . HX_2 consists of two General Motors automotive fluorocarbon evaporator cores connected in

parallel to reduce pressure drop. From HX_2 the air passes to the regenerator then on to the compressor.

A lubrication system was installed to provide oil for the moving parts of the compressor-expander and to reduce compressor-expander leakage. The oil is collected in the sump of HX_1 and at the base of the oil separator. From there the oil flows through 1/4 inch diameter lines to a filter and on into the hollow rotor shaft of the compressor-expander. Additional oil lines are installed from the low pressure side of the regenerator to the compressor inlet manifold to drain any oil collecting there.

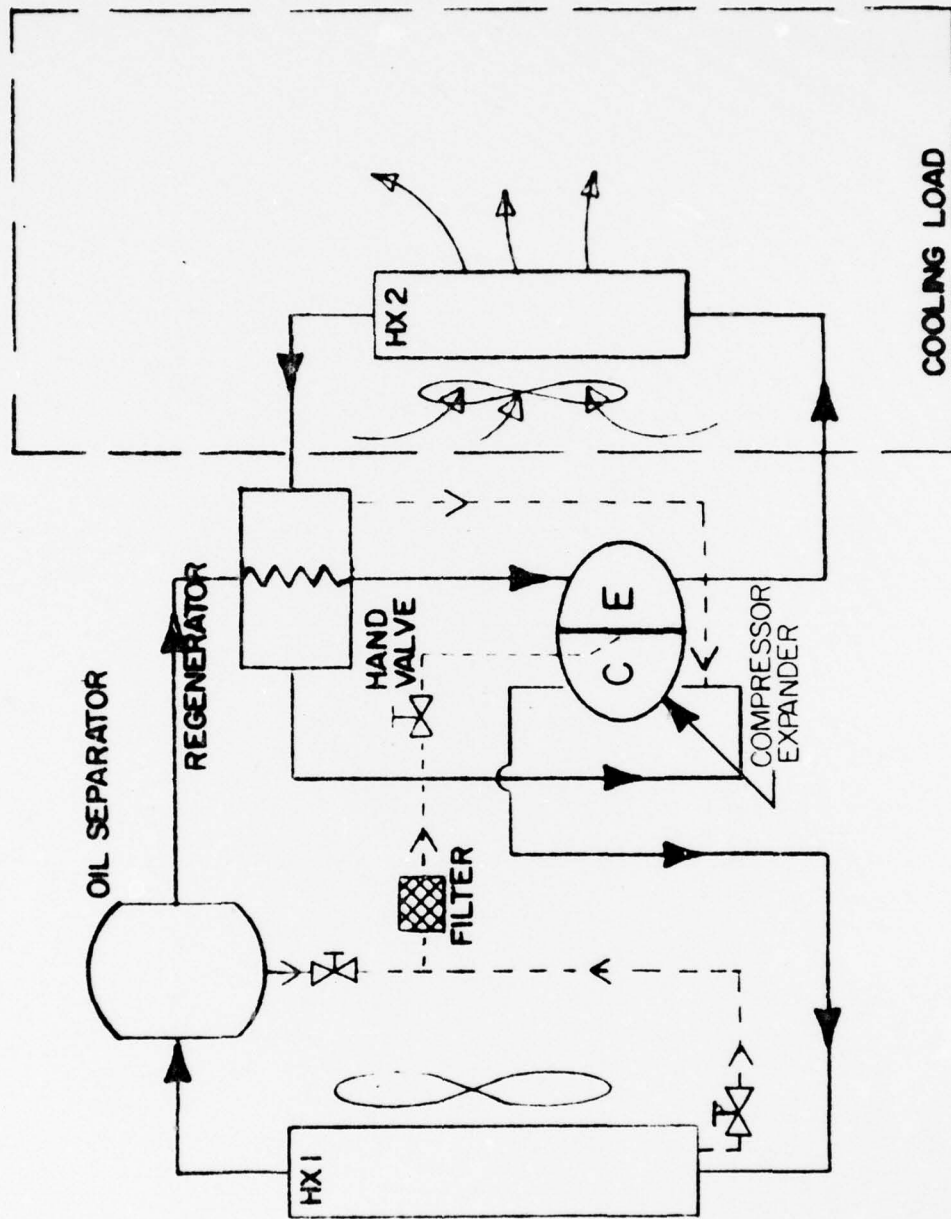


FIGURE 2.1 SYSTEM CONFIGURATION WITH OIL SEPARATOR

SECTION 3

TEST FACILITY

For the testing phase of this program a calorimetric test cell was constructed. The environment of the cell was maintained at the required conditions through the use of heaters, fans, humidifiers and a manual control system. The test chamber and environmental control system are discussed in this section.

3.1 Calorimeter

The environmental test cell used in the test program is a modified prefab walk-in cooler (refer to Appendix A for vendor information) which was purchased from Bally Case and Cooler, Inc. of Bally, Pa. Figure 3.1 (drawing No. G2755) illustrates the chamber as received from the vendor. Its basic inside dimensions are: 10'-11" long, 7'-1" wide and 6'-10" high. The long dimension is broken by a partition which separates the cooling load chamber from the sink or outside chamber. Walls, roof, partition and floor panels are constructed from four inch thick urethane insulation laminated between 22 ga. galvanized steel sheets. This type of construction has several attractive characteristics. First, urethane has a very low thermal conductivity (about half that of fiber glass insulation) which provides for minimum heat transfer loss through the walls. Also, urethane is non-hydroscopic. This and the steel sheets provide for a very effective vapor barrier. Finally, this type of construction constitutes a very rigid and strong structure.

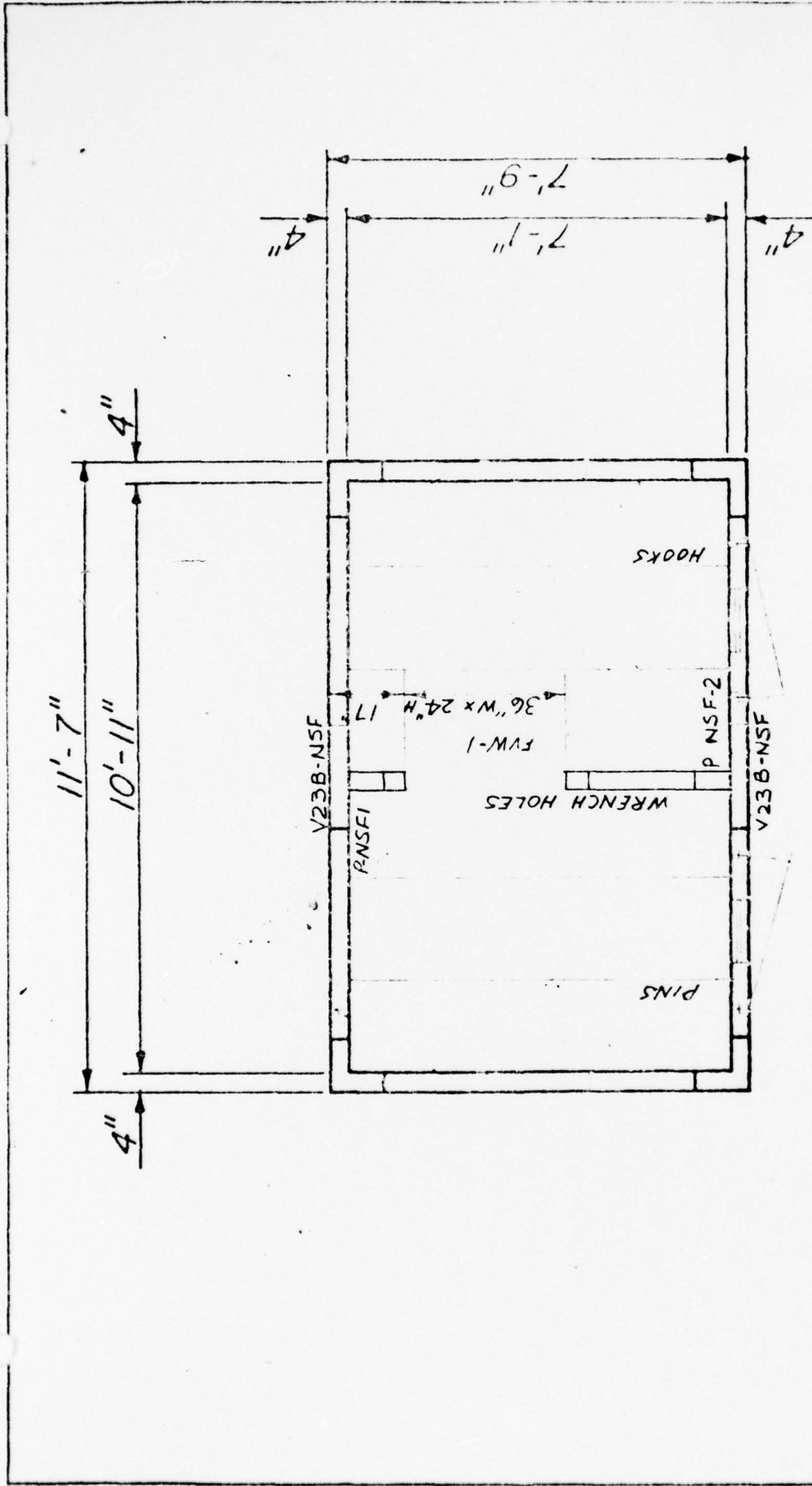


FIGURE 3.1 Test Cell Floor Plan

	DRAWING NO. 62755 DRAWN BY D.G.F.	SCALE 3/8" = 1'-0" DRAWING NO. 1-11-76	DATE 6 19 76
		1041 1174 2111	1 11 1

NOTE:
 EVAPORATOR DRAIN CONNECTIONS BY OTHERS. VENTILATION REQUIRED FOR AIR-COOLED CONDENSING UNITS WHEN IN AN ENCLOSED LOCATION. 750 CFM PER H.P.

As shown in Figure 3.2, the chamber was modified to transform it into an environmental test cell. Most of the modifications were made to the cooling load side. To separate the secondary heat exchanger (the evaporator) upstream air flow from its down-stream air flow to prevent "short-circuiting", a partition was erected at the appropriate location. A mixing chamber with a resistance heater and fans was constructed at the far side of the cooling load chamber to facilitate proper mixing and heating of the air. Humidification or dehumidification of the air stream can also be accomplished here.

The hot side of the test cell is equipped with a circulation fan to keep the air well mixed and help remove the hot air from the chamber.

3.2 Calorimetric Environmental Controls

In order to maintain the required environmental conditions in the heat rejection and cooling load chambers, manual controls are used. In the heat rejection chamber the opening of the door is adjusted so that hot air can escape from the chamber and be replaced by ambient air. A circulator fan is placed in the chamber to keep the air from stagnating. At steady-state the door can be easily manipulated to achieve the proper chamber temperature.

In the cooling load chamber the controls consist of a variable heater and an electrically heated water container. The dry bulb temperature of the chamber is maintained by adjusting the heater output. Humidity in chamber is controlled by drying out the ambient air and blowing it through the cell before the test began. When the cell door is closed the vapor

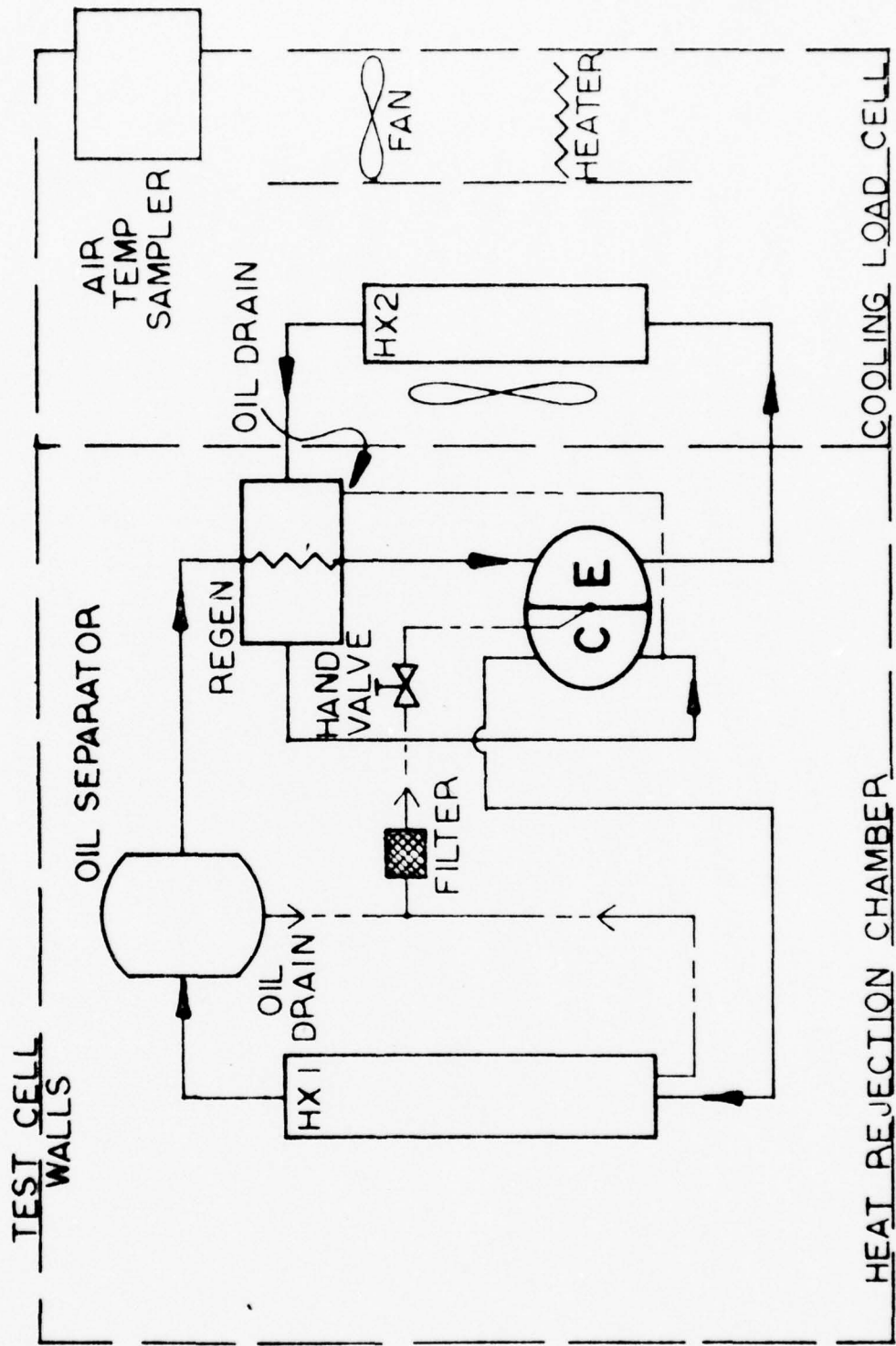


FIGURE 3.2 Test Cell with System Installed

content of the air can be increased to the required conditions by boiling water from an electrically heated container. With these controls and experience gained in the first tests the room air was maintained at the required environmental conditions during steady-state testing.

SECTION 4

INSTRUMENTATION

The calorimetric test cell and the Model 606 system under test were instrumented to provide data on test cell environmental conditions, compressor-expander drive motor horsepower, system cooling capacity, and heat exchanger performance. Figure 4.1 is a schematic diagram of the facility showing the locations of all instrumentation. Table 4.1 gives measurement number, location of measurement and purpose.

Environmental conditions were monitored through thermocouple assemblies (T7, T8, and T9) and wet and dry bulb temperatures (T13 and T14). Wattmeters (W1 and W2) were used to monitor the electrical power consumed by the three-phase compressor-expander drive motor. The drive motor was calibrated to enable calculation of motor shaft horsepower from the electrical power data.

The cooling capacity of the system was calculated from wattmeter data and checked by using psychrometric data. Wattmeters (W3 and W4) were installed to monitor the electrical power utilized in the cooling load cell to maintain the required environmental conditions. Data on the secondary heat exchanger were used to calculate the cooling capacity of the system using psychrometrics. The psychrometric method of determining cooling capacity was used as a check on the data recorded from the wattmeters.

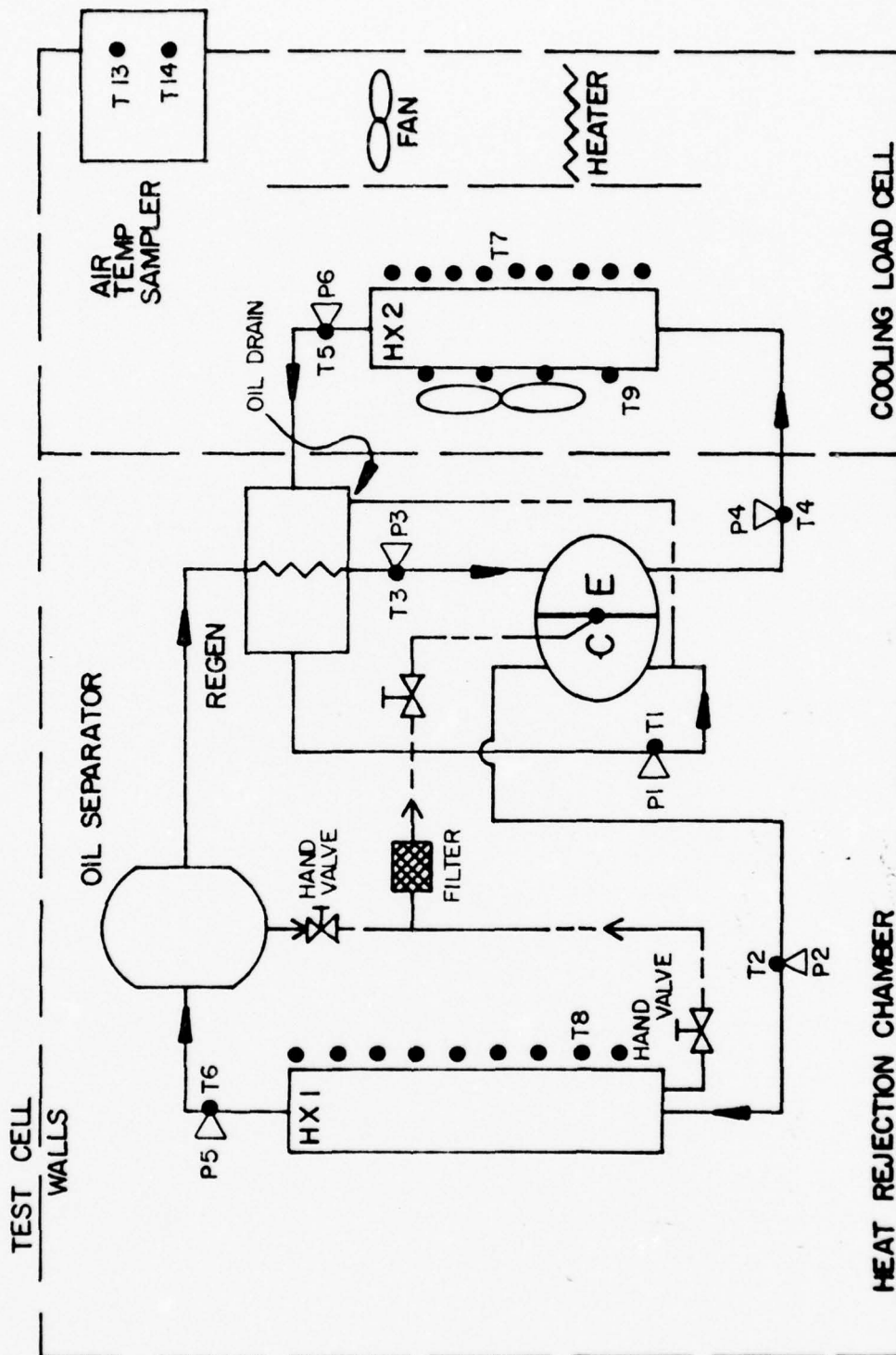


FIGURE 4.1 Test Cell with System and Instrumentation

The performance of the heat exchangers was determined through the use of thermocouples and pressure gages. The effectiveness of the primary heat exchanger (HX_1) was calculated from the thermocouples T2, T6 and T8. The pressure drop across HX_1 was determined from pressure data at P2 and P5. For the secondary heat exchanger HX_2 the effectiveness was calculated from T4, T5 and T9 and pressure drop information was derived from P4 and P6. The effectiveness of the regenerative was determined from thermocouples T1, T3 and T5. Pressure data from P3, P5, P1 and P6 was used to determine regenerative heat exchanger pressure losses.

TABLE 4.1 MEASUREMENT LOCATION AND PURPOSES

<u>MEASUREMENT</u>	<u>LOCATION</u>	<u>PURPOSE</u>
DP2 (psi)	Differential pressure across HX ₂ (primary side)	Indicates pressure drop across HX ₂
DP5 (in.H ₂ O)	Differential pressure across cooling coil blower	Indicates static pressure differential across HX ₂ fan
P1 (psig)	Compressor inlet pressure	Indicates low side loop pressure
P2 (psig)	Compressor inlet pressure	Indicates low side loop pressure
P3 (psig)	Expander inlet pressure	Indicates inlet pressure for calculation of losses
P4 (psig)	Expander outlet pressure	Indicates outlet pressure for calculation of pressure losses
P5 (psig)	HX ₁ outlet, internal flow	For pressure loss calculations
P6 (psig)	HX ₂ outlet, internal flow	For pressure loss calculations
PAMB	Ambient Conditions	Indicates barometric pressure
T1 (°F)	Compressor inlet temperature	Indicates air temperature entering compressor
T2 (°F)	Compressor outlet temperature	Indicates air temperature leaving compressor
T3 (°F)	Expander inlet temperature	Indicates air temperature entering expander

TABLE 4.1 (Continued)

T4 (°F)	Expander outlet temperature	Indicates air temperature leaving expander for calculation of ΔT across expander
T5 (°F)	HX ₂ outlet	Used for T4 and T7 to calculate HX ₂ effectiveness
T6 (°F)	HX ₁ outlet	Used with T2 and T8 to calculate HX ₁ effectiveness and with T1, T3, and T5 to calculate Regenerator effectiveness
T7 (°F)	HX ₂ secondary flow outlet	Indicates cooling air flow temperature from HX ₂
T8 (°F)	HX ₁ secondary flow inlet	Indicates heat rejection chamber temperature
T9 (°F)	HX ₂ secondary flow inlet	Indicates temperature rise across HX ₂
T10 (°F)	Drive motor winding	Indicates temperature of drive motor windings
T11 (°F)	Top of calorimeter	Indicates test cell top temperature for calculation of heat loss
T12 (°F)	Side of calorimeter	Indicates test cell side temperature for calculation of heat loss
T13 (°F)	Thermometer Box	Indicates cooling load chamber dry bulb temperature
T14 (°F)	Thermometer Box	Indicates cooling load chamber wet bulb temperature

TABLE 4.1 (Continued)

W1 (watts)		
W2 (watts)	30 Circulator drive motor	Indicates power consumed by Circulator drive motor
W5 (watts)	220V Resistance heater and HX ₂ fan	Indicates power consumed by resistance in reheating the cooling load chamber air and HX ₂ fan.
W4 (watts)	Air circulating fans (cooling load side)	Indicates power consumed by fans.

SECTION 5

TEST CONDITIONS

Calorimeter tests were made in accordance with a test plan submitted by The ROVAC Corporation based on ASHRAE Standards 16-69, 31-69, 41-66 and approved by the Army Representative. The environmental conditions to be maintained during tests were specified in the original contract number DAAG53-76-C00052. These conditions were as follows: a heat rejection or sink temperature of 125°F, a cooling load temperature of 90°F dry bulb and 67°F wet bulb. These conditions were maintained during all steady state performance tests of the Model 606 system.

SECTION 6

TEST PROCEDURE

The following section outlines the procedure which was followed during testing to determine the cooling capacity and coefficient of performance (COP) of the MERDC ROVAC air cycle system.

1. Verify that all instrumentation is installed and operating properly (thermocouples, thermometers, pressure gages, monometers and wattmeters.)
2. Supply power to the 3-phase Circulator drive motor and primary heat exchanger fans.
3. Verify that oil is flowing through the Circulator lubrication system.
4. Pressurize the system to the desired compressor inlet pressure (closed-loop pressure) as read on P1.
5. Start heater and all fans.
6. Begin taking data at 16 min. intervals on data sheets.
7. Adjust the heater voltage transformer and water evaporator control such that the cooling load chamber wet and dry bulb temperatures (T14 and T13) are at 67°F and 90°F respectively.
8. Adjust the air exchange in the heat rejection chamber until the temperature at T8 is 125°F.
9. When the test cell has reached steady state conditions begin taking data at 15 min. intervals for 1 hour.

Shut down procedure:

1. Vent the Circulator closed-loop pressurization.
2. Shut off power to Circulator drive motor, heater and all fans.

SECTION 7

PERFORMANCE DETERMINATION

The purpose of the testing program was to measure the performance of the ROVAC MERDC air conditioning system. This section outlines the methods which were used to calculate the cooling capacity, cooling coefficient of performance and other performance parameters from the raw data collected during the testing. Also, included in this section are calculations of the existing system performance and optimized system performance.

7.1 Cooling Capacity

The cooling capacity of the system was determined by use of an energy balance method, then checked using enthalpy calculations. The energy balance method consists of measuring the energy input into the cooling load chamber required to maintain the 90°F db and 67°F wb conditions during capacity testing. A graph of the computer predicted heat loss from the chamber is included in this section. This graph was prepared from data generated by Harry Kyser Associates Inc., representatives of the Bally Case Cooler Company. The cooling capacity is calculated by subtracting the heat loss from the energy required during steady state operation of the unit. The following equation will be used to calculate the cooling capacity using the energy method.

$$W3+W4-HL = \text{Cooling Capacity, H(kw)}$$

where: W3 is the steady state wattmeter measurement of energy input to the heater.

~~W4 is the steady state wattmeter measurement of energy~~

input to the fans and blowers.

HL is the heat energy loss from the cooling chamber,

which is the sum of W3 and W4 during the heat loss test.

The enthalpy methods consists of determining the enthalpy change of the air blowing across the secondary heat exchanger. Then, by knowing the mass flow rate of air being cooled, the cooling capacity can be calculated. The enthalpy of the air entering HX_2 is determined by comparing the temperatures at T9 (just down stream of HX_2 fan) with psychrometric charts. The enthalpy of the air leaving HX_2 is determined in a similar manner using T7. The mass flow rate of air blowing across HX_2 is derived from the static pressure versus cfm curve for the fan. The following equation is used to calculate the cooling capacity of the air conditioning unit by the enthalpy method:

$$H = \dot{M}_2 (h_9 - h_7) = \text{Cooling Capacity}$$

where: \dot{M}_2 is the mass flow rate across the secondary heat exchanger (HX_2)

h_9 is the enthalpy of the air entering HX_2 during steady state operation.

h_7 is the enthalpy of the air leaving HX_2 during steady state operation.

Deriving h_7 from the dry bulb temperature at T7 is slightly inaccurate. However, the enthalpy method of determining cooling capacity was used only as a check on the results obtained using the energy method.

Calorimeter Heat Loss Calculation

Predictions of the heat loss from the calorimeter over a range of ambient temperatures have been calculated. Harry Kyser Associates, Inc. P.O. Box 15982, West Palm Beach, Florida 33406, has supplied the computer predicted heat loss data based on test proven values of the coefficient of thermal conductivity. The data was generated for the steady state operating conditions in each chamber, 75°F floor temperature, and a range of ambient temperatures from 60°F to 125°F. Figure 7.1 is a graph of the computer predicted heat loss from the cooling load chamber versus the ambient temperature, TAMB.

7.2 Coefficient of Performance

The coefficient of performance of the ROVAC system was calculated from data indicating the energy supplied to maintain the cooling load chamber at 90°F db and 67°F wb and the energy required to drive the Circulator. The readings on wattmeters W1 and W2 were added to calculate the total energy being used by the 3 phase drive motor during steady state test operation. The losses in the motor due to inefficiencies were compensated for by use of the calibration data supplied by MERDC with the motor. The COP of the compressor-expander was then calculated from the ratio of the cooling capacity to the actual energy supplied to the Circulator. The following equation was used to calculate the COP of the system:

$$\text{COP} = \frac{\text{Cooling Capacity}}{\text{Motor horsepower}}$$

Where Motor horsepower is the actual horsepower of the three phase calibrated drive motor as converted from calibration data. Figure 6.2

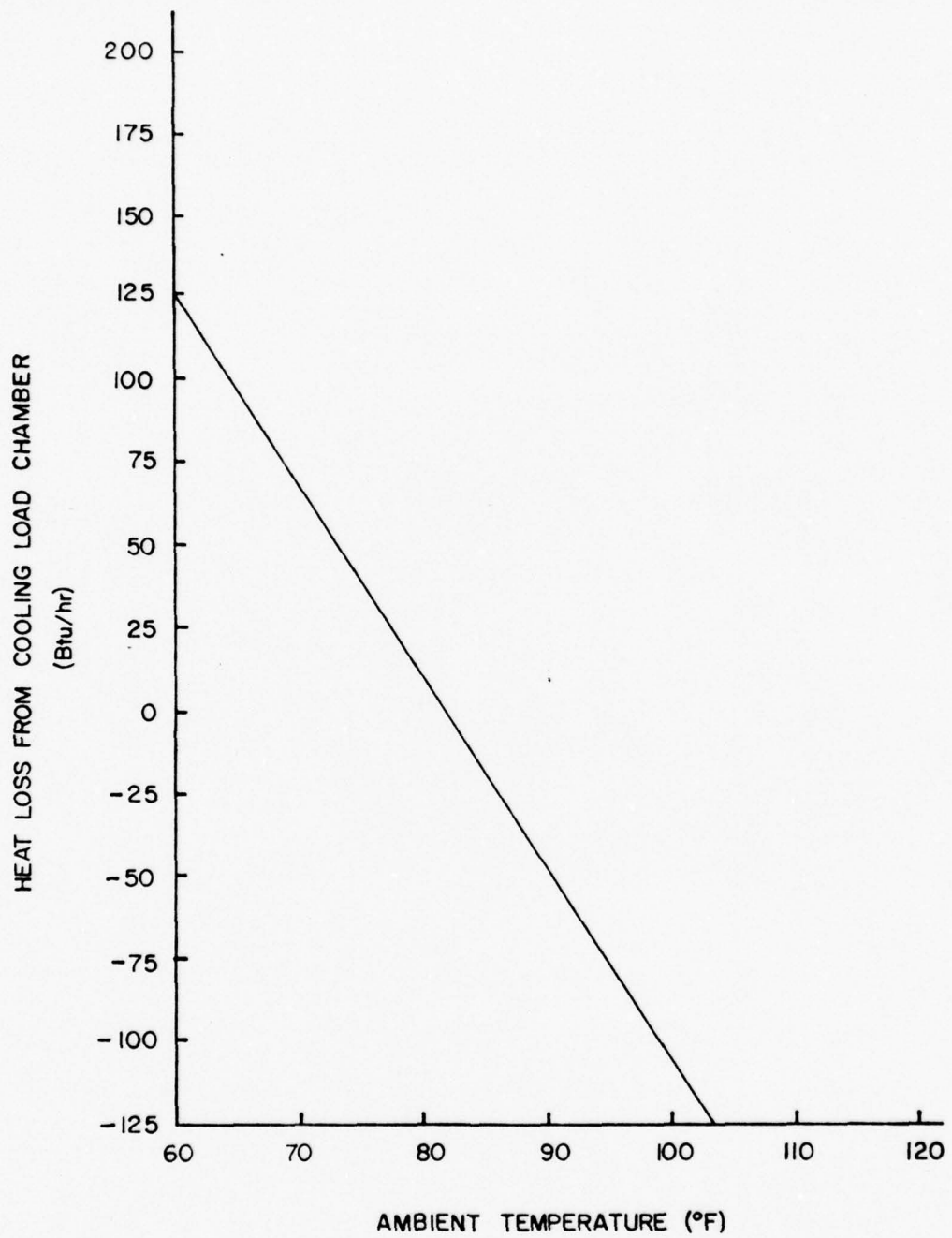


FIGURE 7.1 Computer Predicted Heat Loss From Cooling Load Chamber versus Ambient Temperature

46 1513

K&E 10 X 10 TO THE CENTIMETER 18 X 25 CM
KEUFFEL & ESSER CO. MADE IN U.S.A.

MOTOR 39 60 HZ
DAYTON MODEL A3N221
S/N F-3467-04-B76

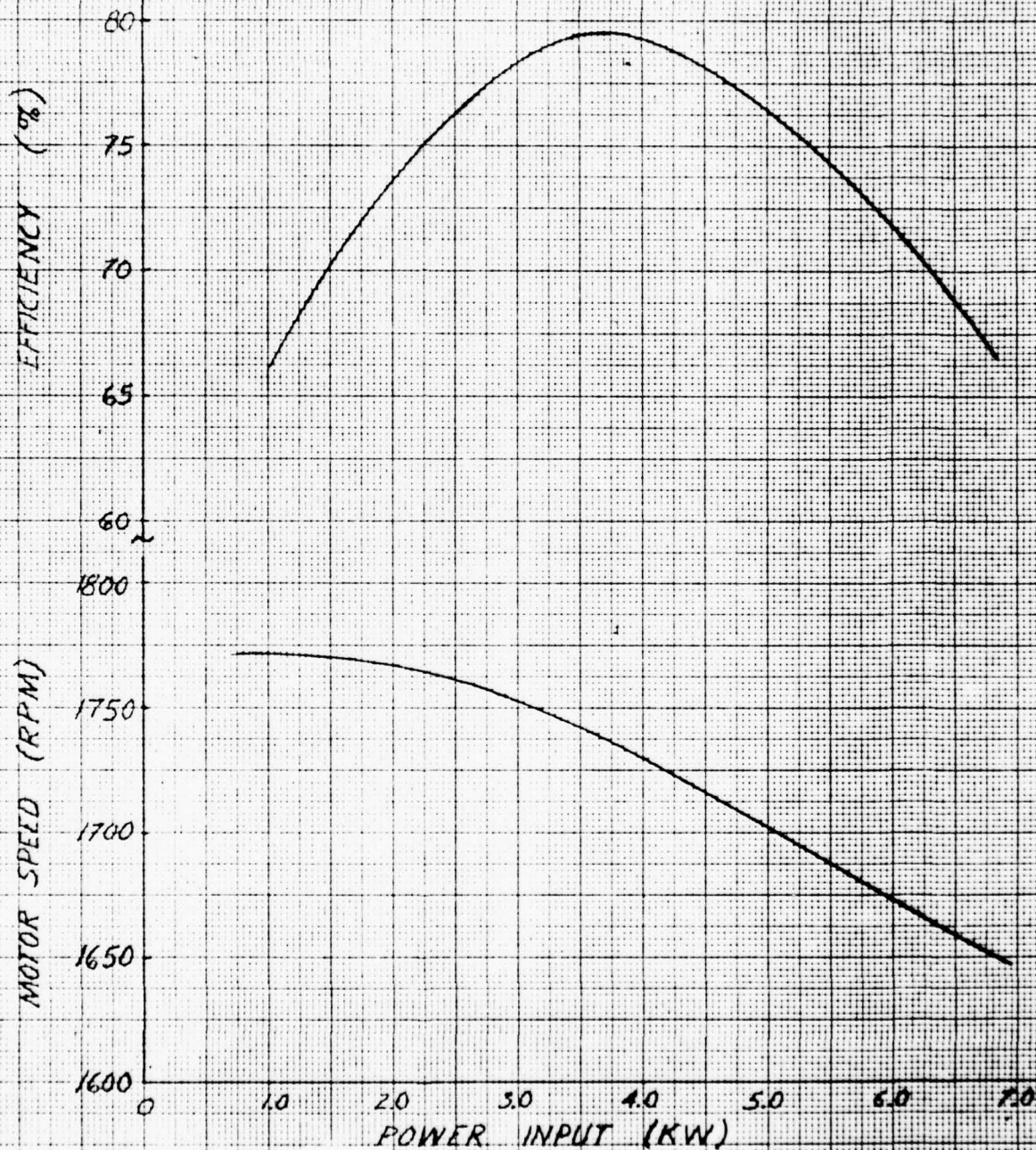


FIGURE 7.2 5 HP MOTOR CALIBRATION CURVE

and 7.3 are graphs made from calibration data on a 5 horsepower motor. Figure 7.4 is a graph of calibration data from a 7 1/2 horsepower motor.

In addition to the calculations performed to determine the cooling capacity and COP of the system from test data, calculations were made to predict the effect of performance of enhanced port and heat exchanger efficiency and minimization of intra-Circulator heat transfer.

7.2.1 Example Calculation of Cooling Capacity (H) and COP of System

(Data Taken In Calorimeter Test on 3/9/77)

Cooling Capacity, Q:

$$Q = W3+W4$$

$$W3 = 1.365 \text{ kW} \quad W4 = .321 \text{ kW}^*$$

$$Q = 1.686 \text{ kW}$$

$$Q = 5754 \text{ Btu/hr}$$

COP:

$$\text{COP} = \frac{\text{Cooling Capacity}}{\text{Work Required}}$$

*One hour average values from steady state test data of 3/9/77.

46 1513

K^oE 10 X 10 TO THE CENTIMETER 18 X 25 CM.
KEUFFEL & ESSER CO. MADE IN U.S.A.

MOTOR 3 @ 60 HZ
DAYTON MODEL A3N221
S/N F-3467-04-B76

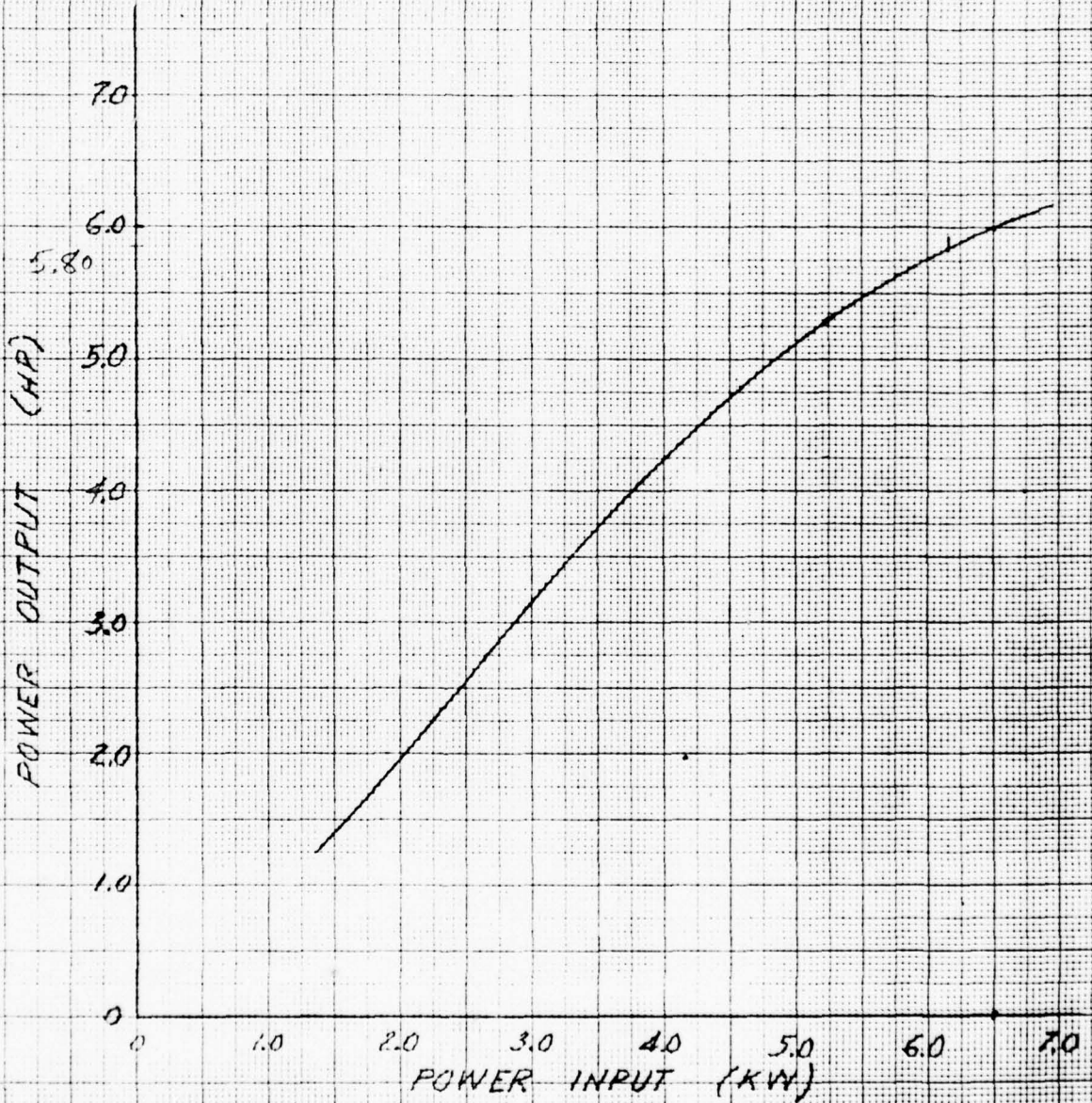


FIGURE 7.3 5HP MOTOR CALIBRATION CURVE

46 1513

NO. 10 X 10 TO THE CENTIMETER 10 X 25 CM
KUFFEL & ESSER CO. MADE IN U.S.A.

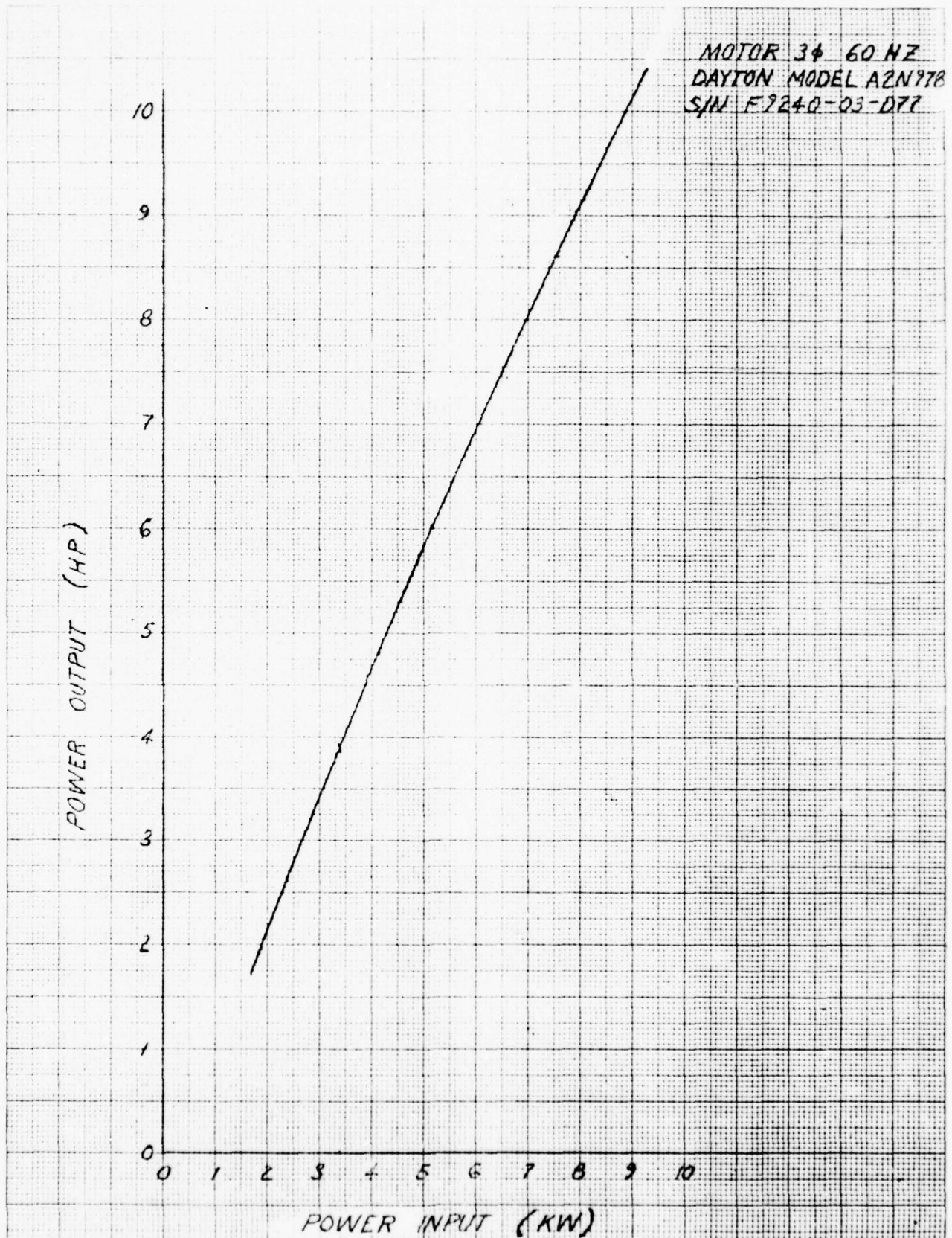


FIGURE 7.4 7 1/2 HP MOTOR CALIBRATED MOTOR CURVE

Work Required = Shaft Horsepower determined from W1+W2
converted from drive motor performance graph
(Figure 6.1)

$$W1 = 1.515\text{kW} \quad W2 = 3.075 \text{ kW}^*$$

$$\text{Work Required} = 4.75\text{hp} = 12,084 \text{ Btu/hr.}$$

$$\text{COP} = \frac{5754}{12,084} = 0.476$$

Check of Cooling Capacity (H) Check Using Enthalpy Method:

$$\text{Cooling Capacity, } H = \dot{M}_2 (h_9 - h_7)$$

$$T7 = 86.25^\circ\text{F}$$

$$T9 = 95.75^\circ\text{F}$$

$$T13 = 90.9^\circ\text{F}$$

$$T14 = 67.75^\circ\text{F}$$

Find h_9 and h_7 :

$$\text{from } T13 \text{ and } T14 \text{ the humidity ratio} = .009 \frac{\text{lbm moisture}}{\text{lbm air}}$$

$$\text{@ } T9 = 95.75^\circ\text{F} \text{ and } .009 \frac{\text{lbm moisture}}{\text{lbm air}}$$

$$\text{@ } T7 = 86.25^\circ\text{F} \text{ and } .009 \frac{\text{lbm moisture}}{\text{lbm air}}$$

$$h_7 = 30.7$$

$$H = \dot{M}_2 (h_9 - h_7)$$

$$\dot{M}_2 = (570 \text{ ft}^3/\text{min}) (.073 \frac{\text{lbm}}{\text{ft}^3}) (\frac{60 \text{ min}}{1 \text{ hr}})$$

*One hour average values from steady state test date of 3/9/77.

$$\dot{M}_2 = 2497 \text{ lbm/hr}$$

$$Q = 2497 \frac{\text{lbm}}{\text{hr}} (33-30.7) \frac{\text{Btu}}{\text{lbm}}$$

$$Q = 5744 \text{ Btuh}$$

7.2.2 Heat Exchanger Performance

The performance of the heat exchangers was analyzed for effectiveness and internal pressure losses. The thermocouples installed in the inlet and outlet of the heat exchangers were used to calculate the effectiveness of the heat exchanger.

The regenerator (RHX) effectiveness is:

$$\text{Eff}_{\text{RHX}} = \frac{T_6 - T_3}{T_6 - T_5}$$

The effectiveness of the primary heat exchanger (HX₁) is:

$$\text{Eff}_{\text{HX}_1} = \frac{T_2 - T_6}{T_2 - T_8}$$

The effectiveness of the secondary heat exchanger (HX₂) is:

$$\text{Eff}_{\text{HX}_2} = \frac{T_4 - T_5}{T_4 - T_9}$$

The internal pressure loss through each heat exchanger is determined from pressure readings taken throughout the system.

Analysis of the performance of the heat exchanger makes it possible to determine if the performance of the system could be improved by replacing the heat exchangers with more efficient ones. Also, the analysis makes it possible to obtain a clearer picture of what the actual performance of the Circulator would be if the characteristic of the peripheral equipment were optimized.

Heat Exchanger Performance Calculations

Steady State Calorimeter Data from March 9, 1977

Regenerator Effectiveness, Eff_{RHX} :

$$Eff_{RHX} = \frac{T_6 - T_3}{T_6 - T_5}$$

$$= \frac{132 - 110.75}{132 - 94.75} = \frac{21.25}{37.25}$$

$$Eff_{RHX} = .57$$

The very low effectiveness of the regenerative heat exchanger imposed an adverse effect upon actual system performance.

Primary Heat Exchanger Effectiveness, Eff_{HX_1} :

$$Eff_{HX_1} = \frac{\dot{M}_i C_p (T_2 - T_6)}{\dot{M}_i C_p (T_2 - T_8)}$$

Where \dot{M}_i is the system internal and minimum mass flow rate:

$$Eff_{HX_1} = \frac{(T_2 - T_6)}{(T_2 - T_8)}$$

$$Eff_{HX_1} = .956$$

Secondary Heat Exchanger Effectiveness Eff_{HX_2} :

$$Eff_{HX_2} = \frac{\dot{M}_i C_p (T_4 - T_5)}{\dot{M}_i C_p (T_4 - T_9)} = \frac{(T_4 - T_5)}{(T_4 - T_9)}$$

$$\frac{30.5 - 94.75}{30.5 - 95.75} = - \frac{64.25}{65.25}$$

$$Eff_{HX_2} = 0.985$$

Pressure losses Across Heat Exchangers

$$\Delta P_{RHX} \text{ high pressure} = 1.0 \text{ psi}$$

$$\Delta P_{RHX} \text{ low pressure} = 0.7 \text{ psi}$$

$$\Delta P_{HX_1} = 0.68 \text{ psi}$$

$$\Delta P_{HX_2} = 0.55 \text{ psi}$$

The pressure losses across the regenerator are relatively high. These values should be more in the 0.25 to 0.35 psi range. This poor regenerator flow efficiency imposes yet another adverse effect upon the efficiency of the actual test system.

7.3 Performance Projections & Discussion

Noting the significant advancement in the performance of the 606 machine as contrasted with that of the original Army 209 system (U.S. Army Contract No. DAAG53-76-C-0052) it becomes important to generate meaningful projections of expected performance in a further developed Circulator and system. It has already been pointed out that the low effectiveness and high pressure loss associated with the regenerative heat exchanger imposed a system adversity. However, the heart of the system, the Circulator, bears the largest potential for overall system performance improvement. Detailed Company-funded research on various present-generation Circulators has delineated two specific areas of future Circulator design improvement:

1. Minimization of Intra-Circulator Heat Transfer
2. Maximization of High Pressure Port Performance

Knowledge of the second item, high pressure port performance, has been in hand for some time. While both the compressor discharge port over-pressure and the expander inlet port drop are both important, the dominant loss is the expander port. This is because a loss here counts twice: first as a reduction in expander energy recovery and second as a reduction in expander flow temperature drop. The compressor discharge over-pressure, on the other hand, only counts once: added compressor work.

It has been theoretically and experimentally determined through in-house development that the major shortcoming of the present 606-type of expander ports are couched in their variable velocity nature. Thus,

steps have been taken to devise constant-velocity (constant-cross sectional flow area) port geometry. A manifestation of this effort has been the so-called "Baby-Bottom" geometry that consists basically of a centrally located radial feed circular inlet region that fans axially and circumferentially to maintain an approximately constant area flow path. This geometry has been tested in a 217 machine and is showing moderately improved performance. It is recommended, of course, that such port flow improvements be factored into any advanced compressor-expander system for MERDC.

Knowledge in the area of intra-circulator heat transfer on the other hand; is relatively recent and also a result of company-funded advanced Circulator development activities. It has been learned that expander efficiency has been eroded by two major factors: high frequency transient heat flow from the rotor surface to the expander as well as stator shell heat conduction from the compressor section to the expander section.

The transient rotor heat transfer arises from the combination of the relatively high temperatures reached by the air during compression and the subsequent high film coefficient arising from the high velocity tangential air flow "scrubbing" past the rotor during the compressor discharge process. This combination forces the flow of heat into the rotor periphery during the compressor discharge process. When this hot rotor surface passes into the expander intake region, the relatively cool expander inlet flow "scrubs" the heat back off the rotor surface thus delivering it into the expander inlet flow.

The stator shell heat flow is fundamentally a heat conduction phenomena which is aggravated by the turbulence-induction caused by the rapidly moving vane tips as they pass very near to the expander (and compressor) stator walls. This induced turbulence serves to increase the net convective film coefficient arising between the expanding air and the hot expander walls.

The high frequency heat transfer factor is to be dealt with through the use of an oil-cooled high diffusivity (aluminum) rotor. The high diffusivity property provides a relatively low rotor surface temperature rise during the compressor discharge process. As well, the rapid propagation of thermal energy through the peripheral surface of the rotor then proceeds to the oil-cooled section of the rotor where it is absorbed and carried away, thus avoiding a substantial rise in the steady-state rotor surface temperature.

The stator conduction flow will be arrested by approximately 1/16" coating of phenolic insulation applied to the endcap surfaces. This coating, due to its very low conductivity will effectively stop stator thermal flow from the compressor to the expander. However, to further enhance the effectiveness of this coating, the endcaps are also to be cooled by the same flow of lubricating/cooling oil passing through the rotor. As well, this thermal insulation is to be applied between the two halves of the stator housing itself as well as to the expander stator section.*

*All the improvements mentioned here have already been factored into the design of the ROVAC model 222 Circulator and actual testing has shown significant improvement in steady-state performance. These improvements are receiving further developmental refinement.

With these basic improvements ahead, meaningful estimates of their advent can be made based upon existing 606 test data. The following section deals with these estimates. The first set of calculations include an improved regenerative heat exchanger; the second set include good heat exchanger performance and improved Circulator ports, and the third set include good heat exchangers, improved ports and reduced compressor-to-expander thermal short-circuiting.

7.3.1 Performance Estimates of 606 System with Industry-Standard Regenerator Performance

The following analysis and calculations employs example data taken during the various tests and identifies an estimate of performance improvement that can be expected by replacing the present regenerator with an optimized industry-standard regenerator.

Actual Regenerative Heat Exchange Performance:

$$\begin{aligned} \text{Eff}_{\text{RHX actual}} &= 0.57 & \Delta P_{\text{RHX high press actual}} &= 1.0 \text{ psi} \\ & & \Delta P_{\text{RHX low press actual}} &= 0.70 \text{ psi} \end{aligned}$$

Optimized Industry-Standard Regenerator Performance:

$$\begin{aligned} \text{Eff}_{\text{RHX opt.}} &= 0.95 & \Delta P_{\text{RHX high press opt.}} &= 0.3 \text{ psi} \\ & & \Delta P_{\text{RHX low press opt.}} &= 0.30 \text{ psi} \end{aligned}$$

Other Component Efficiencies: (analysis employs these actual values)

$$\begin{aligned} \text{Eff}_{\text{HX}_1} &= 0.956 & \text{Eff}_{\text{HX}_2} &= 0.985 \\ \Delta P_{\text{HX}_1} &= 0.68 \text{ psi} & \Delta P_{\text{HX}_2} &= 0.55 \end{aligned}$$

Calculations: State Points

$$T_{\text{AMB}} = 125 \text{ F} = T_8$$

$$T_6 = T_2 - \text{Eff}_{\text{HX}_1} (T_2 - T_8) = 764 - .956 (764 - 585)$$

$$T_6' = 133\text{F} *$$

$$T_4 = 25\text{F} \text{ (measured 9/4/77)}$$

$$T_5' = T_4 - \text{Eff}_{\text{HX}_2} (T_4 - T_9) = 485 - 0.95 (485 - 550)$$

$$T_5' = 87\text{F}$$

$$T_3' = T_6 - \text{Eff}_{\text{RHX}} (T_6 - T_5) = 593 - .95(593 - 547)$$

$$T_3' = 89\text{F}$$

$$P_1 = 14.7 \text{ psia}$$

$$P_2' = 46.30 \text{ psia}$$

$$P_5' = 46.30 - .70 = 45.6 \text{ psia}$$

$$P_3' = 46.60 - .30 = 45.30 \text{ psia}$$

$$P_6' = 14.7 + .30 = 15.00 \text{ psia}$$

$$P_4' = 15.00 + .55 = 15.55 \text{ psia}$$

Net Polytropic Index:

$$n_e = \left[1 + \ln \left(\frac{T_4}{T_3} \right) / \ln \left(\frac{P_3}{P_4} \right) \right]^{-1}$$

*Where (') indicates "improved" values.

$$n_e = \left[1 + \ln \left(\frac{25+460}{109+460} \right) / \ln \left(\frac{45.3}{15.55} \right) \right]^{-1}$$

$$n_e = 1.1727$$

$$T_{4'} = T_{3'} \left(\frac{P_{4'}}{P_{3'}} \right)^{\frac{n_e - 1}{n_e}} = 549 \left(\frac{15.55}{45.30} \right)^{\frac{.1727}{1.1727}}$$

$$= 9^\circ\text{F}$$

$$T_{4'} = 9^\circ\text{F}$$

Thus the cooling capacity would increase by a factor of:

$$\frac{T_9 - T_{4'}}{T_9 - T_4} = \frac{90 - 9}{90 - 25} = 1.246$$

The additional work recovery due to the 0.7 psia loss recovery during expansion is:

$$\begin{aligned} \Delta W_{\text{rec exp}} &= \frac{n_e R T_{4'}}{n_e - 1} \left[\left(\frac{15.55 + .7}{15.55} \right)^{\frac{n_e - 1}{n_e}} - 1 \right] \\ &= \frac{1.1727}{.1727} (53.35) (469) \left(\left(\frac{16.25}{15.55} \right)^{.1473} - 1 \right) \\ &= 1108 \text{ ft-lb}_f \end{aligned}$$

The work recovered with the existing regenerator is:

$$W_{\text{exp}} = \frac{n_e R (T_4)}{n_e - 1} \left[\left(\frac{15.55}{45.30} \right)^{.1473} - 1 \right]$$

$$= 29088 \text{ ft-lb}_f$$

The energy recovery factor can now be calculated as:

$$= \frac{29088 + 1108}{29088} = 1.038$$

Of course, approximately the same magnitude of decrease in compressor work arises due to the decreased pressure loss through the regenerative heat exchanger.

The sum of these improvement factors totals about 32%. Thus the addition of an industry standard regenerator in the present 606 system could increase the coefficient of performance to:

$$\text{COP}' = 1.322 (.541) = .715$$

Thus, the simple substitution of a good quality regenerative heat exchanger into the existing ROVAC system would bring about a substantial performance improvement.

7.3.2 Calculation of System COP with Optimized Constant-Area High Pressure Porting and Industry Standard Heat Exchangers.

The measured pressure loss from compressor discharge to expander inlet has been determined through rotating pressure transducer measurements to be approximately 6.0 psi, accounting for the pressure loss in HX₁. As a result of port flow analysis it is expected that a constant-area/constant velocity high pressure port configuration will reduce this 6.0 psi loss to only a 1.5 psi loss. The following calculations estimate the improvement possible in system performance resulting from optimized port flow.

Increase in expander temperature drop

$$T_{4''} = T_3 \left(\frac{15.55}{45.3 + 4.5} \right)^{.1473}$$

$$T_{4''} = 2.5^\circ\text{F}$$

Thus, the cooling capacity will increase somewhat by the following factor:

$$\frac{T_9 - T_{4''}}{T_9 - T_4} = \frac{90 - 2.5}{90 - 25} = 1.346$$

This amounts to an increase of $\frac{1.346}{1.246} = 1.0802$

over the non-improved port machine employing an improved regenerator.

Increase in expander work recovery

$$\begin{aligned} \Delta W_{\text{ewc exp}} &= \frac{n_e RT_{4''}}{n_e - 1} \left[\left(\frac{15.55 + 4.5}{15.55} \right)^{.1473} - 1 \right] \\ &+ \frac{1.1727}{.1727} (53.35) (463) (.03815) = \\ \Delta W_{\text{rec exp}} &= 6399 \text{ ft-lb}_f \end{aligned}$$

This amounts to an energy recovery factor of

$$\frac{(29088 + 1108) + 6399}{(29088 + 1108)} = 1.212$$

Because the expander was chosen to derive sole benefit from the port improvement i.e.: the entire 4.5 psi recovery, no reduction in compressor work would occur. Thus, this improvement would yield nearly a 30% increase in performance. Specifically,

$$\text{COP}'' = 1.292(\text{COP}') = 1.292(.715)$$

$$\text{COP}'' = 0.924$$

7.3.3 Calculation of System COP with Optimized Heat Exchangers, High Pressure Porting, and Minimized Intra-Circulator Heat Flux.

One of the major effects of minimizing intra-circulator heat transfer is to push the dry air polytropic index of both the compression and expansion process towards the isentropic value (to dry air) of 1.4. For purposes of estimating the performance change due to minimizing the adverse heat flow, however, the polytropic index will be chosen to be 1.350 for both compression and expansion, thus indicating a small but not insignificant remaining element of heat transfer from the compressor and to the expander.

Increase in expander temperature drop

$$T_{4''} = T_{3'} \left(\frac{15.55}{49.80} \right)^{\frac{1.35-1}{1.35}} = 406^{\circ}\text{R}$$

$$T_{4''} = -53^{\circ}\text{F}$$

The cooling capacity will thus increase substantially by the following factor:

$$\frac{90 - (-53)}{90 - 25} = 2.20$$

This amounts to an increase over the improvements included so far of:

$$\frac{2.200}{1.346} = 1.635$$

This very significant factor clearly demonstrates the large performance adversity associated with intra-circulator heat transfer.

Change in Expander Work Recovery

$$W_{\text{exp}} = \frac{1.35(53.35)(549)}{1.35-1} \left\{ \left[\frac{15.55}{49.8} \right]^{.2572} - 1 \right\}$$
$$= 29228 \text{ ft-lb}_f$$

The expander work recovery of the unchanged Circulator or system was 29088 ft-lb_f. Thus only a negligible increase in net expander work would be brought about by decreasing the intra-Circulator heat transfer. This is accounted for by the compensating nature of the increased expander polytropic index and the reduction of port flow pressure loss.

Due to the fact that heat is transferred from the compressing gas principally after compression, no significant change in the compressor work integral would occur. Thus, the performance increase will be due almost entirely to the increase in cooling capacity. Therefore,

$$\text{COP}''' = (1.635) (\text{COP}'') = 1.635(.924)$$

$$\text{COP}''' = 1.51$$

Therefore it is clear that a coefficient of performance of unity or better can be achieved with improved Circulator hardware. Further, by employing an enriched moisture loop*, this performance could be even more substantially increased.

*See Appendix C.

Performance Testing Summary

The following Table 7.1 is a summary of the calorimeter performance testing of the ROVAC Model 606 air conditioning system. The Table was prepared from test data sheets. Information in the Table consists of the date and duration of the test, the compressor inlet pressure, the expander temperature differential and expander outlet temperature, and the Coefficient of Performance (COP) of the compressor-expander. Also included in the Table is a description of modifications and adjustments which were performed on the compressor-expander between tests.

TABLE 7.1
PERFORMANCE TEST LOG
 FOR ROVAC 606

DATE	TIME RUN HR/MIN	PCI	$\Delta T/TEO$	COP	COMMENTS
2/26/77	0/45	Opsig	63/41	N	{ Regenerator modified HX ₁ replaced after this test.
3/3/77	0/50		93/25	N	
3/4/77	0/42		89/28	N	Regenerator reworked to increase effectiveness
3/8/77	1/14	0	65/39	N	Regenerator reworked to decrease pressure drop
3/9/77	2/48	0	80/40	.476	[Run for Army Rep.]
3/10/77	2/0	5.0	82/30	.421	7 1/2 horsepower motor installed
4/9/77	1/30	0	84/25	.544	Rotor temp. observed on 4/9/77
4/10/77	0/20	5.0	85/23	N	
4/11/77	2/20	0	85/26	.459	

TABLE 7.1 (Continued)

DATE	TIME RUN HR/MIN	PCI	$\Delta T/TEO$	COP	COMMENTS
4/13/77	1/05	5.0psig	86/26	N	
4/13/77	1/20	10psig	83/26	0.432	
4/14/77	0/08	0	N	N	
4/14/77	2/33	0	92/19	0.460	
		0	69/39	0.490	
		5.0	73/37	0.482	
4/15/77	2/48	0	69/40	0.495	
4/16/77	1/45	5	74/35	0.488	
4/18/77	1/20	5	73/36	0.481	
4/21/77	1/15	0	68/41	0.525	
4/29/77	3/20	0	68/41	0.541	
					HX ₁ and Circulator removed from system insulation placed on inside of exp. outlet manifold and on comp. inlet hose. Cir. brackets cut in half. Insulation placed under bracket.

Table 7.1 (Continued)

DATE	TIME RUN HR/MIN	PCI	$\Delta T/TEO$	COP	COMMENT
					Circulator Disassembled and Checked. System Reassembled.
5/17/77	2/49	0	66/43	0.519	2 cups oil removed
	1/26	0	66/44	0.522	2 cups oil removed
	1/0	0	65/45	0.472	2 cups oil removed
5/27/77	3/38	≈ 11.3 psia PCD= 22 psia	62/47	0.526	First test with 7.5 HP calibrated motor
6/15/77	2/13/77	0	67/44	0.478	
6/16/77	2/0	0	86/44	0.474	Regenerator removed from system
7/6/77	1/43	0	96/38	0.358	Argon in system

APPENDIX A

INSTRUMENTATION, CALIBRATION, CERTIFICATION

This Appendix contains information and calibration data on all instrumentation used during the calorimeter tests.



INDUSTRIAL VALVE & INSTRUMENT DIVISION NEWTOWN, CONNECTICUT 08470
HEISE PLANT TEL. 203-488-4408 TWX: 710-487-0817

CERTIFICATION REPORT

of
HEISE GAUGE No. CM-18150

This gauge has been calibrated with a piston gauge which has been compared with master piston gauges whose effective areas were determined with an estimated accuracy of 3 parts in 100,000 by the National Bureau of Standards Identification No. P6744 and No. P6745. The weights for these dead weight piston gauges have also been certified by the Bureau of Standards to have an average accuracy of within one part in 35,000.

READING NUMBER	DEAD WEIGHT OR Hg COL. READING	GAUGE READING (Deviation from Dead Wt. or Hg Col.)
1	7.5 psi	-
2	15.0	-
3	22.5	-
4	30.0	-
5	37.5	-
6	45.0	-
7	52.5	-
8	60.0	-
9	67.5	-
10	75.0	-
11	82.5	-
12	90.0	-
13	97.5	-
14	105.0	-
15	112.5	-
16	120.0	-
17	127.5	-
18	135.0	-
19	142.5	-
20	150.0 psi	-

Room Temperature at Test 70°

Maximum Hysteresis .15 psi

Remarks: Caution: all indicated where error is .15 psi or more.

Date Tested July 10 1976

Signed A. K. Arndt



INDUSTRIAL VALVE & INSTRUMENT DIVISION NEWTOWN, CONNECTICUT 06470
 HEISE PLANT TEL. 203-488-4408 TWX: 710-487-0817

CERTIFICATION REPORT

of
HEISE GAUGE No. *271-18149*

This gauge has been calibrated with a piston gauge which has been compared with master piston gauges whose effective areas were determined with an estimated accuracy of 3 parts in 100,000 by the National Bureau of Standards Identification No. P6744 and No. P6745. The weights for these dead weight piston gauges have also been certified by the Bureau of Standards to have an average accuracy of within one part in 35,000.

READING NUMBER	DEAD WEIGHT OR Hg COL. READING	GAUGE READING (Deduction from Dead Wt. or Hg Col.)
1	3.75 <i>psi</i>	-
2	7.50 <i>psi</i>	-
3	11.25	-
4	15.00	-
5	18.75	-
6	22.50	-
7	26.25	-
8	30.00	-
9	33.75	-
10	37.50	-
11	41.25	-
12	45.00	-
13	48.75	-
14	52.50	-
15	56.25	-
16	60.00	-
17	63.75	-
18	67.50	-
19	71.25	-
20	75.00 <i>psi</i>	-

Room Temperature at Test *70° F*

Maximum Hysteresis *0.75 psi*

Remarks: *Corrections are indicated when error is 0.75 psi or more*

Date Tested *July 16, 1976*

Signed *A. K. Arnet*

I.C.P. TRANSDUCER DATA

**P
C
B** **PIEZOTRONICS INC.**

P. O. BOX 33

BUFFALO, NEW YORK 14225

Model # 112A24

Cal. Range 0-100

Input Time Constant 2 Sec

S/N 1213

Rise Time 2 μ Sec

Average Sensitivity* 47.5 mv/psi

Natural Frequency 250 KHz

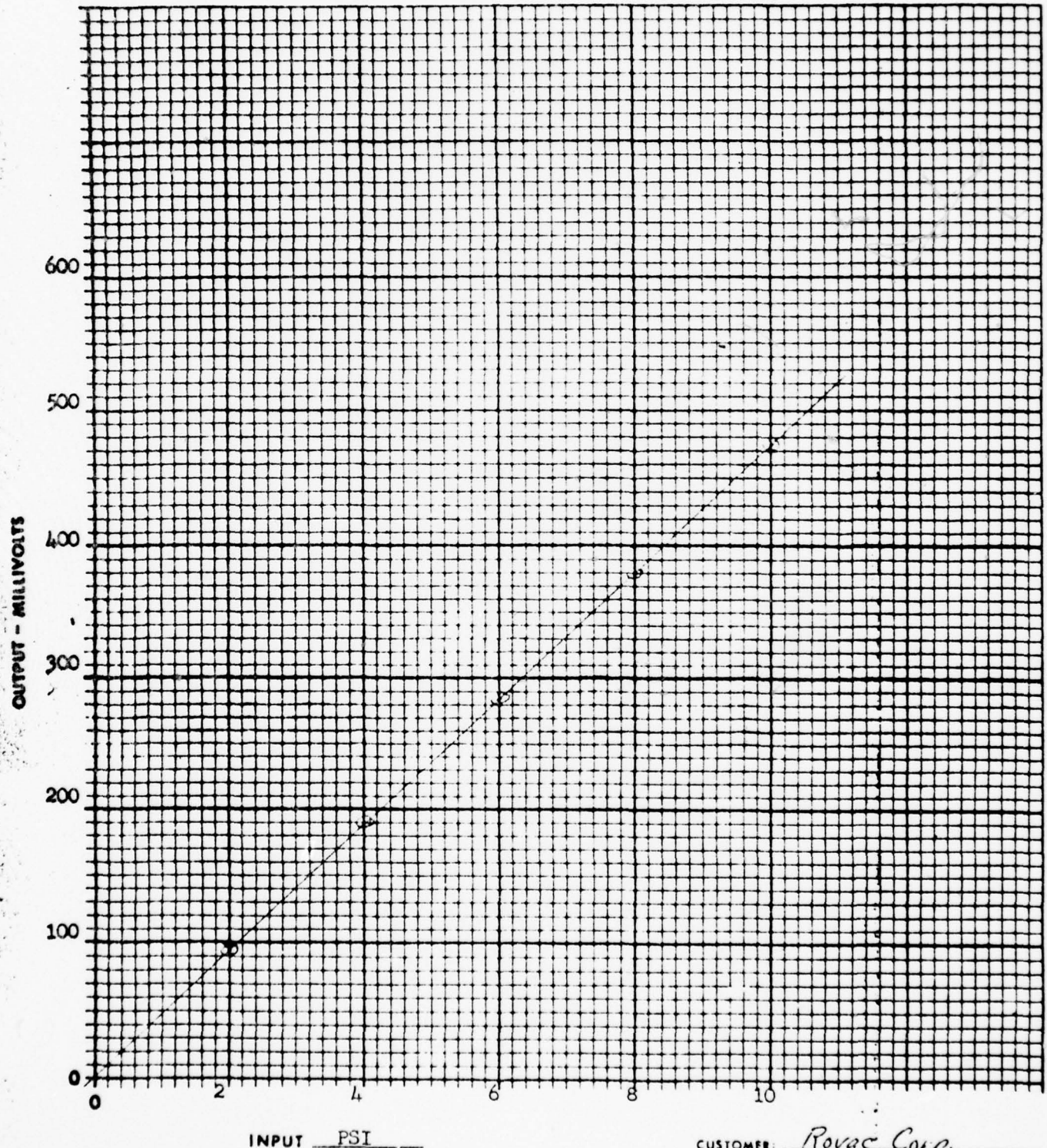
Linearity ± 1.0 % F.S.

Output Impedance <100 Ohms

By T. C. [Signature]

Date 8-8-55

*By comparison with reference Standard per ISA S37.10



CUSTOMER: Rovac Corp.
P.O. NO. 10311

I.C.P. TRANSDUCER DATA

P
C
B
PIEZOTRONICS INC.

P. O. BOX 33

BUFFALO, NEW YORK 14225

Model # 12A21

Cal. Range _____

Input Time Constant _____ Sec

S/N 1213

Rise Time _____ μ Sec

Average Sensitivity* 47.6 mV/psi

Natural Frequency 250 KHz

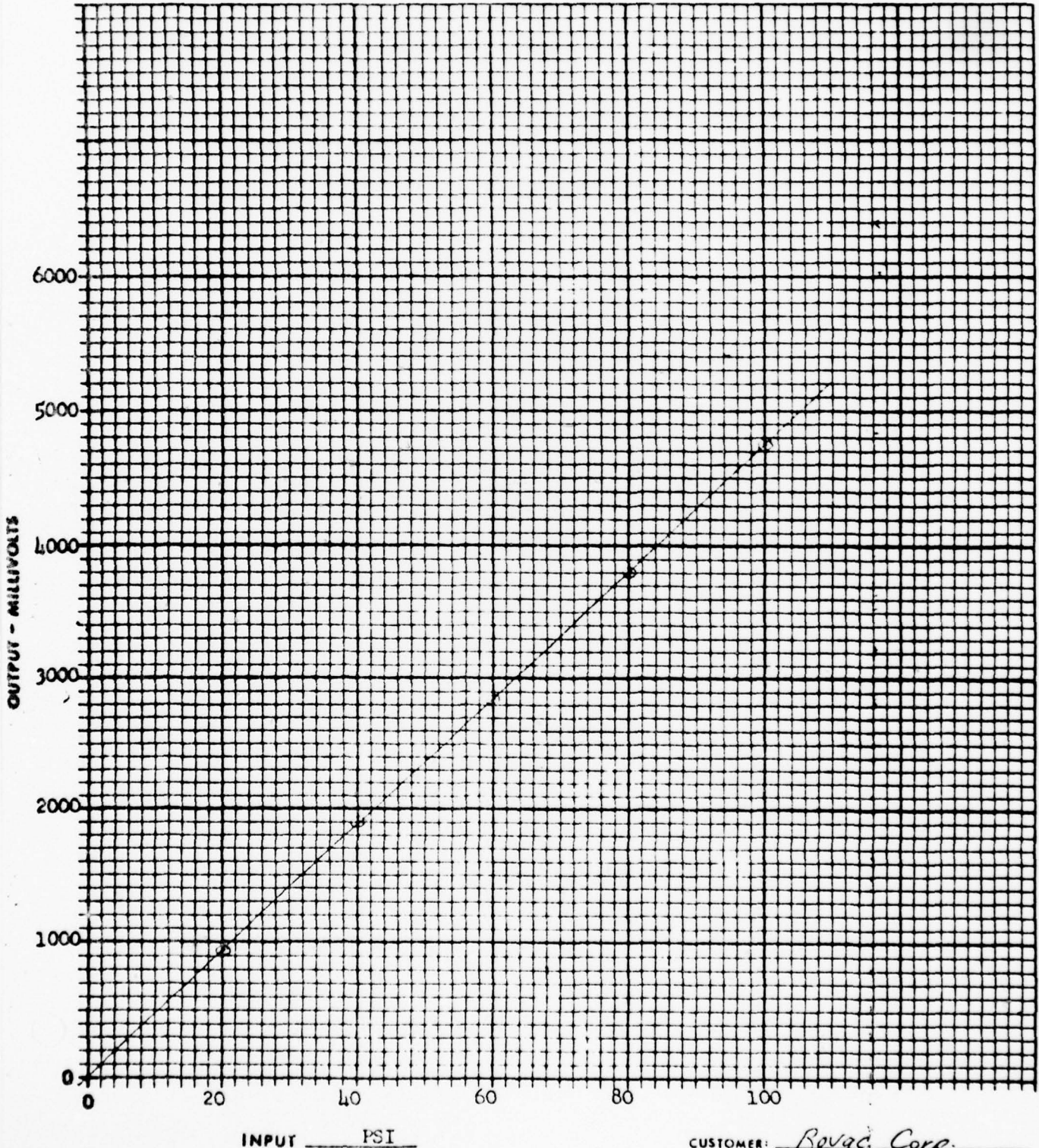
Linearity ±10 % F.S.

Output Impedance _____ <100 Ohms

By T. C. [Signature]

Date 4-27-68

*By comparison with reference Standard per ISA 537.10



CUSTOMER: Bovac Corp.
P.O. NO. 10311

Precision Quality (ASTM TYPE)

These precision thermometers are supplied with white and/or gold backs as indicated. They are designed to meet specifications on graduations and engravings, bulb material, permanency of pigment and others as established by ASTM.

It is recommended that thermometers calibrated for total immersion be used wherever possible. When this cannot be done for various reasons, thermometers calibrated for partial immersion may be selected, or total immersion thermometers may be used with a correction factor.

PRECISION QUALITY THERMOMETERS

Wherever specifications of authoritative bodies are quoted, such as ASTM, the thermometers so listed are checked with master gages for all dimension specifications—in addition to the accuracy test requirements. Permanent SURFMARK or PERMACOLOR graduations and numerals give lifetime readability. All are mercury-filled. They have ring top and are calibrated for total immersion, unless otherwise specified.

Use or Description	Range Limits		Small Divis.	Therm. Length	Cat. No.	Special Notes
	Lower	Upper				
General Testing	-30°F	120°F	1/5°	18"	21020	Furnished in individual felt-lined black oxidized brass case.
General Testing	30°F	120°F	1/10°	21"	21028	
General Testing	30°F	215°F	1/5°	24"	21032	
Bomb-type Fuel Calorimeter	18°C	28°C	1/100°	24"	21510	
Bomb-type Fuel Calorimeter	18°C	30°C	1/50°	18"	21512	

The thermometers in the following table are mercury-filled with a gas-filled capillary above the liquid column. Also, with some exceptions, they have a round top and a stem diameter of 6-7 mm.

ASTM No.	Taylor Cat. Number		Use or Description	Range Limits		Small Div. (in deg.)	Thermometer Length (mm)	Immersion Length (mm)	Special Notes
	White Back	Gold Back		Lower (above zero unless indicated)	Upper				
1G-63		• 21350G	General Test	-20°C	150°C	1	322	76	G-1 } Manufacturing Chemists Association
1F-63		• 21351G		0°F	302°F	2	322	76	
2G-63		• 21351G		-5°C	300°C	1	390	76	
2F-63		• 21355G		20°F	580°F	2	390	76	
3G-63		• 21358G		5°C	400°C	1	413	76	
3F-63		• 21359G		20°F	760°F	2	413	76	
5G-62		21621G	Cloud and Pour	38°C	50°C	1	231	108	(+; 7.8mm)
5F-62		21620G		36°F	120°F	2	231	108	(+; 7.8mm)
6G-62	21625		Low Cloud and Pour	-80°C	20°C	1	232	76	(+; a; 7.8mm)
6F-62	21624			-112°F	70°F	2	232	76	(+; a; 7.8mm)
7G-62		• 21635G	Low Distillation	2°C	300°C	1	386	total	
7F-62		• 21634G		30°F	580°F	2	386	total	
8G-62		21641G	High Distillation	-2°C	400°C	1	386	total	
8F-62		21640G		30°F	760°F	2	386	total	
9G-62		21661G	Flash and Fire; Pensky-Martens.	5°C	110°C	1/2	287	57	(d)
9F-62		• 21660G	Low Range and Tag Closed Tester.	20°F	230°F	1	287	57	(d)
10G-62		• 21663G	Flash and Fire; Pensky-Martens.	90°C	370°C	2	287	57	(d)
10F-62		• 21662G		High Range	200°F	700°F	5	287	57
11G-62		21681G	Flash and Fire.	6°C	400°C	2	308	25	
11F-62		21680G	Cleveland Open Tester.	20°F	760°F	5	308	25	
12G-62		21717G	Gravity	20°C	102°C	1/5	420	total	(7.8mm)
12F-62		21716G		5°C	215°C	1/2	420	total	(7.8mm)

PERMARK pigment

(a) Filled with red PERMACOLOR liquid

(d) Brass Ferrule furnished at extra cost. Specify No. 50S1 Brass Ferrule.



Design and Construction Features

HEISE CLEAN BOURDON TUBE

The most highly developed pressure sensing element in the industry. The first to lend itself to certain and positive cleaning.

EXTERNAL BLEEDER

An integral part of the Bourdon tube. The most effective and convenient means of evacuation or purging.

SOLID FRONT

A solid wall of cast aluminum protects the operator when working with high pressure systems.

INTEGRAL MOVEMENT

A basic concept in unified instrument design.

BALL BEARING PINION SHAFT

Minimizes friction and improves sensitivity.

MICRO SLIDE ADJUSTMENT

A revolutionary development in calibration methods.

THERMAL COMPENSATOR

Holds the gauge in calibration through ambient temperature changes from -25°F to $+125^{\circ}\text{F}$. (optional)

EXTERNAL DIAL ZERO ADJUSTMENT

A convenient means of pre-setting the dial to a bench mark or "tare".

DIAL

Individually engraved to the pressure gradient of its own gauge mechanism. Mirror scales are standard.

POINTER

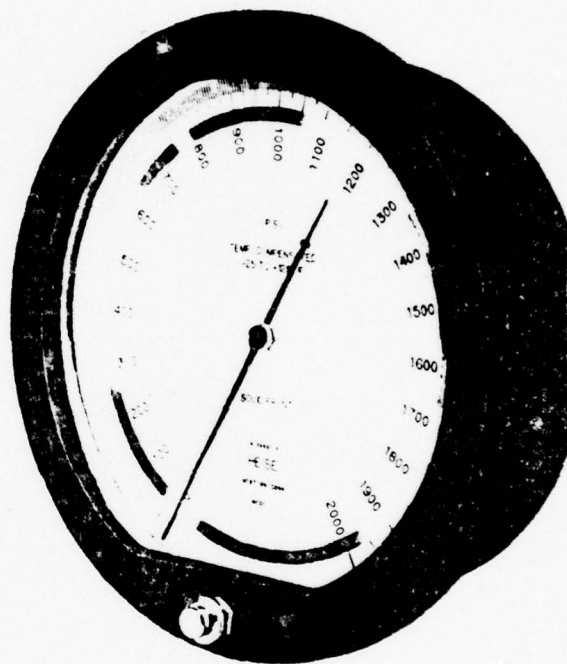
"Gun sight" design eliminates parallax.

CONCENTRIC DIAL MOUNTING

Maintains concentricity of the pointer shaft and dial.

ULTRA HIGH PRESSURE TUBES

The development of precision gauges for the ultra high pressure ranges (above 30,000 psi) was pioneered by Heise laboratories who continue to lead the field in this area.



HEAT TREATMENT

Optimum physical properties in Bourdon tube materials is achieved at Heise laboratories by high vacuum heat treating methods which permit exposure to critical temperatures without oxidation.

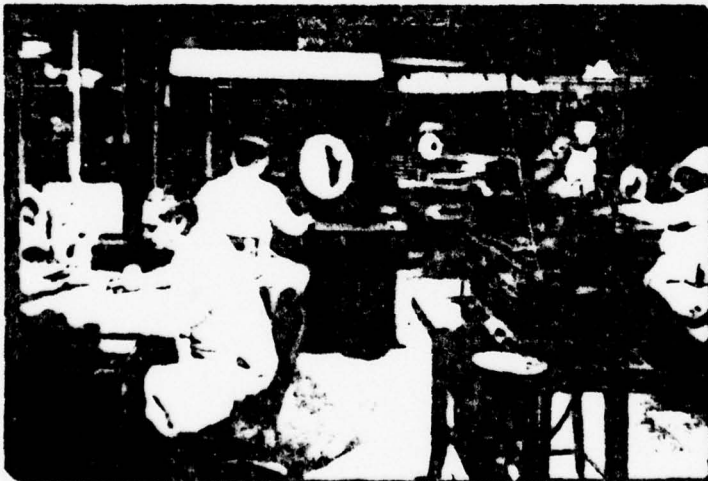
HEISE GAUGES

The Model "C" Gauge is the latest Heise instrument and features a clean tube, a solid front safety case, and many other advances.

As always, Heise laboratories leads the industry in the development of new and better instruments for pressure measurement.

The performance record of the Heise Gauge, unparalleled by any other gauge in the field, qualifies this instrument for the most exacting applications in modern industry and research.

Superior quality takes precedence over production expediency at Heise laboratories where highly skilled technicians give their personal attention to each phase of fabrication, assembly and inspection. Detailed permanent records contain the complete history of each gauge including calibration data and test results.



Research and development projects, continuously probing into the ever expanding field of ultra high pressure testing, add daily to the wealth of knowledge and experience which stands behind the Heise gauge. Specialization in the test gauge field has led to world wide recognition of the Heise name as a guarantee of rugged, dependable and precise instrumentation.

Each instrument is an individual example of superb Heise workmanship.

Specifications Model "C"

ACCURACY

All Heise gauges are accurate to 0.1% of full scale reading throughout the entire 300° dial.

HYSTERESIS

Not greater than 0.1% of full scale reading after application of maximum scale pressure.

GAUGE TYPES (See description on page 12)

P.S.I.
Absolute
Vacuum
Compound

PRESSURE RANGES

From 0-12 psi to 0-30,000 psi.

DIAL SIZES

8½" — 12" — 16" for pressure ranges from 0-12 psi to 0-30,000 psi.

TUBE MATERIALS

Bourdon tubes are available in the following materials:

403 Stainless Steel
Beryllium Copper — for low pressure and for specific purposes up to 20,000 psi.
316 Stainless Steel. In ranges up to 5,000 psi maximum. When used, hysteresis will be three to five times greater than the 0.1% of full scale.

THERMAL STABILITY

The Heise Automatic Thermal Compensator holds precise calibration through ambient temperature variations from -25°F to +125°F. (See Optional Features, pages 12 & 13)

REPEATABILITY

1 Part in 5,000.

READABILITY

An individually engraved dial, an anti-parallax gunsight pointer, and a mirror scale make the Heise gauge the most readable instrument available.

CERTIFICATION

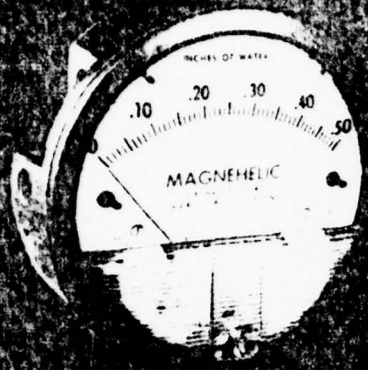
Each Heise gauge is critically tested before shipment and a certified copy of the test results is supplied with the gauge.



SERIES 2000

Magnehelic® Differential Pressure Gages

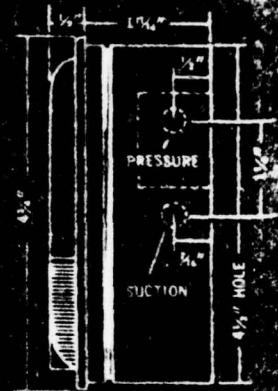
BEST AVAILABLE COPY



Standard Magnehelic® Pressure Gage has a large, easy-to-read 4" dial.



Dimensions, standard Series 2000 Magnehelic® Pressure Gages.



Select the Dwyer Magnehelic® gage for high accuracy — guaranteed within 2% of full scale — and for the wide choice of 61 ranges available to suit your needs precisely. Using Dwyer's simple, frictionless Magnehelic® movement, it quickly indicates low air or non-corrosive gas pressures — either positive, negative (vacuum) or differential. The design resists shock, vibration and over-pressures. No manometer fluid to evaporate, freeze or cause toxic or leveling problems. It's inexpensive, too.

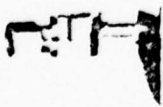
Widely used to measure fan and blower pressures, filter resistance, air velocity, furnace draft, pressure drop across orifice plates, liquid levels with bubbler systems and pressures in fluid amplifier or fluidic systems. It also checks gas-air ratio controls and automatic valves, and monitors blood and respiratory pressures in medical care equipment.

Mounting. A single case size is used for all 61 ranges of Series 2000 Magnehelic gages. They can be flush or surface mounted. Two sets of pressure taps permit either side or back connections. The gages operate in any position and may even be mounted upside down if desired. These characteristics make Magnehelic gages ideal for both stationary and portable applications. Requires 4 1/2" hole in panel for flush mounting. Mounting and connection fittings, plus complete instructions, are furnished with the instrument.



Flush or Surface Mounted

Vent valves



In applications where pressure is continuous and the Magnehelic gage is connected by metal or plastic tubing which cannot be easily removed, we suggest using Dwyer A-371 vent valves to connect gage. Pressure can then be removed to check or re-zero the gage.

HIGH AND MEDIUM PRESSURE MODELS



Mount and install same as standard gage, except requires larger 4 1/4" dia. hole in panel for flush mounting. Will not fit into portable carrying case. High pressure construction to withstand total internal pressures to 100 psig; or medium pressure construction to withstand 35 psig on one or both sides of diaphragm is available in all standard ranges. Weight of the gage is 1 lb. 10 oz. Other specifications same as standard models shown at right above.

PHYSICAL DATA

- Ambient temperature range:** 30° to 140°F.*
- Rated total pressure:** Sustained or highly repetitive pressure: 15 psig.†
- Connections:** 1/8" NPT high and low pressure taps, duplicated — one pair side and one pair on back.
- Housing:** Die cast aluminum. Case and aluminum parts Inidite-dipped to withstand 168 hour salt spray test. Exterior finish is baked dark gray hammerloid.
- Standard ranges:** See facing page.
- Accuracy:** Plus or minus 2% of full scale (3% on -0 and 4% on -00 ranges), throughout range at 70°F.
- Standard accessories:** Two 1/8" NPT plugs for duplicate pressure taps, two 1/4" pipe thread to rubber tubing adapters, back mounting spud with washers and jam nut, three flush mounting adapters with screws (Mounting ring and snap ring retainer substituted for 3 adapters in HP gage accessories).
- Weight:** 1 lb. 2 oz.

*Low temperature models available as special option. †High pressure model available. See left column below.

OPTIONS AND ACCESSORIES

Transparent overlays

Furnished in red and green to highlight and emphasize critical pressures.

Adjustable signal flag

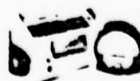
Integral with plastic gage cover, has external reset screw. Available for all ranges (not high pressure). Can be ordered with gage or separately.

Portable units

Combine carrying case with any Magnehelic gage of standard range (not high pressure). Includes 9 ft. of 1/4" I.D. rubber tubing and pipe thread to rubber tubing adapters.

Air filter gage accessory package

Adapts any standard Magnehelic for use as an air filter gage. Includes aluminum surface-mounting bracket with screws, two 5 ft. lengths of 1/4" aluminum tubing, two static pressure taps and two molded plastic vent valves, integral compression fittings on both tips and valves.



BEST AVAILABLE COPY

Quality design and construction features

Bezel provides flange for flush mounting in panel.

Clear plastic face is highly resistant to breakage. Provides undistorted viewing of pointer and scale.

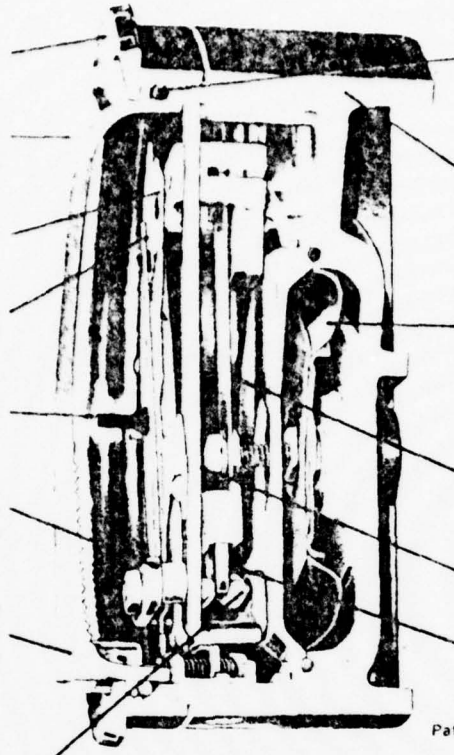
Precision litho printed scale is accurate and easy to read.

Red tipped pointer of heat treated aluminum tubing is easy to see. It is rigidly mounted on helix shaft.

Pointer stops of molded rubber prevent pointer over travel without damage.

Sapphire bearings are shock resistant mounted; provide virtually friction-free motion for helix. Motion damped with high viscosity silicone fluid.

Zero adjustment screw is conveniently located in plastic cover, accessible without removing cover. "O" ring seal provides pressure tightness.



"O" ring seal for cover assures pressure integrity of case.

Die cast aluminum case is precision made. Iridite-dipped to withstand 168 hour salt spray test. Exterior finished in baked dark gray hammerhead. One case size used for all standard pressure ranges, and for both surface and flush mounting.

Silicone rubber diaphragm with integrally molded "O" ring is supported by front and rear plates. It is locked and sealed in position with a sealing plate and retaining ring. Diaphragm motion is restricted to prevent damage due to overpressures.

Calibrated range spring is a flat leaf of Swedish spring steel in temperature compensated design. Small amplitude of motion assures consistency and long life. It reacts to pressure on diaphragm. Live length adjustable for calibration.

"Wishbone" assembly provides mounting for helix, helix bearings and pointer shaft.

Alnico V magnet mounted at end of range spring actuates helix without mechanical linkages.

Patent No. 3,091,123

Helix is precision milled from an alloy of high magnetic permeability, deburred and annealed in a hydrogen atmosphere for best magnetic qualities.

Mounted in jeweled bearings, it turns freely to align with magnetic field of magnet to transmit pressure indication to pointer.

SERIES 2000 MAGNEHELIC® — MODELS AND RANGES

The models below will fulfill most requirements. Page 5 also shows examples of special models built for OEM customers. For special scales furnished in ounces per square inch, inches of mercury, metric units, etc., contact the factory.

Model Number	Range, Inches of Water	Minor Div.	Model Number	Range, Zero Center, Inches of Water	Minor Div.	Dual Scale Air Velocity Units*			Model Number	Range, Metric Scales, CM of Water	Minor Div.	Model Number	Range, Zero Center, Metric, CM of Water	Minor Div.
						Model Number	Range, Inches of Water	Range, Air Velocity, F.P.M.						
2000-00	0-.25	.005	2301	.50-.5	.02	2000-00AV	0-.25	300-2000	2000-1	0-1	.02	2300-4	2-0.2	.02
2000-0	0-.50	.01	2302	1-0-1	.05	2000-00AV	0-.50	500-2800	2000-2	0-2	.05	2300-10	5-0.5	.05
2001	0-1.0	.02	2304	2-0-2	.10	2001-AV	0-1.0	500-4000	2000-5	0-5	.10	2300-20	10-0-10	.10
2002	0-2.0	.05	2310	5-0-5	.20	2002-AV	0-2.0	1000-5600	2000-10	0-10	.20	2300-30	15-0-15	.20
2003	0-3.0	.10	2320	10-0-10	.50	2010-AV	0-10	2000-12500	2000-15	0-10	.5			
2004	0-4.0	.10	2330	15-0-15	1.0				2000-20	0-20	.5			
2005	0-5.0	.10							2000-30	0-30	1.0			
2006	0-6.0	.20							2000-50	0-50	1.0			
2008	0-8.0	.20							2000-80	0-80	2.0			
2010	0-10	.20							2000-100	0-100	2.0			
2015	0-15	.50							2000-150	0-150	5.0			
2020	0-20	.50							2000-200	0-200	5.0			
2025	0-25	.50							2000-250	0-250	5.0			
2030	0-30	1.0							2000-300	0-300	10.0			
2040	0-40	1.0												
2050	0-50	1.0												
2060	0-60	2.0												
2080	0-80	2.0												
2100	0-100	2.0												
2150	0-150	5.0												

*For use with pitot tube.

Special Purpose Ranges	
Scale No. 2401	Scale No. 2402
Square Root	Blank Scale
Specify Range	Specify Range

Suggested Specifications

A differential pressure gage for measuring (state purpose) shall be installed. Gage shall be the diaphragm-actuated dial type 4 1/4" O.D., with white dial, black figures and graduations and pointer zero adjustment. Gage shall be Dwyer Instruments, Inc., Magnehelic®, Catalog No. _____ reading to _____" water column, in _____ divisions.

Model Number	Range, F.P.S.	Minor Div.
2201	0-1	.02
2202	0-2	.05
2203	0-5	.10
2204	0-10	.20
2205	0-20	.5
2210*	0-10	.5
2215*	0-15	.5
2220*	0-20	.5

*These ranges equipped as Medium Pressure Models (see Options).

HOSICA LABORATORIES

CALIBRATION DATA SHEET SINGAC, NEW JERSEY

CUSTOMER **THE BOVAC CORPORATION** DESCRIPTION **WATTMETER**
ORDER No. **10480** DATE **9/2/76**
MAKER **WESTON** MODEL **432** No. **18791**
RANGES **0-.75-1.5 KILOWATTS** SHEET **1** OF **1**

SCALE MARKING	METER INDICATION	TRUE VALUE	CORRECTION	REMARKS
				Temp. ° C
0	0	0	0	21°C
.1	.1	.1	0	
.2	.2	.2	0	
.3	.3	.3	0	
.4	.4	.4	0	
.5	.5	.5	0	
.6	.6	.6	0	
.7	.7	.7	0	
.8	.8	.8	0	
.9	.9	.9	0	
1.0	1.0	1.0	0	
1.1	1.1	1.1	0	
1.2	1.204	1.2	-0.004	
1.3	1.302	1.3	-0.002	
1.4	1.4	1.4	0	
1.5	1.5	1.5	0	
.75	.75	.75	0	

N.B.S. No. **FE-0032Z** MIL-C-45662A CERTIFIED BY *Ted Stultz*

HOSICA LABORATORIES

CALIBRATION DATA SHEET

SINGAC, NEW JERSEY

CUSTOMER THE ROVAC CORPORATION DESCRIPTION WATTMETER
 ORDER No. 10480 DATE 9/2/76
 MAKER WESTON MODEL 905 No. 1076
 RANGES 0-1.5-3-6 KILOWATTS SHEET 1 OF 1

SCALE MARKING	METER INDICATION	TRUE VALUE	CORRECTION	REMARKS
				Temp. ° C
0	0	0	0	21° C
.1	.1	.1	0	
.2	.198	.2	.002	
.3	.298	.3	.002	
.4	.4	.4	0	
.5	.499	.5	.001	
.6	.6	.6	0	
.7	.7	.7	0	
.8	.8	.8	0	
.9	.9	.9	0	
1.0	1.0	1.0	0	
1.1	1.1	1.1	0	
1.2	1.2	1.2	0	
1.3	1.3	1.3	0	
1.4	1.4	1.4	0	
1.5	1.5	1.5	0	
3	3	3	0	
6	6	6	0	

N.B.S. No. #2-00322 NPL-C-45662A CERTIFIED BY Jed. Stultz

HOSICA LABORATORIES

CALIBRATION DATA SHEET SINGAC, NEW JERSEY

CUSTOMER **THE BOVAC CORPORATION** DESCRIPTION **WATTMETER**
ORDER No. **10400** DATE **9/2/76**
MAKER **WESTON** MODEL **432** No. **14315**
RANGES **0-7.5-15 KILOWATTS** SHEET **1** OF **1**

SCALE MARKING	METER INDICATION	TRUE VALUE	CORRECTION	REMARKS
				Temp. ° C
0	0	0	0	21°C
1	1	1	0	
2	2	2	0	
3	2.99	3	+0.01	
4	4	4	0	
5	5	5	0	
6	6	6	0	
7	7	7	0	
8	8	8	0	
9	9	9	0	
10	10	10	0	
11	11	11	0	
12	12	12	0	
13	12.99	13	+0.01	
14	13.98	14	+0.02	
15	14.98	15	+0.02	
7.5	7.49	7.5	+0.01	

T. H. H.

HOSICA LABORATORIES

Singac, New Jersey

CERTIFICATE OF CALIBRATION

Manufacturer **GENERAL ELECTRIC** Model **P-3** Serial **1096850**
Description **0-40-80 HECTOWATT METER** Accuracy **1/2%**

The specified accuracy of the above instrument has been confirmed by comparison to periodically certified reference standards traceable to the National Bureau of Standards and are maintained in our laboratories.

REFERENCE STANDARD

Manufacturer	R.F.L.	Date Certified	4/18/76
Model	829	Serial	86
Certificate No.	4075-5	Date Certified	9/2/76
Ambient Temp.	21 C	Certified By	<i>[Signature]</i>

N.B.S.#E-0032Z MIL-C-45662A

HOSICA LABORATORIES

Singac, New Jersey

CERTIFICATE OF CALIBRATION

Manufacturer **WESTON** Model **432** Serial **8655**
Description **0-3-6 KILOWATT METER** Accuracy **1/2%**

The specified accuracy of the above instrument has been confirmed by comparison to periodically certified reference standards traceable to the National Bureau of Standards and are maintained in our laboratories.

REFERENCE STANDARD

Manufacturer	R. F. L.	Date Certified	4/18/76
Model	829	Serial	86
Certificate No.	4075-4	Date Certified	9/2/76
Ambient Temp.	21°C	Certified By	<i>[Signature]</i>

M. B. S. #B-00322 MIL-C-45662A

HOSICA LABORATORIES

Singac, New Jersey

CERTIFICATE OF CALIBRATION

Manufacturer **WESTON** Model **905** Serial **1076**
Description **0-1.5-3-6 KILOWATTMETER** Accuracy **1/2%**

The specified accuracy of the above instrument has been confirmed by comparison to periodically certified reference standards traceable to the National Bureau of Standards and are maintained in our laboratories.

REFERENCE STANDARD

Manufacturer **R.F.L.** Date Certified **4/18/76**
Model **829** Serial **86**
Certificate No. **4075-1** Date Certified **9/2/76**
Ambient Temp. **21 C** Certified By *[Signature]*
N.B.S.#E-00322 MIL-C-45662A

HOSICA LABORATORIES

Singac, New Jersey

CERTIFICATE OF CALIBRATION

Manufacturer **WESTON** Model **432** Serial **14315**
Description **0-7.5-15 KILOWATT METER** Accuracy **1/2%**

The specified accuracy of the above instrument has been confirmed by comparison to periodically certified reference standards traceable to the National Bureau of Standards and are maintained in our laboratories.

REFERENCE STANDARD

Manufacturer	R.F.L.	Date Certified	8/18/76
Model	829	Serial	86
Certificate No.	4075-2	Date Certified	9/2/76
Ambient Temp.	21° C	Certified By	<i>[Signature]</i>

N.B.S. #E-00322 ML-C-45662A

HOSICA LABORATORIES

Singac, New Jersey

CERTIFICATE OF CALIBRATION

Manufacturer **WESTON** Model **432** Serial **16791**
Description **0-.75-1.5 KILOWATT METER** Accuracy **1/2%**

The specified accuracy of the above instrument has been confirmed by comparison to periodically certified reference standards traceable to the National Bureau of Standards and are maintained in our laboratories.

REFERENCE STANDARD

Manufacturer **R.F.L.** Date Certified **4/18/76**
Model **829** Serial **86**
Certificate No. **4075-3** Date Certified **9/2/76**
Ambient Temp. **21°C** Certified By *[Signature]*

N.B.S. #1-00322 MTL-C-45662A

TEMPERATURE LAST 24 HOURS

75 ° MAX 58 ° MIN

September 15, 1976

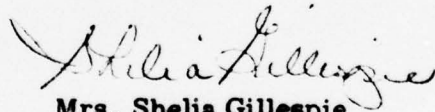
Mr. Walt Sanders
Rovac Corporation
100 Rovac Parkway
Rockledge, FL 32955

Dear Mr. Sanders:

Confirming our phone conversation, our part No. 21028 laboratory thermometer is accurate to 1/10 degree Fahrenheit and is traceable to the National Bureau of Standards.

Feel free to contact us if we may be of further assistance.

Sincerely,



Mrs. Shelia Gillespie
Marketing Specialist

SG/ska

APPENDIX B

TEST DATA

This Appendix contains the test data sheets taken during calorimeter testing.

TEST DATA

DATE: 7/6/77 TIME: 10:53

SYSTEM: COC System ~~PA. 1000~~ TYPE OF TEST: Cal

TEST FACILITY: Cal 7014

OBSERVERS: R.R.J.

COMMENTS: T10 = data furnished [Argon gas as refigerant] judged with Argon

DATA ITEMS:

	10:53	11:06	11:20	11:45	12:00	12:15	12:30	1
TIME	10:53	11:06	11:20	11:45	12:00	12:15	12:30	1
DP2		1.2	1.3	1.4	1.4			
DP5		4.1	4.1	4.1	4.1			
P1		0	0	0	0	0	0	
P2		35	35.0	35.0	35.0	35.0	35.0	
P3		34.0	34.1	34.1	34.1	34.1	34.1	
P4								
P5		34.3	34.2	34.2	34.2	34.1	34.1	
P6								
PAME								
TAMB	77	78	80	80	77	82	82	
T1	87	94	75	76	96	96	96	
T2	220	340	339	342	343	342	343	
T3	27	112	127	120	132	133	134	
T4	5	33	33	35	37	37	38	
T5	94	93	94	94	94	94	94	
T6	92	114	127	129	131	132	133	
T7	82	84	84	85	85	85	86	
T8	92	107	119	122	123	124	125	
T9	95	95	95	95	95	95	95	
T10	97	112	124	127	128	130	130	
T11	77	78	80	81	82	83	83	
T12	77	78	80	81	82	83	83	
T13	90.7	90.2	90.4	90.7	90.6	90.6	90.8	
T14	62.3	66.7	67.1	67.8	68.1	68.3	68.5	
W1	1.63	1.54	1.58	1.54	1.51	1.51	1.55	
W2	2.28	3.73	3.65	3.6	3.61	3.61	3.61	
W3	1.8	1.6	1.57	1.45	1.35	1.35	1.34	
W4	1.26	.26	.26	.26	.26	.26	.26	
TIME ON	10:53							
TIME OFF							12:36	

BEST AVAILABLE COPY

DATE: 3/10/11 10:52

TYPE OF TEST: Calorimeter TEST FACILITY: Calorimeter

SYSTEM: 606 Army

OBSERVERS: W.P.S. J.C.

REMARKS:

1st trace 3rd trace 4/12/11 11:00

DATA ITEMS:

TIME	12:57	1:52	11:10	11:26	11:47	12:00	12:15	12:30	12:45	1:00
DR2	0	0	0	0	0	0	0	0	0	0
DR5	0	0	0	0	0	0	0	0	0	0
P1	0	0	0	0	0	0	0	0	0	0
P2	0	39.2	33.4	48.1	46.6	46.0	45.5	45.2	46.0	45.6
P3	0	32.5	32	32	45.0	44.3	43.8	44.1	45.3	44.2
P4	0	1.8	1.2	8.7	6.5	6.8	6.1	6.5	6.6	6.4
P5	0	33.8	32.7	48.8	43.9	45.1	44.7	45.0	45.8	45.3
P6	0	1.6	1.5	7.3	5.4	5.3	5.1	5.25	5.6	5.3
PAMB	72	72	72	75	74	74.2	74	74.5	76	76
T1	76	25	112	112	115	120	117	118	119	119
T2	76	248	295	295	292	299	297	297	294	294
T3	72	29	108	108	110	113	110	111	108	112
T4	71	-0	17	17	22	29	28	29	27	30
T5	82	102	96	96	92	96	92	94	94	95
T6	74	84	122	122	128	135	133	127	132	138
T7	102	91	87	87	82	87	84	85	85	86
T8	78	86	129	129	124	128	124	127	125	127
T9	105	103	96	96	98	97	93	95	96	96
T10	72	92	172	172	250	295	312	323	326	328
T11	72	70	72	72	76	76	76	76	78	78
T12	70	70	72	72	74	74	74	74	75	75
T13	79	79	91.9	91.9	93.5	92.5	89	90.7	90.5	91
T14	71	71	67.4	67.4	70.4	69	67.3	68.1	68	68.5
W1	0	1.37	1.35	2.3	2.8	2.18	2.23	2.25	2.28	2.20
W2	0	3.16	3.08	3.42	3.96	3.94	3.90	3.92	3.94	3.90
W3	1.5	1.16	1.38	1.60	1.30	1.53	1.54	1.50	1.5	1.5
W4	.33	.32	.33	.33	.325	.33	.33	.33	.32	.32
TIME ON		10:56								
TIME OFF			11:40							

nick

Down Breaker

DATE: 3/13/77 TIME: 1:48

SYSTEM: 606 TYPE OF TEST: Pressure Reg. Test TEST FACILITY: Columbia

OBSERVERS: W.P.L. J.C.

COMMENTS: 7.5 Hg. meter T10 = P-tan temperature

DATA ITEMS:

TIME	1:48	1:56	2:04	2:15	2:30	3:00	3:20
DP2	0	1.8	1.9	1.9	1.9	0	1.0
DP5	0	3.9	3.9	3.9	3.95	0	3.9
PA	0	6	5.5	5.1	5.0	0	5.2
P2	0	37.5	49	48	47.5	0	48
P3	0	33.4	47.5	48.2	47.5	0	46
P4	0	2.1	7.1	6.5	6.5	0	6.8
P5	0	34.2	48.5	47.0	48.8	0	46.5
P6	0	1.0	5.5	5.4	5.2	0	5.4
PAMS	0						
TAMB	79	77	74	75	75	75	76
T1	79	84	112	116	121	106	112
T2	20	266	308	310	309	119	308
T3	77	90	110	110	112	112	108
T4	79	2	20	24	26	65	22
T5	99	109	98	96	95	94	94
T6	79	96	123	120	138	109	127
T7	119	91	80	80	78	23	77
T8	81	99	115	122	120	89	119
T9	117	109	98	97	96	96	96
T10	75	103	136	141	141	91	141
T11	77	74	75	76	77	76	77
T12	71	70	73	74	75	75	76
T13	111	105.5	95.4	93	97	85.5	90.7
T14	77	75	70.7	71.4	68.6	73	68.3
W1	0	1.23	4.1	4.0	3.95	0	1.83
W2	0	3.4	4.1	4.0	3.95	0	4.1
W3	2.0	1.1	.95	1.8	1.9	0	1.68
W4	.27	.27	.27	.27	.27	0	.27
TIME ON	1:53					3:20	
TIME OFF					2:50		

None Above

APPENDIX C

Enriched Loop - Technical Papers

A NEW AIR CONDITIONING,
REFRIGERATION AND HEAT PUMP CYCLE

by
Thomas C. Edwards

The ROVAC Corporation
ROVAC Industrial Center
100 Rovac Parkway
Rockledge, Florida 32955
May 2, 1977

TABLE OF CONTENTS

	<u>Page</u>
Abstract	1
Introduction - Background	1
Expansion and Compression of a Multi-Component/Mixed-Phase Closed System	2
Expansion	2
Compression	4
Process Analyses	6
The Simple Cycle Configuration	11
Sample Comparison - Air Conditioning	13
The New Cycle: A Heat Pump Configuration	16
Sample Comparison - Simple Cycle Ice-Maker Heat Pump	21
A Compressor/Expander Machine	24
Closure	24
References	28
Acknowledgement	28
Appendix A - Details of the Air Conditioning Cycle Calculations Polytropic Process Analysis	29
Sample Calculation - Air Conditioning	30
Appendix B - Details of the Simple Ice-Maker Heat Pump Cycle Calculations Polytropic Process Analysis	36
Sample Calculation - Simple Cycle Ice-Maker Heat Pump	37

LIST OF FIGURES

<u>Figure</u>		<u>Page</u>
1	Multi-Component/Mixed-Phase Closed System Expansion	2
2	Schematic Illustration of Volume-Pressure/Temperature Diagram of a Multi-Component/Mixed Phase Refrigerant Undergoing Expansion	3
3	Compression of a Multi-Component/Mixed-Phase Fluid	4
4	Schematic Illustration of Volume-Pressure/Temperature Diagram of a Multi-Component/Mixed Phase Refrigerant Undergoing Compression	5
5	The Simple Configuration of the New Cycle	11
6	Illustration of Finite Temperature Difference Profiles in Heat Exchangers	15
7	Simple Cycle Ice-Maker Heat Pump	17
8	Regenerative Ice-Maker Heat Pump	20
9	A ROVAC Compressor/Expander Circulator	24

LIST OF TABLES

<u>Table</u>		<u>Page</u>
1	Performance Comparisons Between the Reverse Rankine Cycle and the New Cycle	23

NOMENCLATURE

Symbols

e	$\frac{\text{Btu}}{\text{lb}_m}$	Specific energy
E	Btu	General energy
h	$\frac{\text{Btu}}{\text{lb}_m}$	Specific enthalpy
M	lb_m	Mass
n	-	Polytropic index
p	psia (atm)	Partial pressure
P	psia	Total pressure
q	$\frac{\text{Btu}}{\text{lb}_m \text{ dry air}}$	Specific heat addition
Q	Btu	Total heat addition
T	°F	Temperature
U	Btu	Total internal energy
v	$\frac{\text{ft}^3}{\text{lb}_m}$	Specific volume
w _c	$\frac{\text{Btu}}{\text{lb}_m \text{ dry air}}$	Specific compression work
w _e	$\frac{\text{Btu}}{\text{lb}_m \text{ dry air}}$	Specific expansion work
W	Btu	Total work
ω	$\frac{\text{lb}_m (\text{grains}) \text{H}_2\text{O}}{\text{lb}_m \text{ dry air}}$	Specific humidity ratio

NOMENCLATURE (Continued)

Symbols

$\Delta\phi$	$\frac{\text{lb}_m \text{H}_2\text{O}}{\text{lb}_m \text{dry air}}$	Specific condensed mass of b
--------------	---	------------------------------

Subscripts

1,1',2,3,3',4	State points
a	Dry air (primary component)
b	Secondary component
c	Compression
e	Expansion
fg	Liquid-vapor phase change
i,j	Location points

A New Air Conditioning,
Refrigeration and Heat Pump Cycle

Abstract

This paper discusses the thermodynamics of a new air conditioning, refrigeration and heat pump cycle that embodies two heat transfer processes coupled with both a compression and an expansion process. The working medium of the new cycle is multi-component in nature and, in general, consists of a superheated gaseous carrier component, such as air, in partnership with a phase-changing component, such as water. The basic cycle is described along with variations in system configuration. Simple analytical models and methods are introduced and applied to calculate cycle efficiencies for sample systems.

It is shown that the reverse Brayton and reverse Rankine cycles are subcases of the new cycle. As well, the reverse Carnot can be approximated by this cycle. Further, it is shown that this new cycle yields ideal coefficients of performance (COP) greater than the reverse Brayton and reverse Rankine cycles. For example, in an "ice-making" heat pump configuration, with a source temperature of 32°F and a maximum rejection temperature of 105°F, the ideal heating COP is 9.72 compared to an ideal COP for the R-22 reverse Rankine cycle which is 7.25. In the air conditioning configuration, with a maximum condensing temperature of 150°F and a minimum evaporation temperature of 40°F, the ideal cooling COP is 8.19 compared with an ideal R-12 vapor compression cycle COP of 4.26.

Real compressor/expander machines studied and being developed by the author which can be used in this new cycle have produced adiabatic compressor efficiencies very nearly equal to unity [1]. Such machines have also produced adiabatic expander efficiencies in the low 90% range. Extensive computer models of these machines predict the ultimate attainment of overall compressor and expander efficiencies above 93%. Thus the prognosis for achieving a large fraction of theoretical ideal cycle performance appears favorable.

Introduction - Background

During the period 1967 - 1970 while a doctorate student in the School of Mechanical Engineering at Purdue University (Lafayette, Indiana), the author had the opportunity of investigating a unitary positive displacement device capable of effecting a reverse Brayton cycle when employed with simple air-to-air heat exchangers. This device employs a substantially elliptical stator cavity in concert with a rotating rotor-vane assembly. When in motion, the rotor vane assembly simultaneously compresses, provides for inter-cooling, expands and provides for reheating of the circulating air. This

simple machine, in performing six individual flow processes, produced cool air and illustrated an alternative hardware form of the air cycle system. Since the original work at Purdue, considerable development has taken place toward the advancement of such hardware. Further, the application of such hardware in partnership with extensive theoretical and experimental analyses are confirming the existence of a new efficient thermodynamic heat transfer cycle. While from an engineering standpoint both theory and actualization are important, due to the possible significance of the new cycle, this paper will concentrate primarily on qualitative and quantitative aspects of the ideal thermodynamics of this new cycle from the polytropic viewpoint.

Expansion and Compression of a Multi-Component/Mixed-Phase Closed System

Prior to discussing the complete cycle and various system configurations of the cycle, attention will be directed to the two processes of the present cycle that embody the most interesting thermodynamic aspects. This will involve the examination of the properties of a working fluid which consists of two basic identifiable components: one of which remains in the vapor phase while the other changes phases during a given process.

Expansion

Referring to Figure 1 consider a closed system at equilibrium at an elevated pressure wherein the component that will change phase (secondary component) exists in a saturated vapor condition with the partner non-phase-changing component called the carrier or primary component.

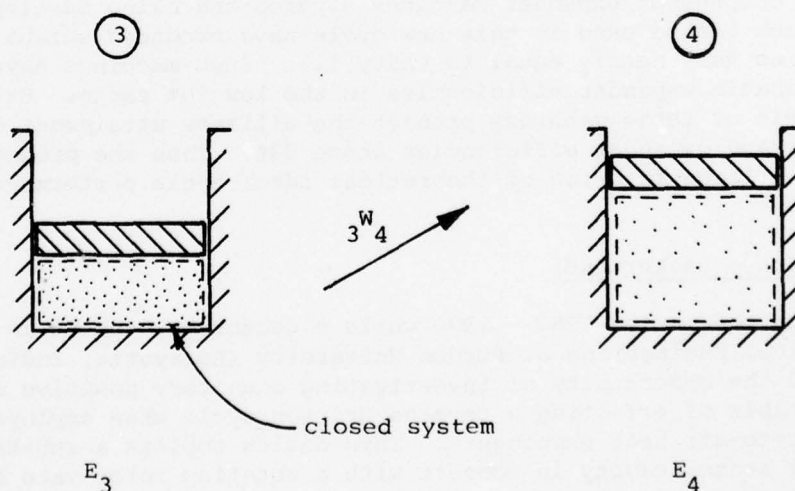


Figure 1: Multi-Component/Mixed-Phase Closed System Expansion

Next, allow the system to expand adiabatically. As expansion begins (depending upon the thermodynamic properties of the working fluid constituents and the actual process path), some of the secondary component will condense due to the temperature decrease. The energy associated with this condensation will be transferred to the primary (gaseous) component thus increasing both its pressure and its temperature over the values which would have been reached if the condensing secondary component had not been present. As further expansion takes place, further condensation will also take place, further perturbing the mixture temperature and pressure state points. Figure 2 represents a graphical illustration of this effect. As can be seen, the process can be considered to consist of a very large number of differential volume increases resulting in a like number of differential temperature (δT) and pressure (δP) changes. This sequence of processes describes the solid line in Figure 2 where the broken line represents an expansion process wherein the mass of the secondary component is zero.

An immediately obvious consequence of this multi-component process is an increase in work of expansion as seen by $\int PdV$. It is also apparent from the first law of thermodynamics that the final expanded energy state is relatively smaller due to the increase in the work integral. These two conclusions will play a major role in the ultimate conclusions to be brought forth and discussed in this paper.

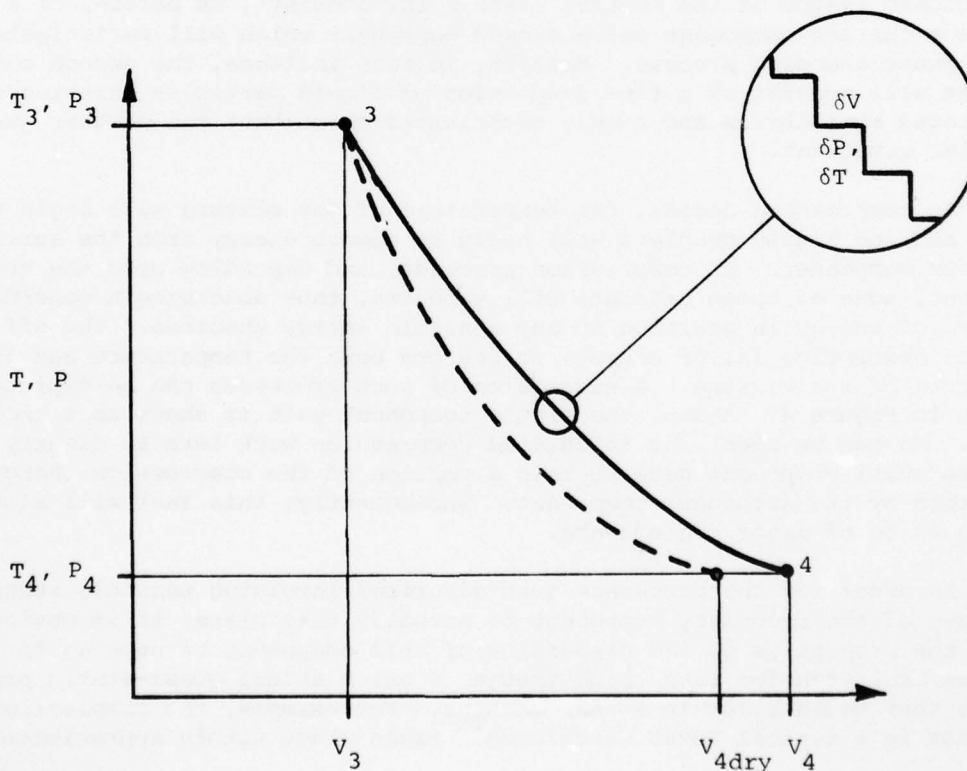


Figure 2: Schematic Illustration of Volume - Pressure/Temperature Diagram of a Multi-Component/Mixed Phase-Refrigerant Undergoing Expansion

Compression

Next, turn to the companion compression process as depicted in Figure 3.

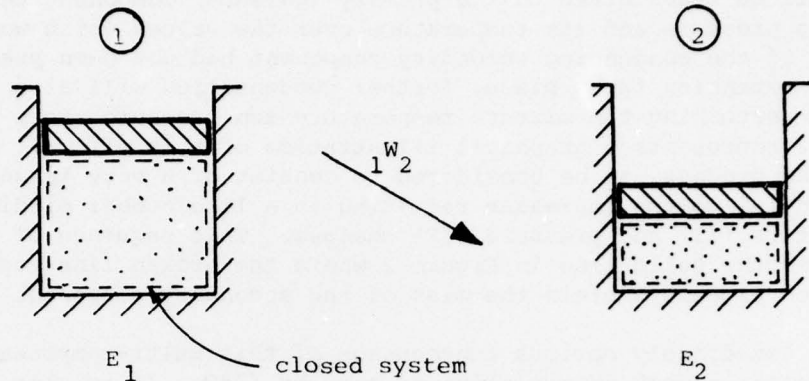


Figure 3: Compression of a Multi-Component/Mixed-Phase Fluid

The closed system at its initial state point consists, as before, of a gaseous carrier component and a second component which will participate in a phase-changing process. However, in this instance, the second component will consist of a fine dispersion of liquid particles existing in saturated equilibrium and evenly distributed throughout the partner gaseous carrier component.

As compression begins, the temperature of the mixture will begin to rise and the liquid droplets will begin to absorb energy from the surrounding gaseous component. As compression proceeds, and depending upon the quantity present, some of these droplets will vaporize, thus absorbing a considerable amount of energy in addition to any sensible energy absorbed. The effect of energy absorption is, of course, to depress both the temperature and the pressure of the mixture. A succession of such processes can be depicted as shown in Figure 4. Again, the single component path is shown as a broken line. As can be seen, the integrated compression work term is clearly less in the multi-component case wherein a portion of the compression energy is absorbed by the secondary component. Subsequently, this fact will also be shown to be of major consequence.

In order for the processes just described involving sensible state changes of the secondary component to actually take place, it is obvious that the properties of the dispersion of this component be such as to permit heat transfer rates high enough to match actual quasi-static process rates that would occur in a real machine. For example, the compression process in a typical ROVAC CirculatorTM takes place within approximately 5

milliseconds. During that time heat transfer rates on the order of 20 Btu per pound of dry air must be transferred to or from the secondary enrichment component. Presuming this secondary component to be water, and further specifying that the maximum temperature difference between the carrier component and the water to be, say, 0.5°F , it can easily be shown through "fog" heat transfer analysis that the diameter of the dispersed particles can be as large as 0.001 inch [2,3]. This value is easily reached by usual liquid spray methods.

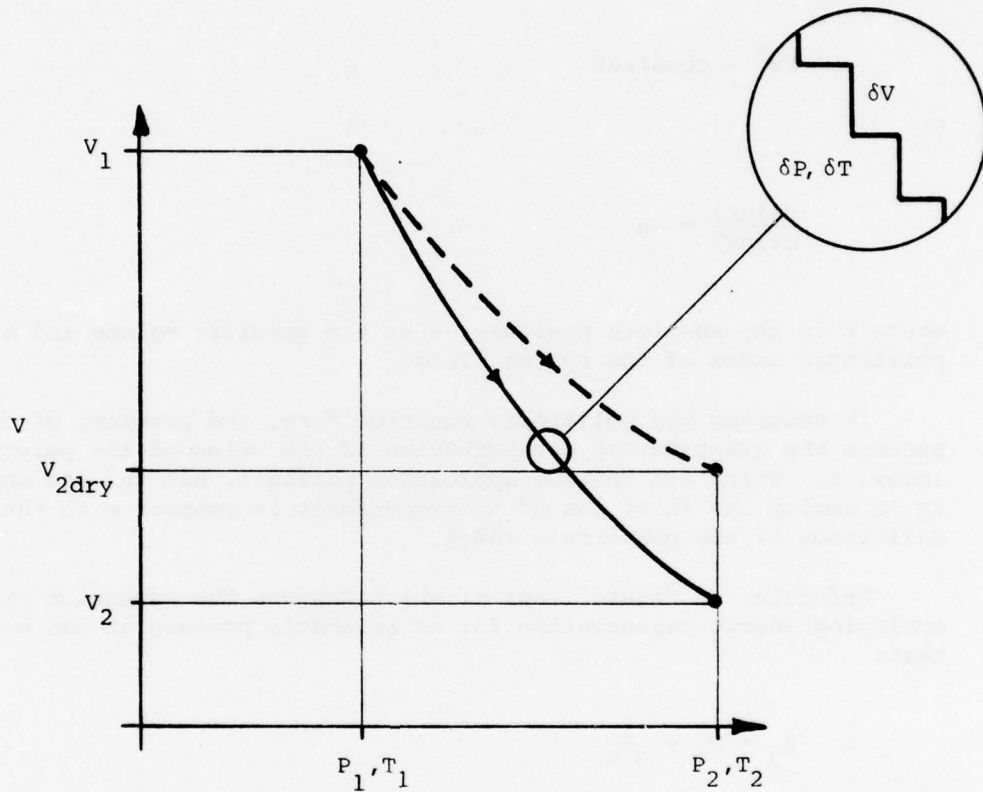


Figure 4: Schematic Illustration of Volume-Pressure/Temperature Diagram of a Multi-Component/Mixed-Phase Refrigerant Undergoing Compression

Process Analyses

In order to make a quantitative assessment of the numerical differences between the multi-component processes and the single component one, the process paths must be adequately postulated. To begin, the generalized nature of the process must first be hypothesized. One simple process path that has proven historically to be accurate (and therefore chosen here) is the exponential or polytropic process wherein the variables are related for a constant n process as:

$$pv^n = \text{constant} \quad \dots (1)$$

or

$$\frac{d(\ln P)}{d(\ln v)} = -n \quad \dots (2)$$

where P is the absolute pressure, v is the specific volume and n is the polytropic index of the system fluid.

In choosing the polytropic equation form, the problem, of course, becomes the quantitative determination of the value of the polytropic index, n . There are various approaches possible, but the one chosen here is to employ the first law of thermodynamics in concert with the mathematical definition of the polytropic index.

Referring to Figure 1 again, which depicts the expansion process and employing energy conservation for an adiabatic process it can be written that:

$$E_3 = E_4 + {}_3W_4 \quad \dots (3)$$

In this expression, E denotes the total energy of the refrigerant fluid and W represents the process work term. Further, the sum of these energies can be written as:

$$U_{a_3} + E_{b_3} = U_{a_4} + E_{b_4} + {}_3W_4 \quad \dots (4)$$

Here subscript a refers to the carrier component and subscript b refers to the secondary phase-changing component and U represents internal energy.

Eqn. (4) can be arranged as:

$${}_3W_4 = (U_{a_3} - U_{a_4}) + (E_{b_3} - E_{b_4}) \quad \dots (5)$$

where $(E_{b_3} - E_{b_4})$ can be considered to be a "heat addition" term, \bar{Q}_e ,

insofar as the carrier component is concerned. While this term has been discussed in connection with a condensation process, it is apparent that it can, in general, consist of sensible components also, as well as others:

$$\bar{Q}_e = (E_{b_3} - E_{b_4}) = M_{b_{\text{latent}}} (\text{latent energy change}) + M_{b_{\text{liquid}}} (\text{sensible energy change})$$

$$+ M_{b_{\text{vapor}}} (\text{sensible energy change}) + \text{other energy additions that may be present (chemical, nuclear, magnetic, etc.)}$$

Where the M's represent masses of the various components undergoing state change. Depending, of course, upon the state condition, the properties and amounts of components, the constituent terms can have various contributions to the total term. If, as previously postulated, only enough of component b exists to just provide saturation (no excess liquid) prior to expansion, the "heat addition" term reduces to:

$$\bar{Q}_e = \Delta M_b (e_{b_3} - e_{b_4}) = \Delta M_b \bar{q}_e$$

where ΔM_b is the amount of component b that has condensed and \bar{q}_e can be treated as $h_{b_{fg}}^*$ (neglecting the generally small sensible effect of the vapor).

Proceeding with the saturation condition assumption (no liquid present), and assuming that component a with the attendant vapor portion of component b

* $h_{b_{fg}}$ is chosen instead of $u_{b_{fg}}$ because, from the standpoint of the secondary fluid, the system is "open". In any case, the choice is somewhat academic in that the desired process path is achieved not only by the specific energy of the secondary fluid but also the amount present.

can be suitably approximated as an ideal gas, one can write

$${}_3W_4 = M_{ab} C_{v_{ab}} (T_{ab_3} - T_{ab_4}) + \Delta M_b (h_{b_{fg}}) \quad \dots (6)$$

where the ab subscript indicates the mixture property of the carrier a and the vapor portion of the secondary component b. On a specific mass basis (based upon component a) Eqn. (6) yields:

$${}_3W_4 = C_{v_{ab}} (T_{ab_3} - T_{ab_4}) + \Delta\phi_e (h_{b_{fg}}) \quad \dots (7)$$

where $\Delta\phi_e$ represents the condensed mass of component b per unit mass of component a.

Following through with the polytropic process definition along with the quasi-static work integral, the work can be represented as:

$${}_3W_4 = \frac{R_{ab} (T_{ab_3} - T_{ab_4})}{n_e - 1} \quad \dots (8)$$

where R_{ab} is the mixture gas constant consisting of component a and the vapor portion of component b, and n_e is the polytropic index of expansion. It is further indicated that the temperature of both components are equal, thus specifying a quasi-static equilibrium condition.

Equating Eqns. (7) and (8) and solving for the polytropic expansion index yields:

$$n_e = 1 + \frac{R_{ab} (T_{ab_3} - T_{ab_4})}{C_{v_{ab}} (T_{ab_3} - T_{ab_4}) + \Delta\phi_e h_{b_{fg}}} \quad \dots (9)$$

and, solving for the "heat addition" term,

$$\Delta \phi_{e, b_{fg}} = \bar{q}_e = \frac{R_{ab} (T_{ab_3} - T_{ab_4})}{(n_e - 1)} - C_{v, ab} (T_{ab_3} - T_{ab_4}) \dots \dots (9')$$

Another relation for this polytropic index can be derived from its mathematical definition:

$$\frac{T_{ab_4}}{T_{ab_3}} = \left(\frac{P_{ab_4}}{P_{ab_3}} \right)^{\frac{n_e - 1}{n_e}} \dots \dots (10)$$

Solving for n_e yields:

$$n'_e = \left[1 + \ln \left(\frac{T_{ab_4}}{T_{ab_3}} \right) / \ln \left(\frac{P_{ab_3}}{P_{ab_4}} \right) \right]^{-1} \dots \dots (11)$$

(Where the prime is added in order to denote the difference in origin of the two representations of the index.)

Note that two Equations, (9) and (11), are available which represent the polytropic index; one from the first law and one from the definition of the polytropic. Further, note that the indices are represented in terms of initial and final temperatures and pressures. In general, the pressure ratio of the process, as well as the initial pressure and temperature will be known. Thus the final temperature, T_{ab_4} and n_e (or n'_e) are the only unknowns. Since two expressions for these variables are available, their values can be computed. However, since one equation is of a transcendental form, it is a simple matter to find the polytropic index of expansion in an iterative manner. In other cases, however, the final temperature will also be known (or postulated) so that Eqns. (9) and (11) can be applied directly.

Considering next the analytical relations for the polytropic index of compression, it is clear that the inverse process occurs so that the respective polytropic relationship can appear as follows:

$$n_c = 1 + \frac{R_{ab} (T_{ab_2} - T_{ab_1})}{C_{v_{ab}} (T_{ab_2} - T_{ab_1}) + \Delta\phi_c h_{b_{fg}}} \dots (12)$$

or, solving for the "heat absorption" term,

$$\Delta\phi_c h_{b_{fg}} = \bar{q}_c = \frac{R_{ab} (T_{ab_2} - T_{ab_1})}{n_c - 1} - C_{v_{ab}} (T_{ab_2} - T_{ab_1}) \dots (12')$$

and

$$n'_c = \left[1 + \ln \left(\frac{T_{ab_1}}{T_{ab_2}} \right) / \ln \left(\frac{P_{ab_2}}{P_{ab_1}} \right) \right]^{-1} \dots (13)$$

Again, the pressure ratio will normally be known, along with the initial pressure and temperature and sometimes the final temperature. Therefore both equations can be solved in order to obtain the final compression temperature of the mixture and the polytropic compression index.

Before proceeding further, however, a word should be stated regarding the actual calculation of $\Delta\phi$. When the final temperature is not specified but is instead calculated on the basis of Eqns. (9) and (11) or Eqns. (12) and (13), some iteration must take place on final temperature states in order to apply numerical thermodynamic properties of the secondary component. For example, considering the expansion process, the quantity of component b in the initial state can be found because the initial state points and the properties of the component are known. However, in order to compute the final temperature of a given process from, say, Eqns. (9) and (11), $\Delta\phi$ must be known. That is, the final quantity of component b in the vapor^e phase must be known so that the difference between the initial

vapor quantities and final vapor quantities ($\Delta\phi_e$) can be computed. Therefore, in the actual application of these Eqns., $\Delta\phi_e$ is assumed based upon an assumed final temperature. Then, after the computation is made, a check on the assumed values is made and corrected, if necessary. In practice, especially if the secondary component proceeds to the solid phase, little error occurs in only a single calculational cycle because so little component would exist in the vapor phase.

Armed with these relations, meaningful comparisons of compression and expansion work and initial state point information can be made as amounts of component b are varied with respect to component a. Next these processes will be assembled into a cycle.

The Simple Cycle Configuration

Figure 5 depicts a simple configuration of the new cycle. As can be seen, the system consists, in addition to the multi-component refrigerant, of three basic components: The primary condensing heat exchanger, HX_1 (hot side), the compressor/expander device, C/E, and the secondary evaporating heat exchanger, HX_2 (cold side). During operation, working fluid flows from HX_2 at state point (1), is compressed by C/E to state point (2), where thermal energy is rejected through HX_1 . The flow emerges from HX_1 at state point (3) and expands through C/E to state point (4). Finally, the working fluid passes through HX_2 where it receives thermal energy until it emerges at state point (1). The cycle is then continuously repeated.

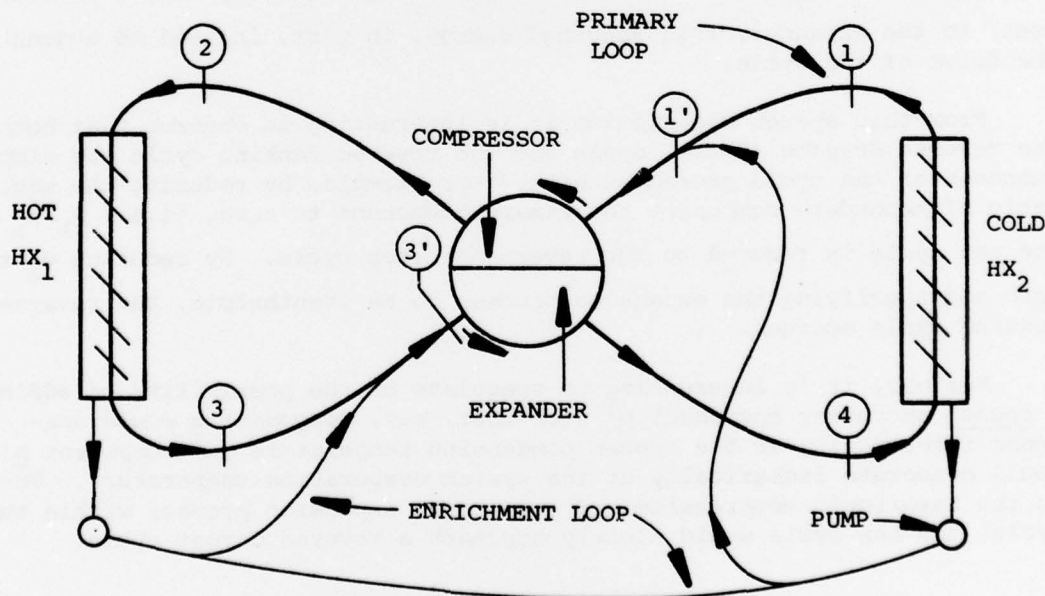


Figure 5: The Simple Configuration of the New Cycle

In general, the secondary component in the liquid phase will collect in both heat exchangers. Therefore, again in general, only the vapor phase of the secondary component will accompany the primary component (this is termed the "non-enriched" case). The amount of this type of secondary component circulation will, of course, be dependent upon the thermodynamic properties of the two components as well as the state point values existing throughout the cycle.

In order to take full advantage of the characteristics of this cycle, it is important to control the ratio of mass of the secondary component with respect to the primary carrier component at various locations in the system. A schematic means for achieving this is depicted in Figure 5 by the solid lines denoted "Enrichment Loop". These lines represent the enrichment flow of the secondary component in liquid form to two important locations in the system. Considering previous discussions related to compression and expansion process involving mixed primary and secondary components, it is apparent from this diagram that the injection of liquid component b (continually collecting in the heat exchangers) into component a at (1), yielding state point (1'), will tend to decrease the work of compression required to reach a given pressure ratio. Likewise, additional secondary liquid injected downstream of state point (3), yielding state point (3'), will increase the energy of expansion. Of course, the continuously recirculating secondary component also greatly influences the heat rejection and absorption rates and heat exchanger temperature profiles. (A very small parasitic liquid pumping requirement exists in order to elevate the pressure of the liquid secondary flow from P_{HX_2} to P_{HX_1} .)

It is worthwhile to note that due to the recirculation of secondary component from HX_2 (where it has absorbed energy from the source environment) to the expander, this absorbed energy, in part, is used to augment the drive of the cycle.

From this system description it is interesting to observe that both the reverse Brayton (Joule) cycle and the reverse Rankine cycle are simply subcases of the cycle presented here. For example, by reducing the mass ratio of secondary component to primary component to zero, (i.e.: $M_b/M_a = 0$), the new cycle is reduced to the reverse Brayton cycle. By reducing M_a to zero and specifying the expansion process to be isenthalpic, the reverse Rankine cycle emerges.

Further, it is interesting to speculate on the possibility of adding a second secondary component b' such that, say, component b would condense isobarically at the system condensing temperature and component b' would evaporate isobarically at the system evaporation temperature. Due to the isentropic compression and isentropic expansion process within the cycle, the new cycle would closely approach a reverse Carnot cycle.

Sample Comparison - Air Conditioning

In order to assess the theoretical ideal performance of this cycle an example configuration will be chosen and a given set of conditions will be specified. For simplicity, this example will be modeled after Figure 5 and the ideal cooling coefficient of performance will be estimated.*

Operating Conditions

Ambient: $T_{\text{outside}} = 95^{\circ}\text{F}$

$T_{\text{inside}} = 80^{\circ}\text{F}$

System: $T_1 = 80^{\circ}\text{F}$

$T_2 = 205^{\circ}\text{F}$

$T_3 = 95^{\circ}\text{F}$

$T_4 = 0^{\circ}\text{F}$

Pressure Ratio = 3:1

Refrigerant: Primary Component = Air

Secondary Component = Water

*Details of this entire calculational process is presented in Appendix A

As noted, ordinary atmospheric air has been chosen as the carrier component and water as the secondary constituent. It can also be seen that, consistent with ideal calculations, the effectiveness of HX_1 and HX_2 are chosen as 100%, and, as will become apparent, the values of T_2 and T_4 are chosen in order to provide a very conservative basis for comparison of theoretical cycle performance between the new cycle configuration and two of its important subcases. (That is, the average condensing temperature is 150°F and the average evaporating temperature is 40°F.)

The pressure ratio of 3.0 was somewhat arbitrarily chosen because the temperature ratio, in addition to being a function of the pressure ratio, is also a function of the specific quantities of secondary component injected. Therefore, once a pressure ratio is chosen, the amount of secondary component added can be varied to reach the desired temperature ratios. This fact, although not explored here, has obvious ramifications related to cycle optimization and variable capacity over a wide range of operating conditions.

Applying the foregoing analytical models to the set of conditions put forth yields the following coefficient of performance:

$$\text{COP}_{E_c} = 5.22$$

Now compare this performance with the ideal performance (i.e. superheating to 80°F and subcooling to 95°F) of a reverse Rankine cycle using fluorocarbon 12 operating under the same ambient conditions. (Refer to Figure 5, where $h_3 = h_4$.)

$$\begin{aligned} \text{COP}_{R_c} &= \frac{h_1 - h_4}{h_2 - h_1} \\ &= \frac{87.731 - 29.902^*}{101.292 - 87.731} \end{aligned}$$

$$\text{COP}_{R_c} = 4.26$$

*Enthalpy values taken from ASHRAE Handbook of Fundamentals, American Society of Heating, Refrigerating and Air Conditioning, Engineers Inc. New York, 1972.

The results are quite interesting in that the new cycle actually demonstrates a higher theoretical ideal coefficient of performance than the popular Rankine fluorocarbon cycle, (and, of course, the reverse Brayton cycle).

Interpretation of this rather respectable ideal performance comparison may be manifested in the fact that the new cycle actually extracts energy from the condensing secondary constituent during an isentropic expansion whereas the reverse Rankine cycle employs an irreversible throttling expansion process. This must be an important factor because it overcomes the non-isothermal heat rejection and acceptance process seen in the new cycle. In this connection, however, it must be recognized that in a real system the condensation or evaporation temperature is generally well separated from the ambient temperature. This, of course, introduces irreversibilities due to heat transfer across finite temperature differences between the working fluid and the environment.

This can be graphically observed in Figure 6 below where $\Delta T_{\text{amb/HX}}$ expresses the difference in temperature between the ambient and the refrigerant working fluid plotted against physical location in a linear heat exchanger.

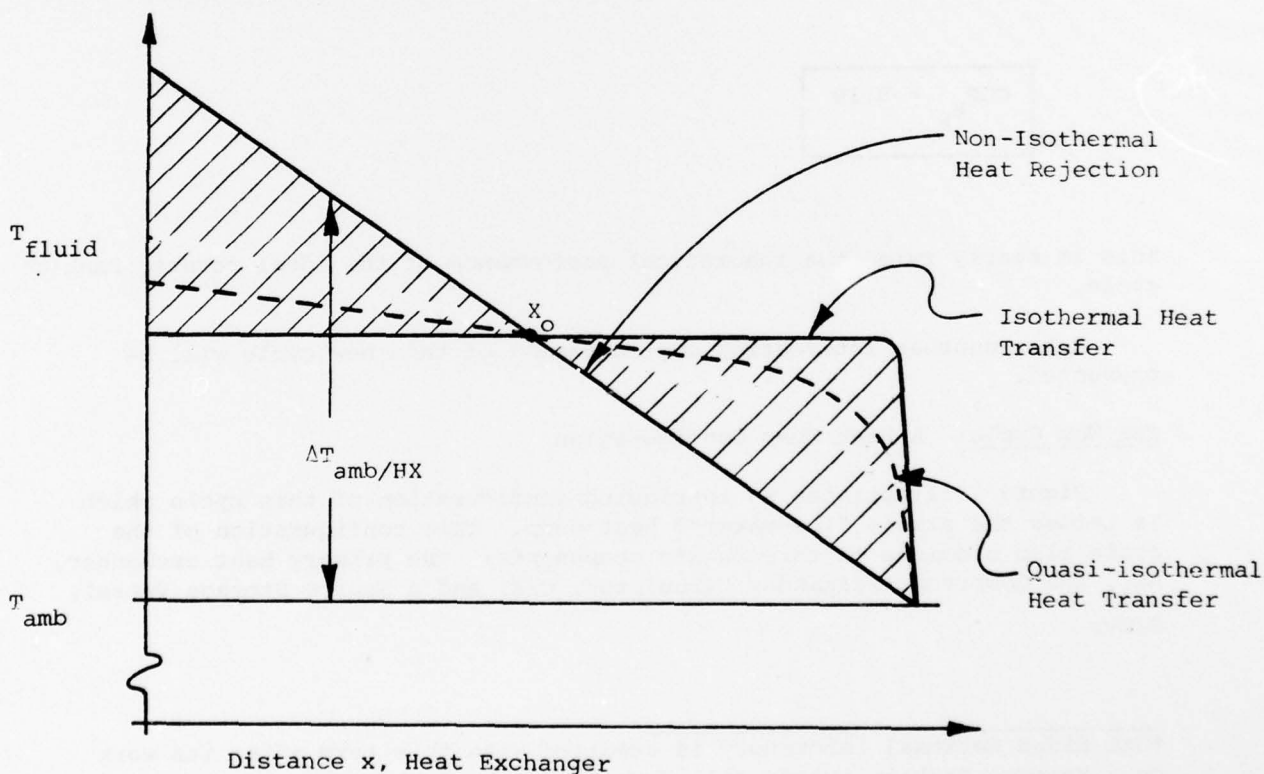


Figure 6: Illustration of Finite Temperature Difference Profiles in Heat Exchangers

It can be noted in a qualitative fashion from Figure 6 that while irreversibilities in the non-isothermal heat exchange process are generally greater to the left of point X_o , they are generally smaller to the right of this point with respect to the isothermal heat transfer process. It can be further stated that due to the nature of the new cycle, one can approach isothermal heat transfer quite closely because relatively large quantities of heat are rejected or accepted through latent effects of the secondary refrigerant and the relative magnitude of the latent components is directly controllable through the thermodynamic properties of the working fluid constituents as well as their relative mass ratios. (In fact, in the present example, two-thirds of the heat transferred is due solely to latent effects.) A conceptual representation of a quasi-isothermal heat rejection process is portrayed by the dotted line of Figure 6.

From this discussion it should be amply apparent that employing "mean" heat exchanger temperature values on the new cycle indeed imposes an unrealistic constraint on theoretical performance when comparing such performance to the reverse Rankine cycle. It is therefore interesting to note in the present example that if the maximum condensing temperature of 150°F is employed along with the minimum evaporating temperature of 40°F (as employed in the previous fluorocarbon 12 example) the performance rises substantially to:

$$\text{COP}_{E_h} = 8.19$$

This is nearly twice the theoretical performance of the ideal reverse Rankine cycle.

Next, another interesting configuration of this new cycle will be presented.

The New Cycle: A Heat Pump Configuration

Figure 7 illustrates an intriguing configuration of this cycle which is termed the simple "ice-maker"* heat pump. This configuration of the cycle also consists of three basic components: The primary heat exchanger, HX_1 , the Compressor/Expander Circulator, C/E, and a Source Storage Vessel, S/SV.

*Oak Ridge National Laboratory is credited with this term after its work on a reverse Rankine system called an "ice maker" heat pump.

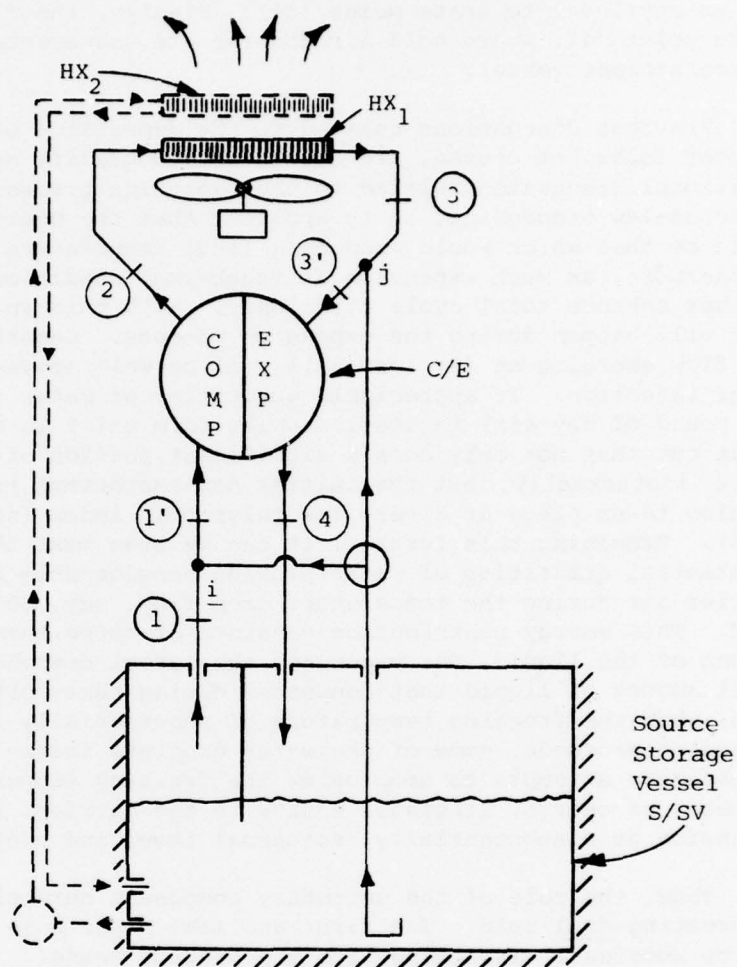


Figure 7: Simple Cycle Ice-Maker Heat Pump

In describing this configuration it will be again specified that the primary carrier component is air and the secondary component is water. Further, it will be specified that S/SV initially contains liquid water at 32°F, one atmosphere pressure. In operation, saturated air at 32°F, (state point (1)) on its way to the compressor, flows to water injection point *i*. Liquid water in a fine spray mist form is injected at this point to yield state point (1'). This air/water mixture is then compressed to state point (2). The warm emerging flow then proceeds through HX₁ where a portion of its thermal energy is rejected to the area being heated. The flow continues

to state point (3) after which additional 32°F water from the storage source tank can be injected (or rejected) at location j , thus changing the energy level to state point (3'). Finally, the flow is expanded to state point (4), where cold air and ice are transported back to the source/storage vessel.

Previous discussions related to the depression of the polytropic compressor index, of course, are sufficient to qualify here. However, some additional discussion related to the expansion process is worthwhile. From a second-law standpoint, it is apparent that the most effective expansion would be that which would produce a final temperature of substantially 32°F. Furthermore, as much expansion at isothermal conditions as possible would further enhance total cycle efficiency. With this in mind, one can explore what will happen during the expansion process. Generally speaking, of course, the flow emerging at (3) (or (3')) will be well above 32°F (say, 50°F) after water injection. If appreciable quantities of water (say, 2000-4000 grains per pound of dry air) in small droplet form exist in state point (3'), it turns out that not only does a significant portion of the expansion take place isothermally, but the initial non-isothermal portion of the expansion takes place at a very low polytropic index (say, on the order of 1.15). Examining this further, it can be seen that this occurs because the substantial quantities of water provide considerable energy transfer to the carrier air during the temperature drop from, say, 50°F to substantially 32°F. This energy contribution consists of three terms: the sensible component of the liquid, the vapor and the latent component arising from the small amount of liquid that condenses during that portion of expansion. Then, when the freezing temperature of substantially 32°F is reached, but expansion proceeds, some of the water droplets freeze as the expansion temperature attempts to drop below the freezing temperature. The freezing process, of course, liberates energy to the carrier, and maintains the expansion at a substantially isothermal level and continuously produces ice.

Thus, the role of the secondary component here plays an especially interesting dual role. The first and most basic role is that of a thermal source because it is coming from the storage vessel. However, the second and less obvious role, is that of directly enhancing cycle efficiency through optimally influencing the work recovery process path.

During the cold season, the heat pump will continuously draw thermal energy from the source tank. In so doing, a considerable quantity of the water will be converted to ice. Therefore, when warm weather returns, an essentially free source of air conditioning is available. In order to employ this source of air conditioning, one simply circulates the ice-cold water remaining near the bottom of S/SV through HX_2 . During the summer months, then, the ice is slowly melted as energy from the house is transferred back to the source for use during the winter.

A somewhat more complex configuration of this type of heat pump is represented in Figure 8. This embodiment employs a regenerative heat exchanger to transfer some of the thermal energy from the sink to the flow proceeding to the compressor. The effect of this added component is interesting: it provides for an increase in heating capacity while providing for an isothermal expansion essentially over the entire expansion process. Further, if allowances are made in compressor temperature ratio (say, by a reduction in pressure ratio or, more likely, an increase in compressor enrichment flow) that would provide for the same compressor discharge temperature as the comparable non-regenerative case, a small increase in theoretical COP occurs.

The flow diagram pictured in Figure 8 can be understood by following the flow circuit. The primary component is again chosen to be air with the secondary component being water. For the sake of description it will once more be assumed that the storage source temperature is 32°F with some ice floating in the tank. Beginning at state point (1), saturated air at 32°F from the clearance volume of the tank source flows into the regenerative heat exchanger, RHX, where it receives heat from the counter-flowing mass emerging from the condensing heat exchanger, HX_1 . After emerging from RHX, the flow enthalpy at state point (2) approaches the counterflowing enthalpy at state point (4) by the action of RHX. After emerging from (2), 32°F liquid water spray fog is mixed with the flow, thus emerging at state point (2'). The total enthalpy of the flow is somewhat increased, principally due to the water mass addition occurring across (2)-(2'). Depending upon the operating conditions, some 200 grains of liquid water droplets are added per pound of dry air at this location.

After compression, the air-water mixture flows into the heating heat exchanger- HX_1 at state point (3). Of course, the enthalpy at (3) is the sum of the incoming enthalpy at (2') and the amount of compression work applied between (2') and (3). As the hot air/water mix travels through HX_1 , fan air passes across the heat exchanger, thus providing heating. Simultaneously, of course, the loop flow is yielding a like quality of energy so that state (4) is reached. At this point, the air/water mixture is unable to further deliver thermal energy to the sink. Nonetheless, a respectable quantity of heat still remains. Therefore, the flow, instead of going directly to expansion, detours through the regenerative heat exchanger, RHX, and yields further energy to the counter-flowing mass on its way to the compressor. This flow thus emerges from RHX at state (5) where its enthalpy is reduced to a level on the order of state (1), depending upon the effectiveness of RHX. Next, liquid water at 32°F is injected into the flow wherein it reaches state (5'). Again, the purpose of water injection is to increase the work of expansion. This is achieved by depressing the polytropic index, but, as previously indicated, now it will be depressed all the way down to the isothermal value, i.e., $n_e = 1$. This occurs again

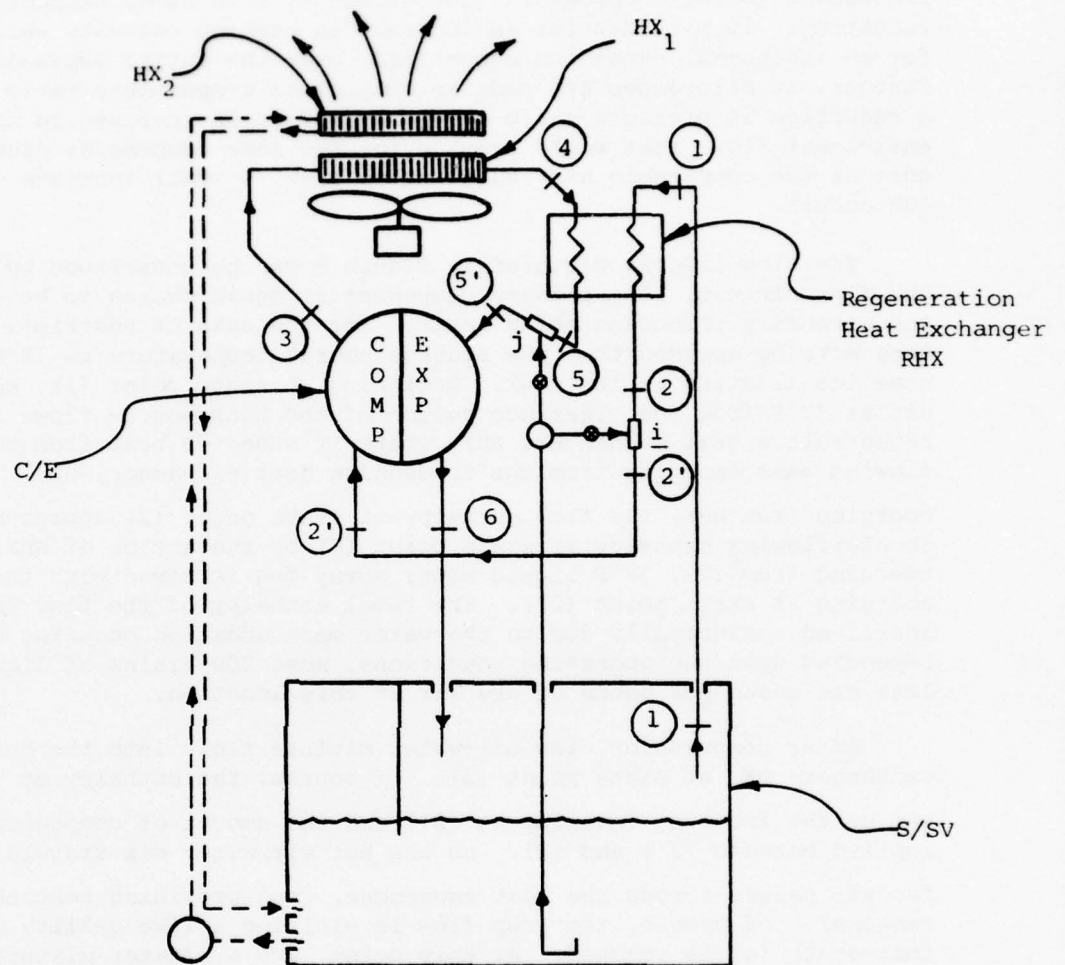


Figure 8: Regenerative Ice-Maker Heat Pump

by providing a sufficiently large number of grains of liquid water in small droplet form. As the expansion process begins, the air temperature will attempt to drop below the freezing value. Once more, due to the presence of the water droplets, as soon as even a small temperature difference develops between the air and water, some of the tiny droplets will freeze. This freezing process liberates energy which is transferred directly to the

air, thus bring the air/mix temperature back to the freezing value. This process continues in a quasi-static isothermal fashion so long as expansion takes place and liquid water droplets exist. As previously discussed, isothermal expansion yields maximum work of expansion thus maximizing the cycle efficiency.

Sample Comparison - Simple Cycle Ice-Maker Heat Pump

The ideal heating coefficient of performance for the simple "ice-maker" heat pump cycle configuration as shown in Figure 7 is next presented in order to assess its ideal performance.* The ideal performance of this cycle is compared to a similar ice-maker system employing fluorocarbon 22 in the reverse Rankine cycle such as the unit being developed at Oak Ridge National Laboratory, Oak Ridge, Tennessee.

Operating Conditions

Ambient: $T_{\text{inside}} = 70^{\circ}\text{F}$

System: $T_1 = 32^{\circ}\text{F}$, saturated

$T_2 = 140^{\circ}\text{F}$

$T_3 = 70^{\circ}\text{F}$

$T_4 = 32^{\circ}\text{F}$

Pressure Ratio = 3:1

Refrigerant: Primary Component = Air

Secondary Component = Water

As noted on the preceding page, ordinary atmospheric air and water has again been chosen as the carrier and secondary component, respectively. Consistent with ideal calculations, the effectiveness of HX_1 is chosen as 100% (the return air flowing over HX_1 in a warm air system, typically, is 5-10 degrees cooler than room temperature) and T_2 of 140°F ** has been selected to obtain an average condensing temperature of 105°F with the source temperature at 32°F . Immediately apparent in this system configuration is the absence of an evaporating heat exchanger (HX_2) and the

*The entire calculational procedure for this example is presented in Appendix B.

**See discussion on pages 15 and 16.

isolation of the system from the varying outside atmospheric temperature because the heat source is the water in the storage vessel.

Application of the foregoing analytical models to the heat pump conditions set forth yields the following ideal coefficient of performance:

$$\text{COP}_{E_h} = 7.38$$

If a maximum condensing temperature of 105°F is chosen, the ideal coefficient of performance rises substantially to:

$$\text{COP}_{E_h} = 9.72$$

The performance of the 'ice-maker' heat pump configuration of the new cycle is next compared to an ideal R-22 reverse Rankine system which employs subcooling of the condensed liquid to 70°F and operates with a condensing temperature of 105°F and a source temperature of 32°F. Again, referring to Figure 5 and R-22 tables, the heating coefficient of performance is found as:

$$\begin{aligned} \text{COP}_{R_h} &= \frac{h_2 - h_3}{h_2 - h_1} \\ &= \frac{119.84 - 30.116}{119.84 - 107.459} \end{aligned}$$

$$\text{COP}_{R_h} = 7.25$$

This ideal COP for the reverse Rankine system is somewhat unrealistic because an evaporative heat exchanger is required to absorb the source energy. Typically, a 10-16°F temperature difference is necessary for use of the heat source (Ref. 4). Employing a more realistic ideal evaporating temperature of 20°F instead of 32°F, the ideal heating coefficient of performance for the reverse Rankine "ice-maker" heat pump falls to:

$$\text{COP}_{R_h} = 6.12$$

The results of the foregoing analyses and calculations are presented in Table 1.

Table 1: Performance Comparisons Between the Reverse Rankine Cycle and the New Cycle

Air Conditioner	Conditions		COP
	Condenser	Evaporator	
Reverse Rankine Cycle	150°F	40°F	<u>4.26</u>
New Cycle a)	205°F	0°F	<u>5.22</u>
b)	150°F	40°F	<u>8.29</u>
Heat Pump			
Reverse Rankine Cycle a)	105°F	32°F	<u>7.25</u>
b)	105°F	20°F	<u>6.12</u>
New Cycle (no regeneration) a)	140°F	32°F	<u>7.38</u>
b)	105°F	32°F	<u>9.72</u>

A Compressor/Expander Machine: The ROVAC CirculatorTM

As indicated in the Introduction of this paper, the author has been involved in appreciable activity directed toward the development of actual hardware that can be used to efficiently effectuate both the non-enriched and enriched version of the thermodynamic cycle discussed here. The device that has received the majority of attention is termed a ROVAC CirculatorTM. This machine, basically an anti-friction constrained rotary-vane device, is unitary in nature in that it simultaneously produces in a single unit all the processes required to achieve cooling and heating in the new cycle. Figure 9 shows a photograph of one of these units. This particular machine, known as the Model 217, provided the engineering basis for the Model 222 automotive air conditioning unit scheduled for light pilot production beginning in mid-1977 at ROVAC Industrial Center. Real machines have produced adiabatic compressor efficiencies very nearly equal to unity. Such machines have also produced adiabatic expander efficiencies in the low 90% range. The respectable efficiencies of these Circulators is due in large part to the anti-friction nature of the machines. That is, the vane tips do not contact the stator wall due to the simple constrained vane/cam geometry. In addition, the closed loop machines carry lubricating fluid and the specially designed vane flank surface designs insure full hydrodynamic film lubrication of the vanes within the vane slots.

Closure: General Discussion and Conclusions

This paper has disclosed, discussed and analyzed a new and interesting thermodynamic cycle. The results of analytical models and methods developed here predict that the ideal performance of the new cycle is greater than the well-known fluorocarbon reverse Rankine cycle which is currently the "backbone" of the present air conditioning, heat pump and refrigeration industry.

As indicated in the abstract, although the polytropic model employed here does provide considerable insight into the nature and character of both the compression and expansion processes of this cycle, this model as employed, does not precisely provide for ideal isentropic processes. In fact, in the example calculations made, (see Appendices) small gains in entropy were generally noted for both the compression and expansion processes. Of course, this indicates that the "ideal" performance prediction for the new cycle is somewhat pessimistic [5].

The basic attributes of the new cycle may be intuitively apparent. As noted earlier, the new cycle can be conceptualized as a synergistic union between the air cycle and the vapor-compression cycle. This is because the new cycle is structured in such a way as to simultaneously employ the energy recovery advantage of the air cycle and the isothermal heat transfer processes of the vapor compression cycle. By its nature, the new cycle is able to recover energy from a condensable component that can provide significant volume change effects in a gaseous carrier component. As well, the isothermal

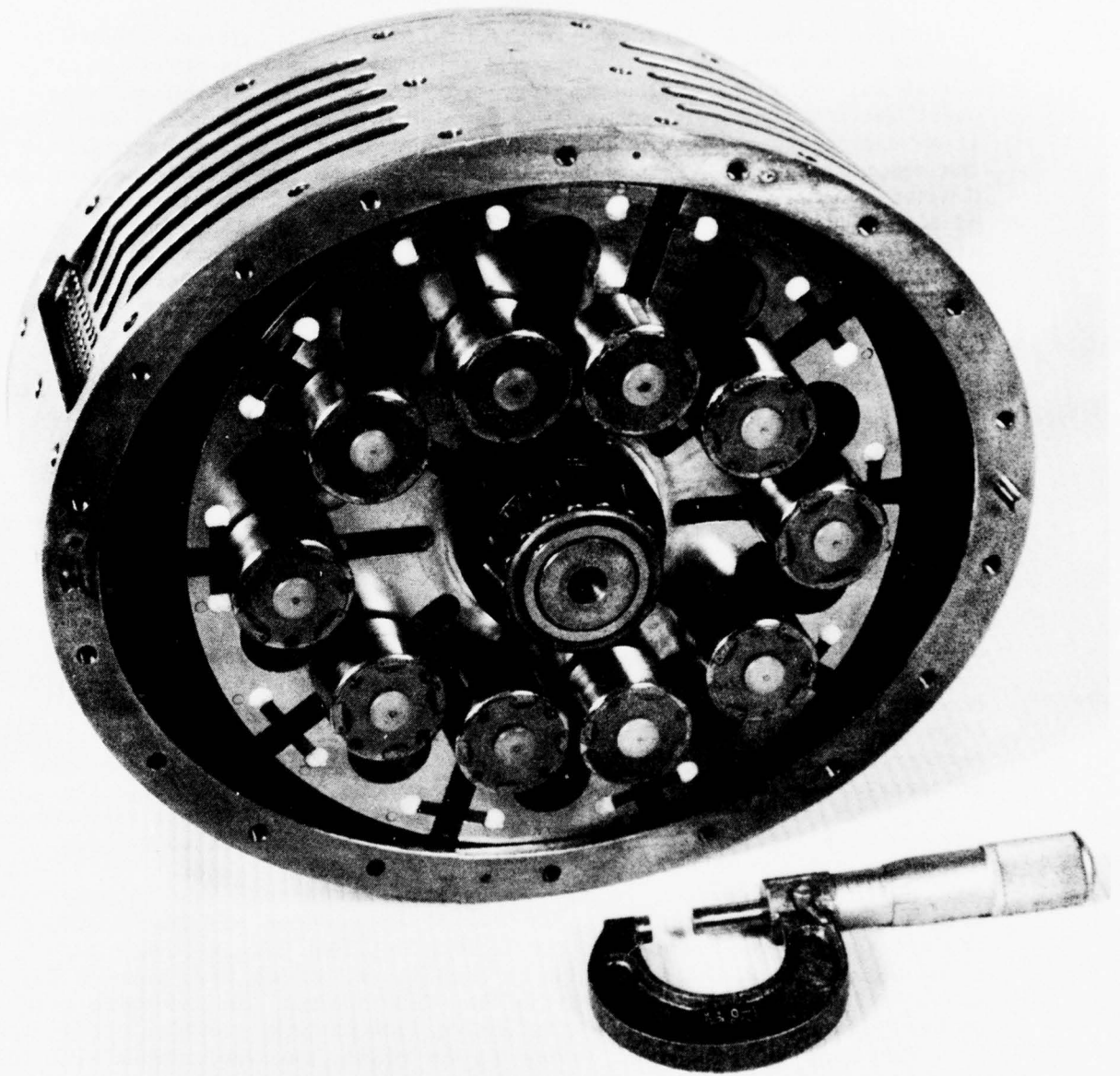


Figure 9: A ROVAC Compressor/Expander Circulator

heat transfer characteristics of the reverse Rankine cycle can be closely approximated by the properties of the working fluid mixture, thus adopting this very positive attribute of the vapor-compression system. Further, the effects of the secondary component on both the compression and expansion processes of the new cycle are favorable.

Once one has accepted the fundamental superiority of the ideal properties of the new cycle, obvious and important questions arise regarding its actual practical implementation. For example, one of the well-known practical attributes of the reverse Rankine cycle is that cycle efficiency is a function of the efficiency of only one volume-changing component: the compressor. This is not the case with the new cycle (and the reverse Brayton cycle) which is dependent upon the product of the efficiencies of both a compression device and an expansion device. Thus, actual cycle efficiency attainment is more sensitive to machine efficiency in the case of the new cycle than the vapor compression system. (Considering the vapor compression cycle, however, it appears reasonable to note that even some expansion efficiency is better than none at all.)

Regarding further the matter of compressor and expander efficiencies, it has been the author's experience with the ROVAC Circulator that the machine exhibits a high volumetric efficiency. Tests made by the Environmental Control Section of the Air Force Flight Dynamics Laboratory at Wright-Patterson Air Force Base (Ref.1) have confirmed volumetric flow efficiency levels very nearly equal to unity. This is an important factor that must be considered carefully when comparing the reverse Rankine cycle to the new cycle. This is because volumetric efficiency is itself a multiplier in determining overall vapor compression system performance. That is, the overall reverse Rankine performance is the product of the compressor efficiency and the volumetric efficiency. While by no means does the unitary compressor/expander device ameliorate the basic need for good efficiency of both the compression and expansion processes, the unitary nature of the Circulator does offer clear economies in efficiency because it is basically a single machine. Further, it is well known that the use of a regenerative heat exchanger (or recuperator) in the reverse Brayton cycle can be used to mitigate the sensitivity of that cycle to the irreversibilities inherent in real compressor and expander devices. The same option, of course, is open to the new cycle.

Continuing with the topic of heat exchangers, it is important to note that even minute quantities of moisture present in the loop air drastically improve the internal heat transfer film coefficient of air-to-air heat exchangers (Ref. 2, Ref 3). In this connection, it has been interesting to learn in actual tests that unmodified fluorocarbon fin-and-plate evaporator cores used in automobile air conditioning systems have provided cross-flow heat exchanger effectiveness values in the ninety percent bracket with less than 1 psi pressure loss. (Of course, a cross-counter flow core configuration would be better.)

It is worthwhile to note that in the closed system configuration, pressurization of the closed system effectively "dilutes" the machine's

frictional losses over the resulting increase in produced cooling. That is, if a system is operating at a given set of conditions and the evaporative heat exchanger reference pressure is, say doubled from one atmosphere to two atmospheres, the cooling capacity is essentially doubled. However, the "over-head" friction of the machine which consists principally of bearing friction and hydrodynamic lubricant shear will increase only very slightly. Thus, the system can inherently improve its performance through pressurization. It is further interesting to note that the positive benefits of pressurization are not limited to mechanical friction; to the contrary, they extend to dilution of adverse heat transfer, porting losses (velocity-squared losses vs. gas density losses), and internal leakage.

In conclusion, the results of the analyses of the new cycle indicate that this natural refrigerant cycle offers a partial solution to the growing world-wide energy shortage as well as a solution to the global pollution and toxic substance problems related to conventional fluorocarbon refrigerants.

REFERENCES

- [1] Smolinski, R.E., Midolo, L.L., "Performance of a New Positive Displacement Air Cycle Machine", AIAA Meeting, September, 1976, Dallas, Texas.
- [2] Takahara, E.W., "Experimental Study of Heat Transfer from a Heated Circular Cylinder in Two-Phase, Water-Air, Flow", MS Thesis, Air Force Institute of Technology, May, 1966.
- [3] Albrecht, J.R., "An Experimental Investigation of the Heat Transfer Near the Stagnation Point in a Two-Phase Air-Water Spray Flow", MS Thesis, Air Force Institute of Technology, March, 1967.
- [4] Fisher, H.C., Nephew, E.A., "Application of the Ice-Maker Heat Pump to an Annual Cycle Energy System" ASME Winter Meeting, N.Y., N.Y., December, 1976.
- [5] Ecker, A.L., Edwards, T.C., and Wark, Kenneth, "A Tabular Data Boundary-State Analysis of the Edwards Cycle", ASHRAE Symposium, to be published December, 1977.

Acknowledgements

The Author wishes to express his appreciation to shareholders of The ROVAC Corporation for their continued faith and support of his work. The Author is also indebted to scientists and engineers of the Oak Ridge National Laboratory, Purdue University, and the Massachusetts Institute of Technology for thoughtful and constructive review of this paper.

Appendix A

Details of the Air Conditioning Cycle
Calculations Polytropic Process Analysis

Sample Calculation - Air Conditioning

The following presents the calculational details of the theoretical assessment of the air conditioning configuration of the new cycle.

Operating Conditions

Ambient: $T_{\text{outside}} = 95^{\circ}\text{F}$

$T_{\text{inside}} = 80^{\circ}\text{F}$

System: $T_1 = 80^{\circ}\text{F}$

$T_2 = 205^{\circ}\text{F}$

$T_3 = 95^{\circ}\text{F}$

$T_4 = 0^{\circ}\text{F}$

Pressure Ratio = 3:1

Refrigerant: Primary Component = Air

Secondary Component = Water

As noted, ordinary atmospheric air has been chosen as the carrier component and water as the secondary constituent. It can also be seen that, consistent with ideal calculations, the effectiveness of HX_1 and HX_2 are chosen as 100%, and, as will become apparent, the values of T_2 and T_4 are chosen in order to provide a very conservative basis for comparison of theoretical cycle performance between the new cycle configuration and two of its important subcases. (That is, the average condensing temperature is 150°F and the average evaporating temperature is 40°F .)

The pressure ratio of 3.0 was somewhat arbitrarily chosen because the temperature ratio, in addition to being a function of the pressure ratio, is also a function of the specific quantities of secondary component injection. Therefore, once a pressure ratio is chosen, the amount of secondary component added can be varied to reach the desired temperature ratios.

To begin the calculation, we can apply Eqn. (13) to compute the polytropic index of compression n'_c :

$$n'_c = \left[1 + \ln\left(\frac{665}{540}\right) / \ln\left(\frac{1}{3}\right) \right]^{-1}$$

$$n'_c = 1.234$$

From n'_c , $\Delta\phi_c$ can be calculated from Eqn. (12'), after calculating mean values for R_{ab} , $C_{v_{ab}}$ and $h_{b_{fg}}$ (to account for their variation over the process due to variations in quantity of vapor component of the water):

$$\Delta\phi_c = \frac{7000}{1012.5} \left[\frac{55.9(665-540)}{778(1.234-1.0)} - .185(665-540) \right]$$

$$\Delta\phi_c = 104.6 \frac{\text{grains H}_2\text{O}}{\text{lb}_m \text{ dry air}}$$

It can be seen from the conditions at hand that almost 105 grains will be vaporized between these state points.

The energy level at the compressor inlet can now be calculated by the following Eqn. (A-1), which represents the enthalpy of moist air with liquid water in thermal equilibrium:

$$h = C_p T + \frac{\omega_{\text{sat}}}{7000} (1061 + C_{p_{wv}} T) + \frac{\omega_{\text{liq}}}{7000} C_{pw} T \quad \dots (A-1)$$

where C_p is the specific heat at constant pressure of dry air, ω_{sat} is the number of grains held at saturation, ω_{liq} is the number of grains of liquid, $C_{p_{wv}}$ is the specific heat at constant pressure of the water vapor, C_{pw} is the specific heat of liquid water and T is the temperature in degrees Fahrenheit. This yields:

$$h_1 = .24(80) + \frac{155.6}{7000} (1061 + .444(80)) + \frac{104.5}{7000} (1.0)(80)$$

$$h_1 = 44.77 \frac{\text{Btu}}{\text{lb}_m \text{ dry air}}$$

Continuing to the expansion process, Eqns. (11) and (9') are employed in order to find the polytropic expansion index and the amount of water injected:

$$n'_e = \left[1 + \ln\left(\frac{460}{555}\right) / \ln\left(\frac{3}{1}\right) \right]^{-1}$$

$$n'_e = 1.206$$

$$\bar{q}_e = \left[\frac{53.9(555-460)}{778(1.206-1.0)} - .174(555-460) \right]$$

$$\bar{q}_e = 15.42 \frac{\text{Btu}}{\text{lb}_m \text{ dry air}}$$

The amount of water, $\Delta\phi_e$, at 95°F that must be injected to effect \bar{q}_e , is calculated by taking into consideration the latent effect of water bound in vapor form and the sensible and latent cooling of the injected water.

That is:

$$15.42 = \bar{q}_e = \frac{(82.1-7.1)}{7000} (1210) + \frac{\Delta\phi_e}{7000} \left[(1.0)(555-460) + 143.5 \right]$$

or

$$\Delta\phi_e = 72.1 \frac{\text{grains H}_2\text{O}}{\text{lb}_m \text{ dry air}}$$

Thus, a total of 72.1 grains of water per pound of dry air must be injected into the air stream prior to expansion in order to transfer sufficient energy to the air.

The enthalpy at the expander inlet with the air fully saturated can now be computed by means of Eqn. (A-1);

$$h_3 = .24(95 + \frac{82.1}{7000}(1061 + .444(95))) + \frac{72.1}{7000}(1.0)(95)$$

$$h_3 = 36.72 \frac{\text{Btu}}{\text{lb}_m \text{ dry air}}$$

With this information one can proceed to calculate the two work terms as well as the cooling capacity term that will be needed in order to compute the cooling coefficient of performance of this example. Thus the steady-flow compression work per pound mass of dry air can be calculated as:

$$1^w_2 = \frac{\frac{n}{c} R_{ab} T_1}{n_c - 1} \left[\left(\frac{P_2}{P_1} \right)^{\frac{n_c - 1}{n_c}} - 1 \right] \dots \dots (A-2)$$

$$= \frac{1.234(55.9)(540)}{778(1.234 - 1.0)} \left[\left(\frac{3}{1} \right)^{\frac{.234}{1.234}} - 1 \right]$$

$$1^w_2 = 47.39 \frac{\text{Btu}}{\text{lb}_m \text{ dry air}}$$

Next, the steady-flow expansion work per pound of dry air can be calculated as:

$$\begin{aligned}
 {}_3w_4 &= \frac{n_e R_{ab} T_3}{n_e - 1} \left[1 - \left(\frac{P_3}{P_4} \right)^{\frac{n_e - 1}{n_e}} \right] \\
 &= \frac{1.206 (53.9) (555)}{778 (1.206 - 1.0)} \left[1 - \left(\frac{1}{3} \right)^{\frac{.206}{1.206}} \right] \\
 {}_3w_4 &= 38.52 \frac{\text{Btu}}{\text{lb}_m \text{ dry air}}
 \end{aligned}$$

The cooling capacity is simply the difference in the enthalpies across HX_2 and can be written as:

$${}_4q_1 = (h_1 - h_4) - q_{liq} = h_1 - (h_3 - {}_3w_4) - q_{liq}$$

where q_{liq} is the amount of cooling energy required to cool the liquid excess collected in the high pressure heat exchanger from 95°F to 80°F prior to injection into the compressor inlet flow. Thus:

$${}_4q_1 = 44.77 - (36.72 - 38.52) - \frac{(155.6 + 104.6 - 82.1 - 72.1)}{7000} - (1.0) (555 - 540)$$

$${}_4q_1 = 46.34 \frac{\text{Btu}}{\text{lb}_m \text{ dry air}}$$

Finally, then, the theoretical cooling coefficient of performance is calculated as:

$$\text{COP}_{E_C} = \frac{4^q_1}{1^w_2 - 3^w_4}$$

$$\text{COP}_{E_C} = \frac{46.34}{47.39 - 38.52}$$

$$\text{COP}_{E_C} = 5.22$$

Applying the same calculational process using a maximum condensing temperature of 150°F and a minimum evaporating temperature of 40°F (which simply encompasses an increase in the secondary enrichment flow rate), the coefficient rises substantially to:

$$\text{COP}_{E_C} = 8.19$$

Appendix B

Details of the Simple Ice-Maker Heat Pump
Cycle Calculations Polytropic Process Analysis

Sample Calculation - Simple Cycle Ice-Maker Heat Pump

The following presents the calculational and analytical details of the theoretical assessment of the ice-maker heat pump configuration of this new cycle.

Operating Conditions

Ambient: $T_{\text{inside}} = 70^{\circ}\text{F}$

System: $T_1 = 32^{\circ}\text{F}$, saturated

$T_2 = 140^{\circ}\text{F}$

$T_3 = 70^{\circ}\text{F}$

$T_4 = 32^{\circ}\text{F}$

Pressure Ratio = 3:1

Refrigerant: Primary Component = Air

Secondary Component = Water

As noted on the preceding page, ordinary atmospheric air and water has again been chosen as the carrier and secondary component, respectively. Consistent with ideal calculations, the effectiveness of HX_1 is chosen as 100% and T_2 of 140°F has been selected to obtain an average condensing temperature of 105°F with the source temperature of 32°F .

A pressure ratio of 3.0 is again chosen. By specifying both the pressure and the temperature ratio, the amount of secondary component necessary to reduce the polytropic index for a given set of conditions can be computed. Therefore, beginning with Eqn. (13), the polytropic index of compression, n'_c , is calculated as:

$$n'_c = \left[1 + \ln\left(\frac{600}{492}\right) / \ln\left(\frac{1}{3}\right) \right]^{-1}$$

$$n'_c = 1.220$$

From n'_c , and Eqn. (12), \bar{q}_c , the amount of heat to be transferred from the carrier component to the secondary component during the compression process, can be calculated (after having calculated mean values for R_{ab} , $C_{v_{ab}}$ and $h_{b_{fg}}$) as:

$$\bar{q}_c = \left[\frac{54.3(600-492)}{778(1.220 - 1.0)} - .176(600-492) \right]$$

$$\bar{q}_c = 15.25 \frac{\text{Btu}}{\text{lb}_m \text{ dry air}}$$

Neglecting the sensible contribution of the water vapor, $\Delta\phi_c$ can be calculated by Eqn. (12') as:

$$\Delta\phi_c = \frac{\bar{q}_c (7000)}{h_{b_{fg}}} = \frac{15.25(7000)}{1044.9}$$

$$\Delta\phi_c = 102.2 \frac{\text{grains}}{\text{lb}_m \text{ dry air}}$$

Therefore, 102.2 grains of liquid water at 32°F must be injected prior to compression to achieve the necessary polytropic index.

A check can be made to determine whether equilibrium saturation conditions will allow an additional 102.2 grains of water at state point (2)

in vapor form. At compressor inlet conditions, a maximum of 26.4 grains can be held in saturation at 32°F and atmospheric pressure; while at the compressor discharge, a maximum of 35.6 grains can be held in saturation at 140°F and 3 atmospheres. Thus, the 102.2 grains can be held in vapor form and a large portion of the heat transfer will be due to the latent heat of the vaporization of the injected water.

The enthalpy at state point (1') can be computed using Eqn. (A-1) of Appendix A and by realizing that the temperature at state point (1') will remain at 32°F:

$$h_{1'} = .24(32) + \frac{26.4}{7000}(1061 + .444(32)) + \frac{102.2}{7000}(1.0)(32)$$

$$h_{1'} = 12.20 \frac{\text{Btu}}{\text{lb}_m \text{ dry air}}$$

The steady-flow compression work per pound mass of dry air can now be calculated:

$${}_{1'}w_2 = \frac{1.220(54.3)(492)}{778(1.220-1.0)} \left[\left(\frac{3}{1} \right)^{\frac{.220}{1.220}} - 1 \right]$$

$${}_{1'}w_2 = 41.72 \frac{\text{Btu}}{\text{lb}_m \text{ dry air}}$$

Since the temperature at exit of HX_1 (state point (3)) is stipulated to equal 70°F, the energy remaining in the working fluid mixture can again be computed via Eqn. (A-1):

$$h_3 = .24(70) + \frac{36.2}{7000}(1061 + .444(70)) + \frac{(192.2 + 26.4 - 36.2)}{7000}(1.0)(70)$$

$$h_3 = 23.37 \frac{\text{Btu}}{\text{lb}_m \text{ dry air}}$$

Water at 32°F will be injected into the flow at this point, (3'), to insure partial isothermal expansion for maximum work recovery. For calculational purposes, assume that 1200 grains of water per pound of dry air is injected into the stream and the energy at state point (3') can be computed as:

$$h_{3'} = h_3 + h_{inj} = 23.37 + \frac{1200}{7000}(1.0) \quad (32)$$

H_2O

$$h_{3'} = 28.86 \frac{\text{Btu}}{\text{lb dry air}_m}$$

The temperature existing at state point (3') is found in an iterative fashion by matching constituent and mixture enthalpies and coordinating this matching process with actual thermodynamic property data. The result is:

$$T_{3'} = 58.72^\circ\text{F}$$

The expansion work must now be calculated. In the first approach taken here, the work will be calculated by postulating a two-step expansion process, i.e., first a non-isothermal expansion from 58.72°F to 32°F and then an isothermal expansion at 32°F down to atmospheric pressure. This result will be compared to that obtained by assuming an average polytropic index over the entire expansion process to demonstrate both analytical approaches.

To determine the pressure at which the expansion process changes from non-isothermal to isothermal, an iteration procedure is again necessary. Assuming the transition pressure, P_4 , to be 30.2 psia, the polytropic index for the initial expansion phase can be calculated as follows:

At 32°F and 30.2 psia, 12.8 grains of water can be held in equilibrium, while at 58.72°F and 44.1 psia, 24.6 grains of water can be held at saturated conditions. Therefore, during the first expansion process, 11.8 grains of water per pound of dry air can be condensed from the refrigerant medium. This condensation of 11.8 grains represents the latent contribution to q_e needed in the first expansion phase while the sensible change of the remaining liquid water from 58.72°F to 32°F constitutes the remaining portion of q_e . That is:

$$\bar{q}_{3'e_4'} = \frac{(24.6 - 12.8)}{7000}(1067.8) + \frac{(26.4 + 102.2 + 1200 - 24.6) - (1.0)(58.72 - 32)}{7000}$$

$$\bar{q}_{3'e_4'} = 6.78 \frac{\text{Btu}}{\text{lb}_m \text{ dry air}}$$

Again employing mean process values for R_{ab} and $C_{v,ab}$, the polytropic index of expansion, n'_e , for the first portion of expansion (3' to 4'), can be found using Eqn. (9):

$$n_e = 1 + \frac{53.6(518.72 - 492)}{778(.172(518.72 - 492) + \bar{q}_e)}$$

$$n_e = 1.162$$

The assumed value of $P_{4'}$, must be checked:

$$P_{4'} = P_{3'} \left[\frac{T_{4'}}{T_{3'}} \right]^{\frac{n_e}{n_e - 1}}$$

$$P_{4'} = 44.1 \left[\frac{492}{518.72} \right]^{\frac{1.162}{.162}}$$

$$P_{4'} = 30.18 \text{ psia}$$

This checks closely with our assumed value of $P_{4'}$, so we can continue. At this pressure, the saturation humidity ratio is 12.8 grains of water per pound of dry air.

The steady-flow expansion work per pound of dry air for the first portion of expansion can be found as:

$$3'w_{4'} = \frac{1.162(53.6)(518.72)}{778(1.162-1.0)} \left[1 - \left(\frac{30.18}{44.1} \right)^{\frac{.162}{1.162}} \right]$$

$$3'w_{4'} = 13.20 \frac{\text{Btu}}{\text{lb}_m \text{ dry air}}$$

The second step of the expansion process occurs isothermally from 30.18 psia down to atmospheric pressure. The steady-flow expansion work for an isothermal process can be computed as follows: (For an isothermal expansion process, the amount of expansion recovery work is identically equal to the amount of heat transferred to the carrier component.)

$$\begin{aligned} 4'w_4 &= -R_{4'ab_4} T_4 \ln \left(\frac{P_4}{P_{4'}} \right) \\ &= \frac{-53.6(492)}{778} \ln \left(\frac{14.7}{30.18} \right) \end{aligned}$$

$$4'w_4 = 24.38 \frac{\text{Btu}}{\text{lb}_m \text{ dry air}}$$

Next, then, a check can be performed to determine if enough liquid secondary component was injected into the flow prior to expansion to permit an isothermal process:

$$4'\bar{q}_4 = 4'w_4 = 24.38 \frac{\text{Btu}}{\text{lb}_m \text{ dry air}}$$

Almost all of the heat transfer would be due to the latent heat of fusion, $h_{b \text{ fusion}}$ of the water. Therefore, the amount of liquid component necessary for a final isothermal expansion phase $\Delta\phi_{e\ell'}$ can be found as:

$$\Delta\phi_{el} = 4, \bar{q}_4 \frac{(7000)}{h_{b \text{ fusion}}}$$

$$= \frac{24.38 (7000)}{143.5}$$

$$\Delta\phi_{el} = 1189 \frac{\text{grains of water}}{\text{lb}_m \text{ dry air}}$$

Since the amount of water injected at state point (3') was 1200 grains, sufficient water was available for the partial isothermal expansion process.

The ideal heating coefficient of performance can now be calculated for the new cycle operating in an 'ice-maker' heat pump configuration:

$$\begin{aligned} \text{COP}_{E_h} &= \frac{2q_3}{w_c - w_e} \\ &= \frac{(h_{1'} + w_c) - h_3}{1'w_2 - (3'w_{4'} + 4'w_4)} = \frac{(12.20 + 41.72) - 23.37}{41.72 - (13.20 + 24.38)} \end{aligned}$$

$$\text{COP}_{E_h} = 7.38$$

If a maximum condensing temperature of 105°F is chosen, the ideal coefficient of performance rises substantially to:

$$\text{COP}_{E_h} = 9.72$$

The analytical approach using a two-step expansion process taken in the above calculation differs from the previous example which modeled the expansion as a continuous single-step process employing a single value for n_e .

Upon review of the assumptions implicit in this method, it becomes immediately obvious that the method of 'index averaging' is a surprisingly accurate averaging method. That is, a single-step process path approximation is very nearly as accurate as the two step approximation. This statement can be proven by recalculating the expansion work employing an overall constant index as follows:

The overall 'average' polytropic index of expansion is calculated as:

$$n'_e = \left[1 + \ln\left(\frac{492}{518.72}\right) / \ln\left(\frac{3}{1}\right) \right]^{-1}$$

$$n'_e = 1.051$$

The steady-flow expansion work from state point (3') to (4) per pound mass of dry air is computed as:

$${}_{3'}w_4 = \frac{1.051(53.6)(518.72)}{778(1.051-1.0)} \left[1 - \left(\frac{1}{3}\right)^{\frac{.051}{1.051}} \right]$$

$${}_{3'}w_4 = 38.23 \frac{\text{Btu}}{\text{lb}_m \text{ dry air}}$$

This value compares closely with the previously calculated expansion work:

$${}_{3'}w_4 = {}_{3'}w_4 + {}_{4'}w_4$$

$$= 13.20 + 24.38 = 38.58 \frac{\text{Btu}}{\text{lb}_m \text{ dry air}}$$

Employing the average polytropic index calculational approach represents only 1.7% error in the computation of the work term. The primary source of this small error exists in the variation of R_{ab} due to the continuous

variation in the amount of water existing in vapor form across the process. Because only the end states are necessary for computation of the reasonably accurate performance estimated and iteration steps are eliminated, this analytical tool allows for more rapid and convenient computation of the cycle state points. A note of caution in this connection, however, should be added. Due to the fact that various calculations involving work terms require subtraction of numerical values which are similar, small errors can result. Very good accuracy can therefore be had by proceeding with a number of steps through the volume-changing processes. Obviously a digital computer can be easily employed for such calculations. It is quite interesting to note that, in the final analysis, exact knowledge of the process paths is not necessary to prove the basic efficiency of the cycle simply because these paths are infinitely variable according to the instantaneous ratio of M_b/M_a .

A TABULAR DATA BOUNDARY-STATE ANALYSIS

OF THE
EDWARDS CYCLE

by

Amir Leif Ecker

Thomas C. Edwards

The ROVAC Corporation

and

Kenneth Wark

Purdue University

The ROVAC Corporation
ROVAC Industrial Center
100 Rovac Parkway
Rockledge, Florida 32955
February 23, 1977

TABLE OF CONTENTS

	<u>Page</u>
Abstract	1
Introduction: The Edwards Cycle	1
Tabular Boundary-State Analysis Method	4
Example Calculation: Air Conditioning Cycle Analysis	6
Discussion - Optimization of the Edwards Cycle	17
References	20

LIST OF FIGURES

<u>Figure</u>	<u>Page</u>
1 The General Configuration of the Edwards Cycle	2
2 The Edwards Cycle Employed in an Air Conditioning Configuration Depicting the Moisture Flow	15

LIST OF TABLES

<u>Table</u>	<u>Page</u>
1 Pressure Ratio versus Performance of Edwards Cycle	18

NOMENCLATURE

Symbols

h	$\frac{\text{Btu}}{\text{lb}_m}$	Specific enthalpy
M	lb_m	Mass
p	psia (atm)	Partial pressure
P	psia	Total pressure
q	$\frac{\text{Btu}}{\text{lb}_m \text{ dry air}}$	Specific heat addition
R	$\frac{\text{Btu}}{\text{lb}_{\text{mole}} \text{ } ^\circ\text{R}}$	Gas constant
s	$\frac{\text{Btu}}{\text{lb}_m \text{ } ^\circ\text{R}}$	Specific entropy
T	$^\circ\text{F}$	Temperature
v	$\frac{\text{ft}^3}{\text{lb}_m}$	Specific volume
w_c	$\frac{\text{Btu}}{\text{lb}_m \text{ dry air}}$	Specific compression work
w_e	$\frac{\text{Btu}}{\text{lb}_m \text{ dry air}}$	Specific expansion work
ω	$\frac{\text{lb}_m \text{ (grains) H}_2\text{O}}{\text{lb}_m \text{ dry air}}$	Specific humidity ratio
x	-	Mole fraction

NOMENCLATURE (Continued)

Subscripts

1,1',2,3,3',4	State points
a	Dry air (primary component)
b	Secondary component
c	Compression
e	Expansion
fg	Liquid-vapor phase change
i,j	Location points
inj	Injected
l,f	Liquid phase of secondary component
r	Refrigerant
s	Saturated
s,i	Solid phase of secondary component
wv	Water vapor

A Tabular Data Boundary-State Analysis

of the

Edwards Cycle

Abstract

This paper develops a simplified analytical method for determining the theoretical ideal performance of the Edwards cycle employing only tabulated boundary-state thermodynamic property data. The ideal Edwards cycle employs a multi-component/mixed-phase refrigerant which undergoes two heat transfer processes and isentropic compression and expansion processes. This cycle has been previously analyzed through the application of a polytropic model for the compression and expansion process [1]. While this previous analytical approach provides insight to the details of the Edwards cycle, it is subject to slight errors resulting from small deviations from true ideal process path models. Conversely, the analytical methods presented here are fully independent of any hypothecon of the details of the compression and expansion process paths; one depends only upon well-known tabulated thermodynamic property data over isentropic processes to calculate the theoretical ideal performance of this cycle. Thus, this analysis is a direct analog of the method now used to compute the ideal performance of fluorocarbon vapor-compression systems.

In an air conditioning system with a maximum condensing temperature of 150°F and a minimum evaporation temperature of 40°F, the polytropic analysis of the Edwards cycle predicts a cooling COP of 8.19. The isentropic boundary-state analysis, on the other hand, results in an ideal cooling COP prediction 8.22 including ideal secondary fluid injection work. A fluorocarbon vapor compression system using R-12 as the refrigerant shows an ideal isentropic COP of 4.26 across the same condensing and evaporation temperatures employing condenser subcooling and evaporator superheating.

Introduction: The Edwards Cycle

Figure 1 portrays a general configuration of the Edwards cycle. As can be seen, the system consists, in addition to the working fluid, of three basic components: the primary condensing heat exchanger, HX_1 (hot side), the compressor/expander device, C/E, and the secondary evaporating heat exchanger, HX_2 (cold side). During operation, working fluid flows from HX_2 at state point (1), is compressed by C/E to state point (2), where thermal energy is rejected through HX_1 . The flow emerges from HX_1 at state point (3) and expands through C/E to state point (4). Finally, the working fluid passes through HX_2 where it receives thermal energy until it emerges at state point (1). The cycle is then continuously repeated.

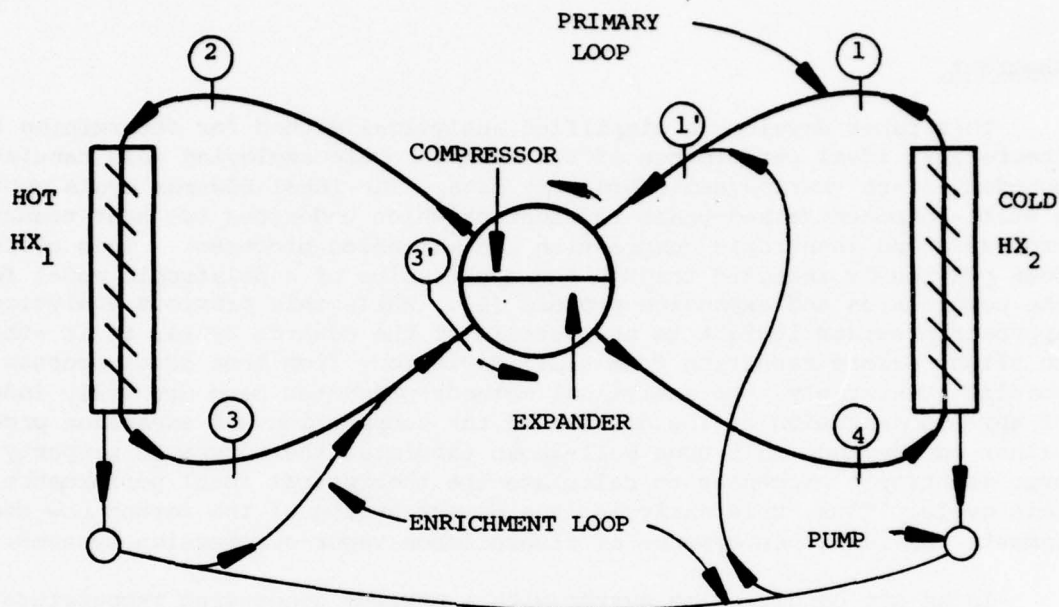


Figure 1: The General Configuration of the Edwards Cycle

In general, the multi-component/mixed-phase refrigerant used in the Edwards cycle consists of a permanently gaseous carrier constituent, termed the primary component, a, and a state and phase-changing constituent termed the secondary component, b. This mixed refrigerant continuously circulates through the system. During operation the secondary component in the liquid phase will collect in both heat exchangers. Therefore, generally speaking, only the vapor phase of the secondary component will automatically accompany the primary component. This condition is termed the "non-enriched" version of the new cycle. The amount of this type of secondary component circulation will, of course, be dependent upon the thermodynamic properties of the two components as well as the state point values around the cycle.

In order to take full advantage of the characteristics of this cycle, it is important to control the ratio of mass of the secondary component with respect to the primary carrier component at various locations in the system. A schematic means for achieving this is depicted in Figure 1 by thin solid lines. These lines represent the enrichment flow of the secondary component in liquid form to two important locations in the system and, hence, this configuration is termed the "enriched" version. The injection of liquid component b (continually collecting in the heat exchangers) into component a at (1), yielding state point (1'), will tend to decrease the work of compression required to reach a given pressure ratio due to the sensible and latent absorption of compression heat. Likewise, additional secondary liquid injected downstream of state point (3), yielding state point (3'), will increase the energy of expansion due to the release of sensible and latent energy to the gaseous carrier component. Naturally, the continuously recirculating secondary component also greatly influences the heat rejection and absorption rates and heat exchanger temperature profiles. Of course, a parasitic liquid pumping requirement exists in order to elevate the secondary flow pressure from P_1 (P_4) to P_3 (P_1).

From this system description it is interesting to note that both the reverse Brayton cycle and the reverse Rankine cycle are subcases of the Edwards cycle. For example, by reducing the mass ratio of secondary component to primary component to zero (ie: $M_b/M_a = 0$), the Edwards cycle becomes the reverse Brayton cycle. By reducing M_a to zero and specifying the expansion process to be isenthalpic, the reverse Rankine cycle emerges.

The Edwards cycle can be conceptualized as a synergistic union between the air cycle and the vapor-compression cycle. This is because the new cycle is structured in such a way as to simultaneously employ the energy recovery advantage of the reverse Brayton cycle and the isothermal heat transfer process of the vapor-compression cycle. By its nature, the Edwards cycle recovers energy from a condensable component through the expansion process simply by suspending it in a gaseous carrier component that can provide significant volume change. As well, the isothermal heat transfer characteristics of the reverse Rankine cycle can be closely approximated by the properties of the working fluid mixture due to the large latent contributions of the secondary component.

In order to generate predictions regarding ideal theoretical performance, various enthalpic state-point data is required. Specified environmental conditions as well as certain arbitrary system conditions and parameters provide portions of this data. For example, if the maximum condensing temperature, minimum evaporation temperature and pressure are specified along with the source and sink temperatures, the initial enthalpy prior to, say, compression can be determined if the refrigerant composition and properties are known.

However, in order to find the enthalpy state after compression, the energy of compression must be found. An approach to this is to assume a general work path function such as the polytropic process and determine the polytropic index of the process. The polytropic index can be found through the simultaneous application of the first law of thermodynamics and the mathematical definition of the polytropic process. Co-author Edwards applied this technique in the original analysis of this cycle [1].

Subsequent analysis employing the second law of thermodynamics disclosed that, from an ideal standpoint, the original analysis was slightly pessimistic. Initial and final entropy state calculations across both the compression and expansion process disclosed that slight gains in entropy resulted from the assumed process paths. Therefore, in order to produce truly ideal performance predictions, either the details of the process paths would have to be modified to provide isentropic processes or an isentropic process could be specified a priori and tabulated thermodynamic property data applied at the boundary states. This latter approach was chosen for the present paper. The advantages of employing this approach are that not only does it obviate the need for knowledge of details of the process path, but the boundary-state analysis method is exact and presents a direct analog to cycle analysis procedures established for fluorocarbon systems. This method also legitimizes the Edwards cycle and clearly demonstrates its validity.

Tabular Boundary-State Analysis Method

Implicit in the following analysis are two basic thermodynamic assumptions: 1), the primary and secondary components (in this case, air and water, respectively) exist together at thermal equilibrium and 2), the moist air portion of the refrigerant behaves essentially as an ideal gas. Exception may be taken to the first above assumption; however, as indicated in Ref. [1], through the application of fog droplet heat transfer analysis, typical liquid atomization methods can achieve the necessary inter-component heat transfer rates to accommodate thermal equilibrium even during rapid compression and expansion processes. Treating the moist air as a perfect gas mixture is permissible since the partial pressure of the water vapor is much smaller in comparison to the total system pressure (Ref. [2]).

Referring to Figure 1, on an enthalpy basis, the cooling coefficient of performance can be generally written as:

$$\text{COP}_{E_C} = \frac{h_1 - h_4}{(h_2 - h_{1'}) - (h_{3'} - h_4)} \quad \dots (1)$$

To effect the evaluation of the coefficient of performance, then, it becomes a matter of computing the enthalpies at various state points. In general, for a refrigerant, all eight basic thermodynamic properties can be found once any two are known. Since the refrigerant employed in the Edwards cycle is multi-component in nature, that is, two distinguishable fluids are present existing simulataneously at the identical system total pressure and temperature at any given location, only two properties (plus relative composition) are required to compute the refrigerant property at that point. Thus the total refrigerant properties can be determined by summing the properties of the individual components. This method then allows use of standard property tables to determine the actual air and water mixture properties.

If the evaporative heat exchanger environment is specified (which will normally be the case) and the low side pressure is set, and further, if the amount of secondary component is known (saturation conditions will prevail at state point (1) because all of the condensed and liquid water will drain in the evaporative heat exchanger and eliminate liquid carry-over), the thermodynamic state of (1) is fully prescribed. That is T_1 , P_1 , and ω_1 are known. From these, all other properties can be determined.

If next, the maximum condensing temperature and pressure ratio of the cycle is prescribed, the entire condition of state (2) can be determined because an isentropic compression is also prescribed, i.e.:

$$s_2 = s_1, \quad \dots (2)$$

The entropy prior to compression, $s_{1'}$, is determined by the equation:

$$s_{1'} = s_1 + \omega_i s_i \quad \dots (3)$$

where s_i is the specific entropy of the injected water (on a per pound of water basis) which will be in liquid form. Thus, the injection entropy is solely a function of injection temperature - which must be additionally specified. As will be seen subsequently, the injection temperature will be taken (somewhat arbitrarily) to be the temperature of the heat source, T_1 .

The continuity equation can be written for the water in terms of the specific humidity across the compressor yielding:

$$\omega_2 = \omega_1 + \omega_i \quad \dots (4)$$

Equations (2), (3) and (4) can be solved iteratively to find ω_i , the amount of secondary fluid injected at i , after which the properties of interest, i.e., h_1 , and h_2 , can be calculated.

Having established all properties at state (2) one can next proceed to determining the thermodynamic state at (3). This can be uniquely determined because the primary condensing process is isobaric, the sink temperature is known, and state (3) is constrained to saturation (all liquid falls out into HX_1).

With all the properties at (3) determined, one can proceed to state point (3') where again the entropy can be written as:

$$s_{3'} = s_3 + \omega_j s_j \quad \dots (5)$$

where s_j is the specific entropy of liquid water at T_1 .

Similar to the compression process, by prescribing an isentropic expansion process in addition to the minimum evaporation temperature (remember: The pressure ratio has already been determined and the evaporative heat exchange process is also isobaric.), the amount of water injected at j can be found directly without iteration. The final enthalpies necessary for computation of the COP, h_3 , and h_4 , can then be readily determined.

As will become apparent in the following section, in order to prevent optimistic performance projections, it is necessary to include a small parasitic cooling term to account for the mass of water condensed in HX_1 at the heat sink temperature and a small power degradation term that arises through injection of additional secondary component prior to the compression and expansion processes.

The following section details an air conditioning cycle analysis in conjunction with actual thermodynamic properties to provide ideal performance projections that will clearly manifest the remarkable ideal performance of the Edwards cycle.

Example Calculation: Air Conditioning Cycle Analysis

This section presents the calculational equations and details for the theoretical assessment of the air conditioning configuration of the Edwards cycle.

Operating Conditions

Ambient: $T_{\text{outside}} = 95^{\circ}\text{F}$

$T_{\text{inside}} = 80^{\circ}\text{F}$

System: $T_1 = 80^{\circ}\text{F}$

$T_2 = 150^{\circ}\text{F}$

$T_3 = 95^{\circ}\text{F}$

$T_4 = 40^{\circ}\text{F}$

$P_1 = P_4 = 1 \text{ atm}$

Pressure Ratio = 3:1

Refrigerant: Primary Component = Air

Secondary Component = Water

Consistent with ideal performance calculations, the heat exchangers are assumed to have a 100% effectiveness with zero pressure loss. The pressure ratio was arbitrarily chosen and was not optimized for the given environmental constraints; rather, the purpose of employing a pressure ratio of 3:1 was to afford a proper cross-check on the performance predictions obtained via the polytropic process paths as taught by Edwards [1].

Since in this cycle, the amount of gaseous primary component does not change, while, on the other hand, the water may be condensing or vaporizing, the properties are hereafter written on the basis that dry air is the reference quantity. The reference state for air was arbitrarily chosen as 0°F and 14.696 psia while the reference state for the water was chosen as 32°F .

At state point (1), the following conditions exist:

$$T_{1,a} = T_{1,b} = T_1 = 80^{\circ}\text{F}$$

$$P_1 = 14.696 \text{ psia} = 1 \text{ atm and the refrigerant is saturated.}$$

The amount of secondary component at state point (1) is determined by the saturation pressure of the water at T_1 and the system pressure P_1 . Employing the following relation, the saturated humidity ratio can be calculated as:

$$\omega_{1,\text{sat}} = \frac{.62198 p_{\text{wv},s}(T_1)}{P_1 - p_{\text{wv},s}(T_1)} 7000 \quad \dots (6)$$

$$\omega_1 = \omega_{1,\text{sat}} = 155.7 \frac{\text{grains H}_2\text{O}}{\text{lb}_m \text{ dry air}}$$

where $p_{\text{wv},s}(T_1)$ is the saturation pressure of the water vapor at T_1 .

The enthalpy of the refrigerant can now be determined by employing the general equation:

$$h_r = h_a + \omega_{\text{wv}} h_{\text{wv}} + \omega_{\ell} h_f + \omega_s h_i \quad \dots (7)$$

$$h_1 = (129.06 - 109.9) + \frac{155.7}{7000} (1096.4)$$

The first term consists of the dry air enthalpy adjusted to the reference state while the second term represents the enthalpy of saturated water vapor per pound of dry air. Performing the calculation, one finds:

$$h_1 = 43.55 \frac{\text{Btu}}{\text{lb}_m \text{ dry air}}$$

The entropy at state (1) can be computed using the following general equation:

$$s_r = s_a + \omega_{\text{wv}} s_{\text{wv}} + \omega_{\ell} s_f + \omega_s s_i \quad \dots (8)$$

Since the entropy of gas is a function of both the partial pressure of the gas and the temperature, the entropy property for a gas is commonly found by using the following relation:

$$s_a = \phi_a - R_a \ln(p_a) \quad \dots (9)$$

where the first term, which accounts for the variation of specific heat with temperature, is dependent only on the temperature and is conveniently tabulated. The second term represents a pressure correction term to be applied whenever the partial pressure of the air is not identically equal to one atmosphere absolute.

The partial pressure of the air is found by first computing the mole fraction as follows:

$$x_a = \frac{1}{1 + \omega \frac{\left[\frac{M_a}{M_{wv}} \right]}{7000}} \quad \dots (10)$$

Applying Dalton's law, one obtains:

$$p_a = x_a P \quad \dots (11)$$

$$p_{wv} = (1 - x_a) P$$

The entropy at state point (1) can be computed by combining the results of Equations (8) through (11), yielding:

$$s_1 = 0.60078 - \frac{1545}{28.97(778)} \ln(.9654) + \frac{155.7}{7000} (2.0356)$$

Here, the first two terms represent the entropy of the air as given by Equation (9), while the last term is the entropy of the saturated water vapor. (Note: The term ϕ_a was not referenced to 0°F). The result is:

$$s_1 = 0.64847 \frac{\text{Btu}}{\text{lb}_m \text{ dry air } ^\circ\text{R}}$$

The properties at state point (1') cannot be fully calculated until the amount of water to be injected at i is found. The relations for the enthalpy and entropy at (1') are shown below having constrained the injection temperature of the water to equal the temperature of the heat source, T_1 :

$$h_{1'} = 43.55 + \frac{\omega_i}{7000} \quad (48.09)$$

$$s_{1'} = 0.64847 + \frac{\omega_i}{7000} \quad (.09332)$$

At state point (2), the following conditions exist:

$$T_{2,a} = T_{2,b} = T_2 = 150^\circ\text{F}$$

$$P_2 = 3 \text{ atm}$$

The continuity equation dictates that:

$$\omega_2 = \omega_1 + \omega_i$$

and the entropy at state point (2) is found by:

$$s_2 = 0.63001 - \frac{1545}{28.97(778)} \ln[(3)x_{a,2}] + \frac{(155.7 + \omega_i)}{7000} s_{wv,2}$$

where $s_{wv,2}$ is the specific entropy of the water vapor which is a function of both T_2 and the partial pressure of the water vapor, $p_{wv,2}$. This equation is valid only as long as ω_2 is less than or equal to $\omega_{2,sat}$.

Prescribing an ideal isentropic compression process yields:

$$s_{1'} = s_2$$

While the only unknown in the above equation is the amount of water to be injected prior to the compressor, the values for $x_{a,2}$ and $s_{wv,2}$ are dependent

on the quantity ω_1 . No exact closed form solution is available for solving this equation when the compressor discharge flow is unsaturated and one must resort to an iteration process. The procedure entails guessing a value for ω_1 , computing $p_{a,2}$ and $P_{wv,2}$, then determining the value of $s_{wv,2}$ from the saturated or superheated steam tables - whichever is applicable. The numerical value obtained from the s_1 equation is compared to that obtained from the s_2 equation. The amount of injected water is varied until these two quantities are equal.

After numerous iterations of the above type, it is found that:

$$\omega_1 = 182.5 \frac{\text{grains H}_2\text{O}}{\text{lb}_m \text{ dry air}}$$

The enthalpies before and after compression can now be calculated as follows:

$$h_{1'} = 43.55 + \frac{182.5}{7000} (48.09)$$

$$h_{1'} = 44.80 \frac{\text{Btu}}{\text{lb}_m \text{ dry air}}$$

$$h_2 = (145.875 - 109.9) + \frac{(155.7 + 182.5)}{7000} (1126.3)$$

$$h_2 = 90.39 \frac{\text{Btu}}{\text{lb}_m \text{ dry air}}$$

At state point (3), the following conditions are known:

$$T_{a,3} = T_{b,3} = T_3 = 95^\circ\text{F}$$

$P_3 = 3 \text{ atm}$ and the refrigerant is saturated.

This state point is completely described and after $\omega_{3,sat}$ and $x_{a,3}$ are found, the enthalpy and the entropy can be computed as:

$$h_3 = (132.66 - 109.9) + \frac{82.1}{7000} (1102.9)$$

$$h_3 = 35.70 \frac{\text{Btu}}{\text{lb}_m \text{ dry air}}$$

$$s_3 = .60732 - \frac{1545}{28.97(778)} \ln[3(.9815)] + \frac{82.1}{7000} (1.9951)$$

$$s_3 = 0.55669 \frac{\text{Btu}}{\text{lb}_m \text{ dry air } ^\circ\text{R}}$$

Similar to state point (1'), the enthalpy value at state (3') cannot be determined until the amount of water to be injected into the expander, ω_j , is found. However, the value of ω_j can be uniquely and directly obtained by specifying an ideal isentropic expansion process. Again, the injected water is taken to be at the source temperature, T_1 . Therefore, the entropy at state point (3') is:

$$s_{3'} = 0.55669 + \frac{\omega_j}{7000} (.09332)$$

Turning next to state point (4), the following conditions exist:

$$T_{a,4} = T_{b,4} = T_4 = 40^\circ\text{F}$$

$P_4 = 1 \text{ atm}$ and the refrigerant is super-saturated.

The refrigerant will necessarily be super-saturated at the expander outlet since the refrigerant entered at saturated conditions. Therefore, the partial pressures of the air and water vapor can be evaluated immediately in addition

to the entropy of the two water terms - which, in this case, are solely a function of temperature. This will permit a closed form solution to obtain ω_j . The entropy at state point (4), which includes contributions by the air, water vapor and liquid water, in conjunction with the mass balance relation, can be written as:

$$s_4 = 0.58233 - \frac{1545}{28.97(778)} \ln (.9917) + \frac{36.3}{7000} (2.1592) \\ + \frac{(82.1 + \omega_j - 36.3)}{7000} (.01617)$$

The value for ω_j is found by equating s_3 , and s_4 to yield:

$$\omega_j = 3403.9 \frac{\text{grains H}_2\text{O}}{\text{lb}_m \text{ dry air}}$$

Finally, the enthalpies at state points (3') and (4) can be found:

$$h_{3'} = 35.70 + \frac{3403.9}{7000} (48.09)$$

$$h_{3'} = 59.08 \frac{\text{Btu}}{\text{lb}_m \text{ dry air}}$$

$$h_4 = (119.48 - 109.9) + \frac{36.3}{7000} (1078.9) + \frac{(82.1 + 3403.9 - 36.3)}{7000} (8.02)$$

$$h_4 = 19.13 \frac{\text{Btu}}{\text{lb}_m \text{ dry air}}$$

The enthalpies at each state point have now been determined and the performance of the Edwards cycle under these particular constraints and conditions can be accomplished. The cooling coefficient of performance is defined as:

$$\text{COP}_c = \frac{\text{cooling delivered}}{\text{net work required}}$$

The Edwards cycle is unique in that the total mass flux varies throughout the system. Therefore, a certain amount of work is required to re-inject the secondary component into the refrigerant stream prior to compression and expansion. While pumping work for low viscosity liquids is relatively small, it should be included when evaluating the performance. Assuming a head pressure of two atmospheres is necessary to inject the water into the expander, the ideal injection work can be computed as follows:

$$\begin{aligned} w_{inj} &= \omega_{inj} v \Delta P \\ &= \frac{(3403.9)}{7000} (.016073) (29.4) \left(\frac{144}{788}\right) \\ w_{inj} &= 0.043 \frac{\text{Btu}}{\text{lb}_m \text{ dry air}} \end{aligned}$$

The cooling capacity can now be determined. Since the refrigerant is multi-component in nature, one of which will undergo considerable latent and sensible energy change, it is necessary to be extremely careful when performing this computation. For the sake of clarity, refer to Figure 2 below which depicts the moisture flow and the system configuration chosen for this particular analysis.

By conserving the mass flow throughout the system and recalling that the injection of water into the compressor and expander was stipulated to be at the source temperature (80°F), it becomes apparent that the amount of water condensed on the high pressure side ($\omega_2 - \omega_3$), would need to be cooled from 95°F to 80°F prior to injection. This can be effected by flowing the liquid excess from HX₁ up to the evaporative heat exchanger for cooling (this could be easily accomplished since the pressure difference existing between the two heat exchangers would automatically pump the fluid). It should be realized that the condensed liquid need not be circulated up to HX₂, rather, this excess liquid could be simply reinjected as point j, as indicated in Figure 1, along with the 80°F water from HX₂. The effect would be to lessen the total amount of injected water required at state point (3') to achieve the desired isentropic expansion.

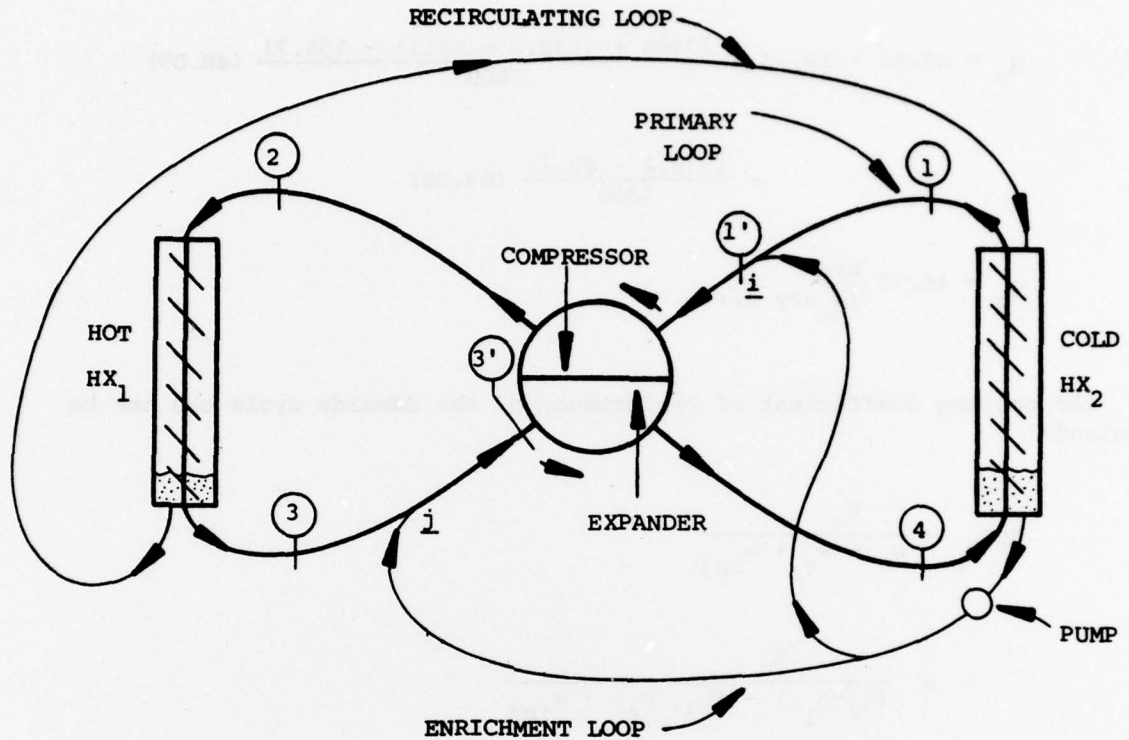


Figure 2: The Edwards Cycle Employed in an Air Conditioning Configuration Depicting the Moisture Flow

Employing the first law of thermodynamics in concert with the continuity equation, an energy balance can be written on the evaporative heat exchanger:

$$q_c + h_4 + \frac{(\omega_2 - \omega_3)}{7000} h_{f,3} = h_1 + \frac{[\omega_4 + (\omega_2 - \omega_3) - \omega_1]}{7000} h_{f,1}$$

Solving for the total cooling capacity, q_c , yields:

$$q_c = 43.55 - 19.13 + \frac{[3486 + (338.2 - 82.1) - 155.7]}{7000} \quad (48.09)$$

$$- \frac{(338.2 - 82.1)}{7000} \quad (63.06)$$

$$q_c = 46.75 \frac{\text{Btu}}{\text{lb dry air}} \text{ m}$$

The cooling coefficient of performance of the Edwards cycle can now be obtained:

$$\text{COP}_{E_c} = \frac{q_c}{w_c - w_e + w_{inj}}$$

$$= \frac{q_c}{(h_2 - h_1) - (h_3 - h_4) + w_{inj}}$$

$$= \frac{46.75}{(90.39 - 44.80) - (59.08 - 19.13) + 0.043}$$

$\text{COP}_{E_c} = 8.22$

All of the thermophysical properties used in the analysis of the Edwards cycle were obtained from the following two sources:

For the dry air:

Source: K. Wark, "Thermodynamics", 2nd ed., McGraw-Hill Book Co., New York, 1971. Data from J.H. Keenan and J. Kaye, "Gas Tables", John Wiley & Sons, Inc. New York, 1945.

For the water:

Source: J.H. Keenan, et al, "Steam Tables", John Wiley & Sons, Inc. New York, 1969.

The performance of the Edwards cycle should be compared with an ideal reverse Rankine cycle employing fluorocarbon 12 with isentropic compression, an evaporating temperature of 40°F and a condensing temperature of 150°F. Further, the fluorocarbon reverse Rankine cycle will superheat from 40°F to 80°F in the evaporator and subcool the liquid from 150°F to 95°F prior to throttling. Using tabulated property values from the ASHRAE "Handbook of Fundamentals" for R-12, the ideal cooling coefficient of performance can be shown to be:

$$\text{COP}_{R_c} = 4.26$$

Discussion - Optimization of the Edwards Cycle

The results obtained in the previous section will now be discussed and compared with the results obtained by the use of the polytropic process analysis [Ref. 1]. A convenient yardstick for determining the validity of any process or cycle is the second law of thermodynamics. The COP obtained by the polytropic index model for cooling under the identical system and environmental conditions was 8.19—not including the secondary component injection work which would slightly reduce this value; whereas, the COP obtained using actual thermophysical property data with isentropic compressor and expander constraints and including ideal injection work was found to be 8.22. The second law was clearly not violated in the analysis presented herein, thus it is this COP value which is the true ideal performance. Therefore, a good cross-check would be to determine whether the compression and expansion polytropic process paths for the multi-component refrigerant were non-isentropic—that is, were the quantities $(s_2 - s_1)$ and $(s_4 - s_3)$ greater than zero. Indeed, as would need be true, the process via polytropic path method generally indicated small increases in entropy which resulted in conclusions that usually tended to be slightly pessimistic.

The coefficient of performance for a system comprising work recovery is a quantity that magnifies small differences in the work terms because the net work input, which is generally a small term, is the result of the difference of two substantially larger terms. In other words, the COP is sensitive to the variations in the work terms. Thus, it is imperative to use tabulated data over ideal process paths to determine the ideal performance of this cycle for comparison with the ideal performance of other well-known thermodynamic cycles.

It should be noted that no attempts have been made to optimize the pressure ratio and the amount of system pressurization for the given external constraints in order to effect an optimum COP. In this connection, a brief parametric study was performed to assess the effect of system pressure ratio on the performance of the Edwards cycle. Table 1 below indicates the analytical results obtained from this study when the identical system conditions were applied. It can be seen from this table that by reducing the system pressure ratio from 3:1 to 2.25:1, an increase in performance of over 18% occurs. While associated with lower pressure ratios is a lower cooling capacity on a per pound of dry air basis, the reduction was only on the order of 30%. Additional benefits accrue from a lower pressure ratio system. Smaller amounts of injected water are necessary to achieve isentropic work processes; therefore, the injection work substantially reduces - although this is quite small. If still smaller quantities of injected secondary component are desired, by dropping the minimum evaporating temperature below the freezing point of the secondary component, substantial reduction (over an order of magnitude) in the amount of required injected component results.

Table 1 -- Pressure Ratio versus Performance of Edwards Cycle

Air Conditioning Mode -- Maximum Condensing Temperature, 150°F - Minimum Evaporation Temperature, 40°F

Pressure Ratio	Cooling Coefficient of Performance	Energy Efficiency Ratio
P_2/P_1	COP_{E_c}	$EER_E \frac{(\text{But/hr})}{\text{watt}}$
3:1	8.22	28.0
2.75:1	8.71	29.7
2.5:1	9.20	31.4
2.25:1	9.67	33.0

Although the combination of two very common, inexpensive and nontoxic fluids - air and water - results in a remarkably good refrigerant, there is nothing sacred about using this combination to achieve the benefits of the Edwards cycle. It may well be that other combinations of a gas and a phase-changing component would produce even higher levels of performance.

The invention of a new and surprisingly efficient thermodynamic cycle so late in the history of thermodynamics is bound to leave a few skeptics. However, several different methods of analysis have all reached the same conclusion: the Edwards cycle is a new and remarkably efficient cycle. The ramifications of such an invention are obviously manifold; not the least of which is the fact that no matter how much effort is put into the perfection of the present fluorocarbon reverse Rankine system, the new cycle will always pose potentially better performance.

To date so little is really known about the effect of all the many different variables. For instance: What is the effect of the injection temperature of the secondary component on the cycle performance? Is discharging from the compressor at saturated conditions more efficient than leaving only partly saturated? What effect does increasing the system pressure have on performance? What other refrigerants could be used to enhance performance? These questions and others open a new field of investigation that should ultimately manifest the Edwards cycle as a highly energy efficient heat transfer system.

REFERENCES

- [1] Edwards, T.C., "A New Air Conditioning, Refrigeration and Heat Pump Cycle", ASHRAE Summer Seminar, Halifax, Nova Scotia, June 29, 1977.
- [2] Bosnjakovic, F., Technical Thermodynamics, Holt, Rinehart & Winston, Inc. New York, 1965.

A POLYTROPIC PROCESS AND BOUNDARY STATE ANALYSIS OF A NEW AIR CONDITIONING CYCLE

Thomas C. Edwards

The ROVAC Corporation
100 Rovac Parkway
Rockledge, Florida 32955

Abstract

This paper discusses the thermodynamics and two methods of analysis of a new air conditioning, refrigeration and heat pump cycle that embodies two heat transfer processes coupled with both a compression and an expansion process. The working medium of the new cycle is multi-component in nature and, in general, consists of a superheated gaseous carrier component, such as air, in partnership with a phase-changing component, such as water.

It is shown that this new cycle yields ideal coefficients of performance (COP) greater than the reverse Brayton and reverse Rankine cycles. For example, with a maximum condensing temperature of 150°F and a minimum evaporation temperature of 40°F, operating across a sink temperature of 95°F and a source temperature of 80°F, the ideal cooling COP of the new cycle is 8.20 compared with an ideal R-12 vapor compression cycle COP of 4.26.

NOMENCLATURE

Symbols

e	$\frac{\text{Btu}}{\text{lb}_m}$	Specific energy
E	Btu	General energy
h	$\frac{\text{Btu}}{\text{lb}_m}$	Specific enthalpy
M	lb _m	Mass
n	-	Polytropic index
p	psia(atm)	Partial pressure
P	psia	Total pressure
q	$\frac{\text{Btu}}{\text{lb}_m \text{ dry air}}$	Specific heat addition
Q	Btu	Total heat addition
s	$\frac{\text{Btu}}{\text{lb}_m \text{ }^\circ\text{R}}$	Specific entropy

T	°F	Temperature
U	Btu	Total internal energy
v	$\frac{\text{ft}^3}{\text{lb}_m}$	Specific volume
w _c	$\frac{\text{Btu}}{\text{lb}_m \text{ dry air}}$	Specific compression work
w _e	$\frac{\text{Btu}}{\text{lb}_m \text{ dry air}}$	Specific expansion work
W	Btu	Total work
w	$\frac{\text{lb}_m \text{ (grains)} \text{H}_2\text{O}}{\text{lb}_m \text{ dry air}}$	Specific humidity ratio
Δφ	$\frac{\text{lb}_m \text{ H}_2\text{O}}{\text{lb}_m \text{ dry air}}$	Specific phase-changing mass of b

Subscripts

1,1',2,3,3',4	State points
a	Dry air (primary component)
b	Secondary component
c	Compression
e	Expansion
f	Saturated liquid
i	Ice
i,j	Location points
l	Liquid water
s	Solid
Sat	Saturated
wv	Water vapor

BACKGROUND AND INTRODUCTION

While at the School of Mechanical Engineering at Purdue University (Lafayette, Indiana, 1967-70), the author investigated a unitary rotary positive displacement device capable of effecting a reverse Brayton cycle when employed with simple air-to-air heat exchangers. This simple machine, in performing six individual flow processes, produced cool air and illustrated an alternative hardware form of the air cycle system. The application of such hardware in partnership with subsequent extensive theoretical and experimental analyses is confirming the existence of a new efficient thermodynamic heat transfer cycle. Due to the possible significance of the new cycle, this paper will concentrate primarily on qualitative and quantitative aspects of its ideal thermodynamics.

THE NEW CYCLE: AIR CONDITIONING CONFIGURATION

Figure 1 presents the general configuration of the new air conditioning cycle. As can be seen, the system consists, in addition to the working fluid, of three basic components: The primary condensing heat exchanger, HX_1 (hot side), the compressor/expander device, and the secondary evaporating heat exchanger, HX_2 (cold side). During operation, working fluid flows from HX_2 at state point (1), is compressed by C/E to state point (2), where thermal energy is rejected through HX_1 . The flow emerges from HX_1 at state point (3) and expands through C/E to state point (4). Finally, the working fluid passes through HX_2 where it receives thermal energy until it emerges again at state point (1).

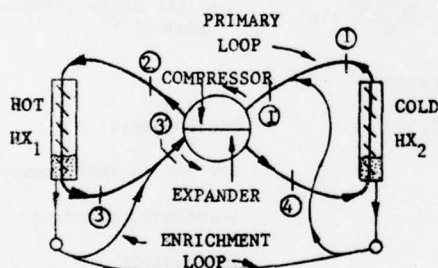


Figure 1: The General Air Conditioning Configuration of the New Cycle

In general, the multi-component/mixed-phase refrigerant used in this cycle consists of a permanently gaseous carrier constituent, termed the primary component, a , and a state and phase-changing constituent termed the secondary component, b . This mixed refrigerant continuously circulates through the system. During operation, the secondary component in the liquid phase will collect in both heat exchangers. Therefore, generally speaking, only the vapor phase of the secondary component will automatically accompany the primary component. The amount of this type of secondary component circulation will, of course,

be dependent upon the thermodynamic properties of the two components as well as the state point values around the cycle.

In order to take full advantage of the characteristics of this cycle, it is important to control the ratio of mass of the secondary component with respect to the primary carrier component at various locations in the system. A schematic means for achieving this is depicted in Figure 1 and is labeled "Enrichment Loop". This loop represents the enrichment flow of the secondary component in liquid form to two important locations in the system. The injection of liquid component b (continually collecting in the heat exchangers) into component a at (1), yielding state point (1'), will tend to decrease the work of compression required to reach a given pressure ratio due to the sensible and latent absorption of compression heat. Likewise, additional secondary liquid injected downstream of state point (3), yielding state point (3') will increase the energy of expansion due to the release of sensible and latent energy to the gaseous carrier component. Naturally, the continuously recirculating secondary component also greatly influences the heat rejection and absorption rates and heat exchanger temperature profiles. (Of course, a parasitic liquid pumping requirement exists in order to elevate the secondary flow pressure from P_1 to P_3 .)

From this system description it is interesting to note that both the reverse Brayton cycle and the reverse Rankine cycle are subcases of the new cycle. For example, by reducing the mass ratio of secondary component to primary component to zero (i.e. $M_b/M_a = 0$), the new cycle becomes the reverse Brayton cycle. By reducing M to zero and specifying the expansion process to be isenthalpic, the reverse Rankine cycle emerges.

The new cycle can be conceptualized as a synergistic union between the air cycle and the vapor-compression cycle. This is because the new cycle is structured in such a way as to simultaneously employ the energy recovery advantage of the reverse Brayton cycle and the isothermal heat transfer processes of the vapor-compression cycle. By its nature, the new cycle recovers energy from a condensable or heat-storing component through the expansion process simply by suspending it in a gaseous carrier component that can provide significant volume change. As well, the isothermal heat transfer characteristics of the reverse Rankine cycle can be closely approximated by the properties of the working fluid mixture due to the large latent contributions of the secondary component. Further, it is interesting to note that some of the energy absorbed at the heat source is "recycled" through the expander process.

THE NEW CYCLE: ANALYTICAL METHODS

Two basic analytical approaches to ascertaining the ideal performance of the new cycle have been developed. In order to generate predictions regarding ideal theoretical performance, various enthalpic state-point data are required. Referring to Figure 1, it can be readily seen that

the cooling coefficient of performance can be generally written in terms of enthalpy as:

$$(\text{COP})_E^C = \frac{h_1 - h_4}{(h_2 - h_1') - (h_3' - h_4)}$$

Specified environmental conditions as well as certain arbitrary system conditions and parameters provide portions of this enthalpy data. For example, if the maximum condensing temperature, minimum evaporation temperature and pressure are specified along with the source and sink temperatures, the initial enthalpy prior to, say, compression can be determined if the refrigerant composition and properties are known. However, in order to find the enthalpy state after compression, the energy of compression must be found. An approach to finding this is to assume a general work path function such as the polytropic process and determine the polytropic index of the process. The polytropic index can be found through the simultaneous application of the first law of thermodynamics and the mathematical definition of the polytropic process. This is termed the "Polytropic Process Model" which provides insight into the details of the processes of the cycle.

The second analytical approach, termed the "Boundary-State Model" is independent of any process path hypotheation; it employs only tabulated state-point data and isentropic compression and expansion processes. While details of the compression and expansion processes are ignored (except, of course, the specification of constant entropy), the advantage of the boundary-state method is that it is fundamentally exact and presents a direct analog to cycle analysis procedures established for fluorocarbon systems.

THE POLYTROPIC PROCESS ANALYSIS METHOD

Expansion and Compression of a Multi-Component/Mixed-Phase Closed System. Attention will next be directed to the two processes of the present cycle that embody the most interesting thermodynamic aspects. This will involve the examination of the properties of a working fluid which consists of two individually identifiable components: One of which remains in the vapor phase while the other changes phases during a given process.

Expansion. Referring to Figure 2, consider a closed system at equilibrium at an elevated pressure wherein the component that will change phase (secondary component) exists in a saturated vapor condition with the partner non-phase-changing component (primary component).

Next, allow the system to expand adiabatically. As expansion begins (depending upon the thermodynamic properties of the working fluid constituents and the actual process path), some of the secondary component will condense due to the temperature decrease. The energy associated with this condensation will be transferred to the primary (gaseous) component thus increasing both its pressure and its temperature over the values which would have been reached if the condensing secondary component had not been present. As further expansion takes

place, further condensation will also take place, further perturbing the mixture temperature and pressure state points.

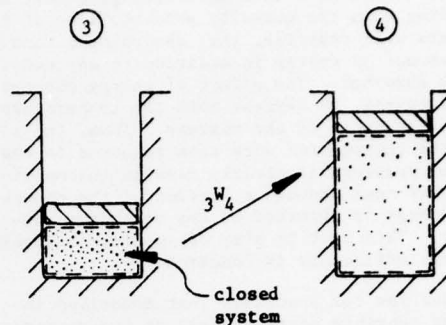


Figure 2: Multi-Component/Mixed-Phase Closed System Expansion

An immediately obvious consequence of this multi-component process is an increase in work of expansion as seen by $\int PdV$. It is also apparent from the first law of thermodynamics that the final expanded energy state is relatively smaller due to the increase in the work integral. These two factors play a major role in the ultimate cycle efficiency.

Compression. Next, turn to the companion compression process as depicted in Figure 3.

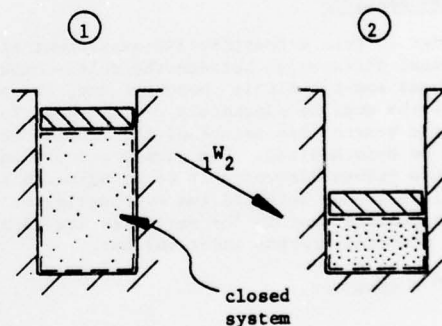


Figure 3: Compression of a Multi-Component/Mixed-Phase Fluid

The closed system at its initial state point consists, as before, of a gaseous carrier component and a second component which will participate in a phase-changing process. However, in this instance, the second component will consist of a fine dispersion of liquid particles existing in saturated equilibrium and evenly distributed throughout the partner gaseous carrier component.

As compression begins, the temperature of the mixture will begin to rise and the liquid droplets will begin to absorb energy from the surrounding gaseous component. As compression proceeds, and depending upon the quantity present, some of these droplets will vaporize, thus absorbing a considerable amount of energy in addition to any sensible energy absorbed. The effect of energy absorption is, of course, to depress both the temperature and the pressure of the mixture. Thus, the integrated compression work term required to reach a given pressure is clearly less in the multi-component case wherein a portion of the compression energy is absorbed by the secondary component. This fact is also of importance insofar as cycle efficiency is concerned.

In order for the processes just described involving sensible state changes of the secondary component to actually take place, it is obvious that the properties of the dispersion of this component be such as to permit heat transfer rates high enough to match actual quasi-static process rates that would occur in a real machine. For example, the compression process in a typical ROVAC Circulator™ takes place within approximately 5 milliseconds. During that time, heat transfer rates on the order of 20 Btu per pound of dry air would be transferred to or from the secondary enrichment component. Presuming this secondary component to be water, and further specifying that the maximum temperature difference between the carrier component and the water to be, say 0.5F°, it can easily be shown that the diameter of the dispersed particles can be as large as 0.001 inch. This value is easily achieved by usual liquid spray methods (Ref. 1, Ref. 2).

PROCESS ANALYSES

In order to make a quantitative assessment of the numerical differences between the multi-component processes and the single component one, the process paths must be adequately postulated. To begin, the generalized nature of the process must first be hypothesized. One simple process path that has proven historically to be accurate (and therefore chosen here) is the exponential or polytropic process wherein the variables are related for a constant process index (n) as:

$$P_v^n = \text{constant} \quad \dots(1)$$

or

$$\frac{d(\ln P)}{d(\ln v)} = -n \quad \dots(2)$$

where P is the absolute pressure, v is the specific volume and n is the polytropic index of the system fluid.

In choosing the polytropic equation form, the problem, of course, becomes the quantitative determination of the value of the polytropic index, n. There are various approaches possible, but the one chosen here is to employ the first law of thermodynamics in concert with the mathematical definition of the polytropic index.

Referring to Figure 1 again (which depicts the expansion process) and employing energy conservation for an adiabatic process, it can be written that:

$$E_3 = E_4 + {}_3W_4 \quad \dots(3)$$

In this expression, E denotes the total energy of the refrigerant fluid and W represents the process work term. Further, the sum of these energies can be written as:

$$(U_a)_3 + (E_b)_3 = (U_a)_4 + (E_b)_4 + {}_3W_4 \quad \dots(4)$$

Here subscript a refers to the carrier component and subscript b refers to the secondary phase-changing component. U represents internal energy. Eqn. (4) can be arranged as:

$${}_3W_4 = [(U_a)_3 - (U_a)_4] + [(E_b)_3 - (E_b)_4] \quad \dots(5)$$

where $[(E_b)_3 - (E_b)_4]$ can be considered to be a "heat addition" term, \bar{Q}_e , insofar as the carrier component is concerned. While this term has been discussed in connection with a condensation process, it is apparent that it can, in general, consist of sensible components also, as well as others. That is:

$$\begin{aligned} \bar{Q}_e &= [(E_b)_3 - (E_b)_4] = (M_b)_{\text{latent}} \text{ (latent energy change)} \\ &+ (M_b)_{\text{liquid}} \text{ (sensible energy change)} \\ &+ (M_b)_{\text{vapor}} \text{ (sensible energy change)} \\ &+ \text{other energy additions that may be present} \\ &\text{(chemical, nuclear, magnetic, etc.)} \end{aligned}$$

where the M's represent masses of the various components undergoing state change.

Depending, of course, upon the state condition, the properties and amounts of components, the constituent terms can have various contributions to the total term. If, as previously postulated, only enough of component b exists to just provide saturation (no excess liquid) prior to expansion, the "heat addition" term reduces to:

$$\bar{Q}_e = \Delta M_b [(e_b)_3 - (e_b)_4] = \Delta M_b \bar{q}_e$$

where ΔM_b is the amount of component b that has condensed and \bar{q}_e can be treated as $(h_b)_{fg}$ (neglecting the generally small sensible effect of the vapor).

Proceeding with the saturation condition assumption (no liquid present), and assuming that component a with the attendant vapor portion of component b can be suitably approximated as an ideal gas, one can write

$$\begin{aligned} {}_3W_4 &= M_{ab} (C_v)_{ab} [(T_{ab})_3 - (T_{ab})_4] \\ &+ \Delta M_b [(h_b)_{fg}] \quad \dots(6) \end{aligned}$$

where the ab subscript indicates the mixture pro-

Perty of the carrier a and the vapor portion of the secondary component b. On a specific mass basis (based upon component a) Eqn. (6) yields:

$$3^w_4 = (C_v)_{ab} [(T_{ab})_3 - (T_{ab})_4] + \Delta\phi_e (h_b)_{fg} \quad \dots(7)$$

where $\Delta\phi$ represents the condensed mass of component b per unit mass of component a.

Following through with the polytropic process definition along with the quasi-static work integral, the work can be represented as:

$$3^w_4 = \frac{R_{ab} [(T_{ab})_3 - (T_{ab})_4]}{n_e - 1} \quad \dots(8)$$

where R_{ab} is the mixture gas constant consisting of component a and the vapor portion of component b, and n_e is the polytropic index of expansion. It is further indicated that the temperature of both components are equal, thus specifying a quasi-static equilibrium condition.

Equating Eqns. (7) and (8) and solving for the polytropic expansion index yields:

$$n_e = 1 + \frac{R_{ab} [(T_{ab})_3 - (T_{ab})_4]}{(C_v)_{ab} [(T_{ab})_3 - (T_{ab})_4] + \Delta\phi_e (h_b)_{fg}} \quad \dots(9)$$

and

$$\Delta\phi_e (h_b)_{fg} = \frac{R_{ab} [(T_{ab})_3 - (T_{ab})_4]}{(n_e - 1)} - (C_v)_{ab} [(T_{ab})_3 - (T_{ab})_4] \quad \dots(9')$$

Another relation for this polytropic index can be derived from its mathematical definition:

$$\frac{(T_{ab})_4}{(T_{ab})_3} = \left[\frac{(P_{ab})_4}{(P_{ab})_3} \right]^{\frac{n_e - 1}{n_e}} \quad \dots(10)$$

Solving for n_e yields:

$$n'_e = \left[1 + \ln \left[\frac{(T_{ab})_4}{(T_{ab})_3} \right] / \ln \left[\frac{(P_{ab})_3}{(P_{ab})_4} \right] \right]^{-1} \quad \dots(11)$$

(Where the prime is added in order to denote the difference in origin of the two representations of the index.)

Note that two Equations, (9) and (11), are available which represent the polytropic index; one from the first law and one from the definition of the polytropic. Further, note that the indices are presented in terms of initial and final temperatures and pressures. In general, the pressure ratio of the process, as well as the initial pressure and temperature will be known. Thus the final temperature, $(T_{ab})_4$ and n_e (or n') are the only unknowns. Since two expressions for these

variables are available, their values can be computed. However, since one equation is of a transcendental form, it is a simple matter to find the polytropic index of expansion in an iterative manner. In other cases, however, the final temperature will also be known (or postulated) so that Eqns. (9) and (11) can be applied directly.

Considering next the analytical relations for the polytropic index of compression, it is clear that the inverse process occurs so that the respective polytropic relationship can appear as follows:

$$n_c = 1 + \frac{R_{ab} [(T_{ab})_2 - (T_{ab})_1]}{(C_v)_{ab} [(T_{ab})_2 - (T_{ab})_1] + \Delta\phi_c (h_b)_{fg}} \quad \dots(12)$$

or, solving for the "heat absorption" term,

$$\Delta\phi_c (h_b)_{fg} = \frac{R_{ab} [(T_{ab})_2 - (T_{ab})_1]}{n_c - 1} - (C_v)_{ab} [(T_{ab})_2 - (T_{ab})_1] \quad \dots(12')$$

and

$$n'_c = \left[1 + \ln \left[\frac{(T_{ab})_1}{(T_{ab})_2} \right] / \ln \left[\frac{(P_{ab})_2}{(P_{ab})_1} \right] \right]^{-1} \quad \dots(13)$$

Again, the pressure ratio will normally be known, along with the initial pressure and temperature and sometimes the final temperature. Therefore both equations can be solved in order to obtain the final compression temperature of the mixture and the polytropic compression index.

Before proceeding further, however, a word should be stated regarding the actual calculation of $\Delta\phi$. When the final temperature is not specified but is instead calculated on the basis of Eqns. (9) and (11) or Eqns. (12) and (13), some iteration must take place on final temperature states in order to apply numerical thermodynamic properties of the secondary component. For example, considering the expansion process, the quantity of component b in the initial state can be found because the initial state points and the properties of the component are known. However, in order to compute the final temperature of a given process from, say, Eqns. (9) and (11), $\Delta\phi$ must be known. That is, the final quantity of component b in the vapor phase must be known so that the difference between the initial vapor quantities and final vapor quantities ($\Delta\phi$) can be computed. Therefore, in the actual application of these Eqns., $\Delta\phi$ is assumed based upon an assumed final temperature. Then, after the computation is made, a check on the assumed values is made and corrected, if necessary. In practice, especially if the secondary component proceeds to the solid phase, little error occurs in only a single calculational cycle because so little component exists in the vapor phase.

Armed with these relations, meaningful comparisons of compression and expansion work can be made as amounts of component b are varied with respect to component a . This, of course, along with specified state point data, enables the computation of all the enthalpy state points required to predict ideal cycle performance.

Next, the elements of the tabular boundary-state analysis method will be presented.

BOUNDARY-STATE ANALYSIS METHOD

Again, in order to evaluate the coefficient of performance of the new cycle, various state point enthalpies are required. Since the refrigerant employed in this cycle consists, as generally discussed here, of two independently identifiable fluids existing simultaneously at identical pressures and temperatures at any given location, only two properties (plus relative composition) are required to compute the total refrigerant property at that point. If the binary refrigerant combination chosen possesses well established thermodynamic data, determination of the refrigerant state points is relatively easy because the mixture properties can generally be determined by the sum of the total properties of the constituents.

If the evaporative heat exchanger environment is specified (which will normally be the case), and the low side pressure is set, and further, if the amount of secondary component is known (saturation conditions will prevail at state point (1) because all of the condensed and liquid water will drain in the evaporative heat exchanger and eliminate liquid carry-over), the thermodynamic state of (1) is fully prescribed. That is, T_1 , P_1 , and ω_1 (specific quantity of a with respect to b) are known from which all other properties can be determined.

If next, the maximum condensing temperature and pressure ratio of the cycle are prescribed, the entire condition of state (2) can be determined because isentropic compression is also prescribed, i.e.:

$$s_2 = s_1' \quad \dots(14)$$

The entropy prior to compression, s_1' , is determined by the equation:

$$s_1' = s_1 + \omega_1 s_1 = s_2 \quad \dots(15)$$

where s_1 is the specific entropy of the injected secondary fluid which will be in liquid form. Thus, the injection entropy is solely a function of injection temperature - which must be additionally specified. The injection temperature can be the temperature of the heat source, T_1 . Because of the cyclic nature of these processes, the net change of entropy of mixing (at the injection points) and "unmixing" (in the heat exchangers) is, of course, zero.

Conserving the mass of secondary component across the compressor yields:

$$\omega_2 = \omega_1 + \omega_i \quad \dots(16)$$

Equations (14), (15) and (16) can be solved by iteration to find ω_i , the amount of secondary fluid injected at i , after which the properties of interest i.e., h_1 and h_2 , can be found.

Having established all properties at state (2) one can next proceed to determine the state at (3). This can be uniquely determined because the primary condensing process is isobaric, the sink temperature is known, and state (3) is constrained to saturation (all liquid falls out into HX_1).

With all the properties at state (3) determined, one can proceed to state point (3') where again the entropy can be written as:

$$s_3' = s_3 + \omega_j s_j = s_4 \quad \dots(17)$$

where s_j is the specific entropy of liquid secondary component injected at T_1 (or T_3 , if chosen).

Because the pressure ratio has already been set, by prescribing the minimum evaporation temperature and noting that the evaporation process is isobaric, the quantity of secondary component injected at j can be found directly. The remaining enthalpies necessary for the determination of $(COP_E)_c$, i.e.: h_3' and h_4' can then be easily determined.

For the sake of exactness it is necessary to include a very small cooling term to account for the mass of water condensed in HX_1 that is cooled from the sink temperature to source temperature and a small parasitic pumping term that arises from the misting and injection of additional secondary component.

The following section summarizes detailed calculational results arising from the application of the two methods of analysis of the new cycle outlined above. Polytropic process model analysis results are from Reference (3) and the companion boundary state results are credited to Reference (4).

Results of Example Calculations:

Ideal Performance of the New Cycle

This section presents the calculational results of applying the two foregoing methods of analysis to the air conditioning configuration of the new cycle operating under the following conditions:

Example Operating Conditions

$$\text{Ambient: } T_{\text{outside}} = 95^\circ\text{F}$$

$$T_{\text{inside}} = 80^\circ\text{F}$$

Example Operating Conditions
(continued)

System: $T_1 = 80^\circ\text{F}$

$T_2 = 150^\circ\text{F}$

$T_3 = 95^\circ\text{F}$

$T_4 = 40^\circ\text{F}$

$P_1 = P_4 = 1 \text{ atm}$

Pressure Ratio = 3:1

Refrigerant: Primary Component = Air
Secondary Component = Water

The following Table I sets forth a summary comparison of the analytical results of operating the new cycle at the above conditions. The results of both methods of analysis are presented along with the results of a COP calculation for an R-12 reverse Rankine cycle operating across the same ambient conditions with a condensing temperature of 150°F , and evaporation temperature of 40°F , and superheating to 80°F and sub-cooling to 95°F .

Table I
Performance Comparisons

	Polytropic Process	Boundary State
New Cycle (air/water)	$(\text{COP}_E)_C = 8.19$	$(\text{COP}_E)_C = 8.22$
Reverse Rankine Cycle (R-12)	—	$\text{COP}_R = 4.26$

The improvement in potential performance over the fluorocarbon system is notable. Further, the close agreement between the two analytical methods is apparent and reinforces the basic conclusion.

No attempts were made in the present example to optimize the pressure ratio for the given external constraints in order to effect a maximum COP. In this connection, a brief parametric study was performed to assess the effect of system pressure ratio on the performance of the new cycle. Table II below indicates the analytical results obtained from this study when the identical system conditions were applied (Ref. 4).

From the results shown in Table II it can be seen that by reducing the system pressure ratio from 3.0:1.0 to 2.25:1, an increase in theoretical performance of nearly 20% is achieved.

Table II

Pressure Ratio Versus COP of New Cycle

Air Conditioning Mode—Maximum Condensing Temperature, 150°F Minimum Evaporative Temperature of 40°F

Pressure Ratio	Cooling Coefficient of Performance	Energy Efficiency Ratio
P_2/P_1	$(\text{COP}_E)_C$	$(\text{EER}_E)_C \frac{(\text{Btu/hr})}{\text{watt}}$
3:1	8.22	28.0
2.75:1	8.71	29.7
2.5:1	9.20	31.4
2.25:1	9.67	33.0

CLOSURE

General Discussion and Conclusions. This paper has disclosed and discussed the analysis of a new and interesting thermodynamic cycle. The results of analytical models and methods summarized here predict that the ideal performance of the new cycle is greater than the well-known fluorocarbon reverse Rankine cycle which is currently the "backbone" of the present air conditioning, heat pump and refrigeration industry. Further, the two methods of analysis presented are basically independent and yet arrive at substantially the same conclusion.

The basic attributes of the new cycle may be intuitively apparent. As noted earlier, the new cycle can be conceptualized as a synergistic union between the air cycle and the vapor-compression cycle. This is because the new cycle is structured in such a way as to simultaneously employ the energy recovery advantage of the air cycle and the isothermal heat transfer processes of the vapor compression cycle. By its nature, the new cycle is able to recover energy from a condensable component that can provide significant volume change effects in a gaseous carrier component. As well, the isothermal heat transfer characteristics of the reverse Rankine cycle can be closely approximated by the properties of the working fluid mixture, thus adopting this very positive attribute of the vapor-compression system. Further, the effects of the secondary component on both the compression and expansion processes of the new cycle are favorable.

Once one has accepted the fundamental superiority of the ideal properties of the new cycle, obvious and important questions arise regarding its actual practical implementation. For example, one of the well-known practical attributes of the reverse Rankine cycle is that cycle efficiency is a

function of the efficiency of only one volume-changing component: the compressor. This is not the case with the new cycle (and the reverse Brayton cycle) which is dependent upon the product of the efficiencies of both a compression device and an expansion device. Thus, actual cycle efficiency attainment is more sensitive to machine efficiency in the case of the new cycle than the vapor compression system. (Considering the vapor compression cycle, however, it appears reasonable to note that even some expansion efficiency is better than none at all.)

Regarding further the matter of compressor and expander efficiencies, it has been the author's experience with the ROVAC Circulator that the machine exhibits a high volumetric efficiency. Tests made by the Environmental Control Section of the Air Force Flight Dynamics Laboratory at Wright-Patterson Air Force Base (Ref. 5) have confirmed volumetric flow efficiency levels very nearly equal to unity. This is an important factor that must be considered carefully when comparing the reverse Rankine cycle to the new cycle. This is because volumetric efficiency is itself a multiplier in determining overall vapor compression system performance. That is, the overall reverse Rankine performance is the product of the compressor efficiency and the volumetric efficiency. While by no means does the unitary compressor/expander device ameliorate the basic need for good efficiency of both the compression and expansion processes, the unitary nature of the Circulator does offer clear economies in efficiency because it is basically a single machine. Further, it is well known that the use of a regenerative heat exchanger (or recuperator) in the reverse Brayton cycle can be used to mitigate the sensitivity of that cycle to the irreversibilities inherent in real compressor and expander devices. The same option, of course, is open to the new cycle.

Continuing with the topic of heat exchangers, it is important to note that even minute quantities of moisture present in the loop air drastically improve the internal heat transfer film coefficient of air-to-air heat exchangers (Ref. 1, Ref. 2). In this connection, it has been interesting to learn in actual tests that unmodified fluorocarbon fin-and-plate evaporator cores used in automobile air conditioning systems have provided cross-flow heat exchanger effectiveness values in the ninety percent bracket with less than 1 psi pressure loss. (Of course, a cross-counter flow core configuration would be better.)

It is worthwhile to note that in the closed system configuration, pressurization of the closed system effectively "dilutes" the machine's frictional losses over the resulting increase in produced cooling. That is, if a system is operating at a given set of conditions and the evaporative heat exchanger reference pressure is, say doubled from one atmosphere to two atmospheres, the cooling capability is essentially doubled. However, the "over-head" friction of the machine which consists principally of bearing friction

and hydrodynamic lubricant shear will increase only very slightly. Thus, the system can inherently improve its performance through pressurization. It is further interesting to note that the positive benefits of pressurization are not limited to mechanical friction; to the contrary, they extend to dilution of adverse heat transfer, porting losses (velocity-squared losses vs. gas density losses), and internal leakage.

In conclusion, the results of the analyses of the new cycle indicate that this natural refrigerant cycle offers a partial solution to the growing world-wide energy shortage as well as a solution to the global pollution and toxic substance problems related to conventional fluorocarbon refrigerants.

References

- 1 Takahara, E.W., "Experimental Study of Heat Transfer from a Heated Circular Cylinder in Two-Phase, Water-Air, Flow", MS Thesis, Air Force Institute of Technology, May, 1966.
- 2 Albrecht, J.R., "An Experimental Investigation of the Heat Transfer Near the Stagnation Point in a Two-Phase Air-Water Spray Flow", MS Thesis, Air Force Institute of Technology, March, 1967.
- 3 Edwards, T.C., "A New Air Conditioning, Refrigeration and Heat Pump Cycle", ASHRAE Summer Seminar, Halifax, Nova Scotia, June 29, 1977.
- 4 Ecker, A.L., et al, "A tabular Data Boundary-State Analysis of the Edwards Cycle", ASHRAE Summer Seminar, Halifax, Nova Scotia, June 29, 1977.
- 5 Smolinski, R.E., Midolo, L.L., "Performance of a New Positive Displacement Air Cycle Machine", AIAA Meeting, September, 1976, Dallas, Texas.